Title
Neurotoxicity of the Parkinson’s Disease-Associated Pesticide Ziram is Synuclein Dependent

Author
Lulla, Aaron

Publication Date
2016

Peer reviewed|Thesis/dissertation

UNIVERSITY OF CALIFORNIA

Los Angeles

Neurotoxicity of the Parkinson's Disease-Associated Pesticide Ziram is Synuclein Dependent

A dissertations submitted in partial satisfaction of the requirements for the degree of Doctor of Philosophy in Molecular Toxicology

by

Aaron Lulla

2016

ABSTRACT OF THE THESIS

Neurotoxicity of the Parkinson's Disease-Associated Pesticide

Ziram is Synuclein Dependent

by

Aaron Lulla

Doctor of Philosophy in Molecular Toxicology

University of California, Los Angeles, 2016

Professor Jeff Bronstein, Chair

Parkinson's disease (PD) is the second most common neurodegenerative disease, affecting seven to ten million people worldwide. Familial forms of PD account for 5-10% of all PD cases suggesting that other factors such as the environment have a role in the development of sporadic cases of PD. Epidemiological studies have indicated that exposure to pesticides increases the risk for PD. Ziram, a dithiocarbamate fungicide commonly used in California, increases the risk of PD for individuals living and working in areas where the pesticide is sprayed. Ziram has previously been found *in vitro* to cause selective dopaminergic cell toxicity, inhibition of the ubiquitin proteasome system (UPS), and increased α-synuclein (α-syn) levels in primary neuronal cultures. In this dissertation we utilize zebrafish embryos (ZF, *Danio rerio*) to study ziram in an *in vivo* system and to determine if ziram's toxicity is mediated via synuclein.

We found that ziram is toxic to ZF at nanomolar concentrations and caused selective

loss of dopaminergic (DA) neurons and impaired swimming behavior in ZF. Since ziram increases α-syn concentrations in rat primary neuronal cultures, we investigated the effect of ziram on ZF γ-synuclein 1 (γ1). ZF express 3 synuclein isoforms and ZF γ1 appears to be a functional homologue of α-syn. We found that recombinant ZF γ1 formed fibrils *in vitro* and overexpression of ZF γ1 in ZF embryos led to the formation of neuronal aggregates and neurotoxicity similarly to α-syn. Importantly, knockdown of ZF γ1 with morpholinos or disruption of oligomers with the molecular tweezer CLR01 protected against ziram's DA toxicity.

Over the course of this dissertation we have demonstrated that ziram is selectively toxic to DA neurons *in vivo* and that its toxicity is synuclein-dependent. These findings provide potentially important mechanistic implications on how ziram and possibly other environmental toxins can contribute to the pathogenesis of neurodegenerative disorders such as PD.

The dissertation of Aaron Lulla is approved.

Patrick Allard

Alvaro Sagasti

David E. Krantz

Carlos Portera-Cailliau

Jeff Bronstein, Committee Chair

University of California, Los Angeles

2016

Table of Contents

Acknowledgements

Over the course of my Ph.D. I have met and worked with so many amazing individuals. I'm so thankful for every one of these friendships and experiences, I have had on this amazing journey. All of these individuals have contributed to my success, and I couldn't have done this without them.

Sharon Li: During my time Sharon helped me to learn how to raise fish, perform experiments, and was always there to help me with setting up my experiments (especially in the last few months). I would not have accomplished any of this without her help and her maintenance of the fish system and lab.

Mark Stahl and Lisa Barnhill: Mark and Lisa have been two of my greatest supporters over the course of my Ph.D. They always stood by me when I was at my lowest, and pushed me to achieve more and to become a better scientist. I am truly grateful to both of them for the hours that we spent discussing science and life. Every grad student ought to have a friend in lab, who can push them to be something more. I am so lucky to had two lab best friends who always pushed me to be better and achieve my goals.

Carlos Portera-Cailliau: Carlos is one of my closest advisors. He has always been there for me when it comes to talking shop, career plans, or life. I am so grateful for his friendship and all the advice he has given me over the past five years. Here's to many years of friendship and to Barcelona always beating Atleti.

Shanta and Victor Lulla: My parents are my greatest supporters and have always pushed me. There were many times over the course of this dissertation when I was ready to give up. They constantly reassured me that I could do it, and even though they live across the country, they were always available for me. I can never say how much I love and appreciate you both.

Jeff Bronstein: I cannot say thank you enough Jeff. You have been more than anything I could have asked for in an advisor. Thank you for always pushing me to be a better scientist and person, for always encouraging and allowing me to push the boundaries of our research, for supporting me in my lowest times and being there to cheer me on, for pushing me to follow my career goals, and for always being my mentor, friend, and treating me like family. I am so grateful for everything, and I look forward to working together and continuing our friendship for many years to come.

"If I have seen further than others, it is by standing upon the shoulders of giants."

-Issac Newton

Vita

Aaron Lulla

B.S. Biochemistry
Rutgers University/Cook College
New Brunswick, New Jersey

Publications:

- **Lulla A.,** Barnhill L., Bitan G., Magdalena., Nguyen B., O'Donnell K., Stahl M.C., Yamashiro C., Klärner F.G., Schrader T., Sagasti A., Bronstein J.M. (2016) Neurotoxicity of the Parkinson's Disease-Associated Pesticide Ziram is Synuclein- Dependent in Zebrafish Embryos. Environmental Health Perspectives (In Press).
- Fitzmaurice A.G., Rhodes S.L., **Lulla A**., Murphy N.P., Lam H.A., O'Donnell K.C., Barnhill L., Casida J.E., Cockburn M., Sagasti A., Stahl M.C., Maidment N.T., Ritz B., and Bronstein J.M. (2013) Aldehyde dehydrogenase inhibition as a pathogenic mechanism in Parkinson disease. Proc. Natl. Acad. Sci. USA 110(2): 636-641. PMID:23267077
- O'Donnell K.C., **Lulla A,** Stahl M.C., Wheat N.D., Bronstein J.M., Sagasti A., (2014) Axon degeneration and PGC-1α-mediated protection in a zebrafish model of α-synuclein toxicity. Dis. Model. Mech. 7(5) 571-582 PMID: 24626988
- Lawal A, Zhang M, Dittmar M, **Lulla A**, Araujo JA. (2015) Heme Oxygenase-1 protects endothelial cells from the toxicity of air pollutant chemicals. Toxicol Appl Pharmacol 284(3) 281-91 PMID: 25620054

Meetings/Presentations:

- Neurotoxicity of the dithiocarbamate fungicide ziram is dependent on synuclein in zebrafish: Implications for Parkinson's disease. **A Lulla**, L Barnhill, M Stahl, A G Fitzmaurice, S Li, J M Bronstein: Society of Toxicology Annual Meeting 2013 (abstract)
- The dithiocarbamate fungicide ziram results in endogenous synuclein aggregation, dopaminergic cell loss, and reduced locomotor behavior in a zebrafish model of parkinson's disease. **A Lulla,** A G Fitzmaurice, M Stahl, S Li, J Bronstein: NIEHS Centers for Neurodegeneration Science Annual Meeting 2012 (abstract)

Awards/Activities:

- 1st Place Graduate Student Poster Award, Neurotoxicology Subspecialty SOT 2013 (National Meeting)
- Colgate-Palmolive Graduate Student Award for Alternative Methods in Research Training
- 1st Place Graduate Student Poster Award, UCLA Neurology Annual Science Day (2012)

Chapter 1

Introduction

Parkinson's disease (PD) was first characterized clinically by Dr. James Parkinson in 1817 as "Shaking Palsy" (Parkinson 2002), and has since been further characterized clinically, pathologically, and genetically. Today, PD is the second most common neurodegenerative disorder behind Alzheimer's disease, and it affects an estimated 5 million individuals world wide (Van Den Eeden et al. 2003), a number that is expected to double by 2030 (Dorsey et al. 2007). Our understanding of PD has allowed for the advancement of clinical care for patients, but no cure nor clear understanding of the causes of PD exists. Through this dissertation, I seek to identify and elucidate the role of environmental factors on the development of PD, and to understand the mechanisms of toxicities of these compounds, to help further our understanding of its etiology.

Clinical Features

Dr. James Parkinson first described PD in 1817, as "Shaking Palsy, the involuntary tremulous motion, with lessened muscular power, in parts not in action and even when supported; with a propensity to bend the trunk forwards, and to pass from a walking to a running pace: the sense and intellects being uninjured." (Parkinson 2002). Today, there are six clinical features of Parkinsonism of the common form, 1. Resting tremor, 2. Bradykinesia, 3. Rigidity, 4. Postural instability, 5. Flexed posture, and 6. Freezing (Jankovic 2008).

Resting tremor is a common symptom of PD that is characterized by supination pronation "pill rolling". During sleep and action, the resting tremor disappears. The number of patients with resting tremor has varied from study to study. One study found that 75% of patients have had resting tremor at some point during the course of the

disease (Hughes et al. 1993). In some patients an essential tremor has been identified prior to the diagnosis of PD, and maybe a risk factor for PD (Shahed and Jankovic 2007).

Bradykinesia is a clinical feature of PD that is characterized by slowness of movement. Patients with PD have a slower reaction time that worsens with progression of the disease, although it has been suggested that this maybe attributed to slowness for executing motor commands. Slowness of movement is likely attributed to muscle weakness, tremor, and rigidity, but the principal cause is insufficient recruitment of muscle force (Berardelli et al. 2001), likely due to effects on the basal ganglia during the course of the disease.

Rigidity is one of the earliest manifestations of PD, specifically pain in the shoulder and is characterized by increased resistance in movement of limbs (Jankovic 2008).

Postural instability is often seen in the late stages of PD, and is the most common cause of falls in patients. This clinical feature is characterized by instability/impairment of balance, a feature that can be tested using the pull test. During the pull test a patient is pulled forward or backward by the shoulders, and the number of steps taken is measured. Absence of a response, or more than two steps backwards are indicative of an abnormal postural response (Jankovic 2008).

Freezing is characterized by loss of movement (akinesia), but is not seen in all patients. There are various forms of freezing including, start hesitation, turn hesitation, and open space hesitation. For most patients with freezing, the legs are affected while walking, but the arms and eyelids may also be affected (Jankovic 2008). Risk factors for freezing include rigidity, bradykineasia, postural instability, and age of onset. To overcome freezing, patients can use tricks such as marching to command, stepping over objects, or walking to music (Jankovic 2008).

Pathology

PD is characterized by the loss of dopaminergic neurons in the substantia nigra pars compacta (SN). The SN is located in the midbrain and is part of the basal ganglia. The SN is characterized by a darkened area of the basal ganglia due to the presence of neuromelanin and is composed of two parts, the pars compacta and pars reticulata. The pars reticulata along with the globus pallidus serves as the main output for the basal ganglia (Deniau et al. 2007). The pars compacta's role in behavior and movement appears to be complex. It is the site of a large population of dopaminergic neurons which are involved in behavior, addiction, and motor activity (Hodge and Butcher 1980); more specifically fine motor movements (Pioli et al. 2008). During the course of PD, dopaminergic neurons are lost in the SN, although the cause of this loss is not well understood.

The pathological hallmark of PD is the Lewy body. These neuronal inclusions are found in neurons of the SN, locus coeruleus, dorsal vagal nucleus, and in several other areas in the brain (Gibb and Lees 1988). Lewy bodies are eosinophilic intracytoplasmic inclusions, characterized by a round shape surrounded by a halo. The primary structural component of the Lewy body and Lewy neurite is the synaptic protein, α-synuclein (α-syn) (Spillantini et al. 1997; Spillantini et al. 1998), but more than 70 other molecules have been identified including tau, synphilin, and components of the ubiquitin proteasome system (Olanow et al. 2004; Wakabayashi et al. 2007). The presence of Lewy bodies has been associated with an increase in neurodegeneration specifically in the SN (Gibb and Lees 1988) but more recently, in other regions of the nervous system (see below). Additionally, Lewy neurites, which are found early in the disease process, have been found to disrupt axonal transport function and may affect survival (Volpicelli-Daley et al. 2014).

The role and effect of Lewy bodies in PD is not well understood. Prior to the discovery of α-syn as the major component of Lewy bodies, they were associated with neurodegeneration as Lewy bodies were found in places of neurodegeneration, and Lewy body cortical density was found to correlate with cognitive impairment in PD (Wakabayashi et al. 2007). More recently it has been suggested that Lewy bodies are not harmful to the cell (Tompkins and Hill 1997), and may actually act as an aggresome to sequester proteins like α-syn, and protect against their neuronal toxicity (Olanow et al. 2004; Tanaka et al. 2004).

Genetics:

α-syn Mutations

Mutations in the SNCA gene (PARK1-4), were the first to be associated with autosomal dominant forms of Parkinson's disease. One of the first mutations was discovered via linkage analysis of an Italian family (Polymeropoulos et al. 1997), on human chromosome 4q21-q23, where α-syn had previously been mapped. The A53T (change of Alanine to Threonine at position 53) variant is one of the most frequent of the missense mutations for α-syn, having been identified in several families worldwide (Choi et al. 2008; Polymeropoulos et al. 1997; Puschmann et al. 2009; Spira et al. 2001). The other missense mutations A30P (change of alanine 30 for proline at position 30) and E46K (change of glutamic acid for lysine at positing 46) have been identified in one family each, but present similar pathology and symptoms to A53T (Kruger et al. 1998; Zarranz et al. 2004). In the case of all of these variants, it appears that structure of α-syn is altered due to the missense mutations, and leads to increased filamentous forms of α-syn and increased distribution of α-syn pathology.

Alterations in gene dosage of α-syn further suggest that a principal cause of PD is demonstrated by genetics. Gene duplication of α-syn has been found in several

families, which presented clinical features typical of idiopathic PD, including age of disease onset (between ages 46-50) as well as response to treatments with levodopa (Chartier-Harlin et al. 2004; Ibanez et al. 2004). Interestingly in cases of patients with gene triplication of PD, the age of onset was approximately 10 years earlier, and the progression of the disease was faster, more severe, associated with dementia and hallucinations (Ibanez et al. 2004), and characterized pathologically by severe neuronal degeneration in the SN and locus coeruleus along with the formation of Lewy bodies throughout the brain (Farrer et al. 2004).

Additionally, alterations in the α-syn promoter have been associated with an increased risk for PD. Specifically, polymorphisms in the REP-1 promoter have been associated with increased risk for α-syn in several studies (Hadjigeorgiou et al. 2006; Maraganore et al. 2006; Myhre et al. 2008; Rajput et al. 2009).

LRRK2 Mutations

Mutations in the Leucine-Rich Repeat Kinase 2 (LRRK2; PARK8) gene have been associated with increased risk for PD. The LRRK2 gene is important for formation of the protein dardarin, which is involved in assembling the cellular cytoskeleton and in protein-protein interactions. Most patients with mutations in LRRK2 have been found to present pathology similar to idiopathic PD (i.e. neurodegeneration in the nigra and the presence of Lewy bodies) (Gilks et al. 2005; Rajput et al. 2006; Zimprich et al. 2004), however, a case without Lewy body inclusions has been previously identified (Gaig et al. 2007). The most common LRRK2 mutation found among patients is the G2019S mutation. This mutation has a large prevalence in Ashkenazi Jews and North African Arabs with PD, as high as 18.3% and 47% respectively (Lesage et al. 2006; Ozelius et al. 2006). The LRRK2 G2019S mutation was the first to demonstrate that a genetic determinant can be involved in sporadic forms of PD (Bonifati 2006).

Parkin and PINK-1 Mutations

Mutations in Parkin (PARK2) are the most common cause of early onset PD. Parkin is an E3 ubiquitin ligase involved with degradation of soluble proteins via the ubiquitin proteasome system (UPS). The Parkin mutation was first identified in a Japanese patient with autosomal recessive juvenile PD (Kitada et al. 1998), and may account for as much as 50% of cases in families with early onset PD (Lucking et al. 2000). Mutations in PINK-1 (PARK6) are the second most common cause of early onset PD. The PINK-1 gene encodes a mitochondrial serine/threonine kinase, and loss of function of PINK-1 is associated with early onset PD. Previous studies have demonstrated that PINK1 and Parkin are associated with the mitochondria and cytosol respectively, but both are important in maintaining and regulating mitochondrial structure and function (Clark et al. 2006; Greene et al. 2003; Park et al. 2006). Clinically, patients with Parkin and PINK1 mutations are indistinguishable from cases of sporadic PD (Abbas et al. 1999; Schneider and Klein 1993). Interestingly, neuropathology of patients with Parkin and PINK1, specifically the presence of Lewy bodies in patients with Parkin mutations, appears to vary (Farrer et al. 2001; Houlden and Singleton 2012; Pramstaller et al. 2005). Additionally, the connection between Parkin/PINK1 mutations and their interaction with α-syn remains unclear (Oliveras-Salva et al. 2014; Stichel et al. 2007; von Coelln et al. 2006).

Mutations in DJ-1 have been found to cause autosomal recessive PD. Mutations in the gene were first identified in Dutch and Italian families, and later found in patients with early-onset PD. DJ-1 appears to have a role in many cellular processes, but with regards to PD, there appears to be an association with parkin and oxidative stress (Bonifati et al. 2003; Martinat et al. 2004; Meulener et al. 2006). DJ-1 has been found to associate with parkin (specifically parkin binding to monomeric DJ-1), and decreased

levels of DJ-1 have been observed in patients with autosomal recessive PD compared to patients with sporadic PD (Moore et al. 2005). DJ-1 appears to have a role in oxidative stress response, specifically protection against oxidative stress. In a study in which MPTP, which increases ROS through inhibition of complex I, was administered to DJ-1 knockout mice, increased striatal denervation and dopaminergic neuron loss was observed (Kim et al. 2005). The connection between DJ-1 and α-syn is unclear, but it appears that DJ-1 associates with α-syn in patients with PD (Meulener et al. 2005). *In vitro* knockdown of DJ-1 was associated with an increase in insoluble α-syn, suggesting that DJ-1 may serve as a chaperone to α-syn (Shendelman et al. 2004).

Mutations in genes involved with protein degradation have also been associated with increased risk for PD. Ubiquitin Carboxyl-Terminal Esterase L1 (UCHL1) is a enzyme that is involved with degradation and recycling of ubiquitin after proteasome degradation of proteins (this protein is discussed below). Another enzyme involved with degradation is the glucocerebrosidase enzyme (GBA). Mutations in GBA are found in individuals with Gaucher's disease, an autosomal recessive disorder in which there is a deficiency of a lysosomal enzyme (glucocerebrosidase). Interestingly, parkinsonism has been found to be associated with many patients with Gaucher's (Goker-Alpan et al. 2004). Studies that have examined loss of GBA function *in vitro* and *in vivo* have found that α-syn aggregates and causes toxicity (Kong et al. 2013; Mazzulli et al. 2011). Further, this is likely related to dysfunction in autophagy, a degradation pathway based on lysosomal degradation that has been implicated in PD (Du et al. 2015; Manzoni and Lewis 2013).

Studies of genetic mutations associated with PD have been invaluable for the PD field. Understanding the mechanisms by which these genetic mutations cause PD, have given great insight into the pathways that maybe altered in sporadic cases of PD. Specifically, the identification of α-syn has provided a target to understand and study

further. Identification of these pathways through genetic mutations has and will continue to provide an opportunity to better understand the etiology of PD, and an opportunity for the development of therapeutics that can help fight the effects of the disease.

α-synuclein characteristics

α-syn is a 140 kD cytosolic protein that is composed of three regions, an amino terminus, a central hydrophobic region (referred to as NAC), and a carboxyl terminus. α-syn is one of three synucleins in the synuclein family (Stefanis 2012). The protein was first identified in a screen of Torpedo electric lobe cDNA library using an antibody against purified cholinergic synaptic vesicles (Maroteaux et al. 1988). Interestingly, α-syn (specifically the NAC region) was not initially identified in PD patients, but rather as a component of amyloid plaques from Alzheimer's disease patients (Ueda et al. 1993). α-syn is expressed widely throughout both the central and peripheral nervous system, however, it can be found outside of the nervous system, in places such as red blood cells and plasma (Barbour et al. 2008). Although α-syn has been identified in synaptic vesicles, its function in neurons is not well understood. Studies have suggested that the protein is involved with regulation of neural plasticity as well as neurotransmitter release and synaptic development (George et al. 1995; Withers et al. 1997). Support for α-syn's role in neurotransmitter release has been demonstrated in several animal models. Knockdown of α-syn in rodent models resulted in a decrease in striatal DA, a decreased response to amphetamine (A Abeliovich et al. 2000) and alterations in dopamine and norepinephrine storage capacity and release, further supporting α-syn's role in synaptic vesicle release (Yavich et al. 2004; Yavich et al. 2006). However, other studies have found that α-syn is not essential for neurotransmitter release or synaptic plasticity, but rather, is involved with long-term regulation and maintenance of presynaptic function

(Chandra et al. 2004). Although the function of α-syn is not well understood, it appears to have a fundamental role in the etiology of PD.

Animal models of α-syn

Several animal models have been generated to study the effects of α-syn's toxicity *in vivo.* One of the first animal models of α-syn overexpressed human wild type (wt) α-syn in mice under the regulatory control of the platelet-derived growth factor-β promoter. α-syn was found to accumulate (as cytoplasmic inclusions) over time in several regions of the mouse's brain including the SN (Masliah et al. 2000). Additionally, the group found that expression of wt α-syn resulted in a loss of dopaminergic neurons (as measured by TH levels), and correlated with alterations in motor behavior. Several other studies have also shown that expression of α-syn in rodent models leads to aggregation of synuclein, alterations in dopamine modulation, α-syn accumulation, loss of dopaminergic neurons, and motor deficits (Chesselet et al. 2012; Lam et al. 2011; Rockenstein et al. 2002). Further, studies have used rodent models to study mutated forms of synuclein, including A53T and A30P. Similar to mice expressing wt human α-syn, mice expressing mutant forms of α-syn (not all models demonstrated the same phenotype) have decreased dopamine levels, motor deficits aggregation of synuclein, and dopaminergic cell loss (Martin et al. 2006; Piltonen et al. 2013; Plaas et al. 2008; Zhou et al. 2008).

The effects of α-syn's toxicity have also been observed in other *in vivo* models. In C. elegans, α-syn was able to form aggregates, and caused a decrease in motility and lifespan of the worms (Bodhicharla et al. 2012). Feany et al. generated transgenic drosophila expressing wt α-syn, A30P, or A53T. They found that expression of any of the variants of α-syn resulted in a loss of TH positive neurons. Additionally, not all dopaminergic neurons were susceptible to α-syn toxicity, and that transgenic drosophila

expressing the A30P variant had quicker loss of climbing ability (measure of motor behavior) as compared to the A53T and wt variants. Interestingly, similar to the rodent models, α-syn was found to form inclusion bodies, reminiscent of human Lewy bodies, in drosophila (Feany and Bender 2000). Similarly in zebrafish (ZF; *Danio rerio*), overexpression of α-syn in developing embryos was found to cause an increase in neuronal toxicity as well as aggregation of α-syn in developing neurons (Prabhudesai et al. 2012).

Native state of α-syn

The native form of α-syn has been a topic of great debate in the synuclein field. Studies using NMR spectroscopy have found that the protein lacks tertiary structure, is unfolded, and is approximately 19kDa as measured under denaturing conditions by immunoblot (Eliezer et al. 2001; Weinreb et al. 1996). Further, α-syn in patients with PD, AD, and DLB was found to be 16kDa when measured under denaturing conditions by immunoblot (Campbell et al. 2000). Other studies have suggested, that α-syn exists not as a monomer, but rather as a stable oligomer (tetramer) that resists aggregation (Bartels et al. 2011; W Wang et al. 2011). However, this finding was recently contested by another group, which found using various molecular techniques (including both denaturing and non-denaturing immunoblot conditions) that α-syn in mouse, rat and human brains exists as an unfolded monomer, which can explain the proposed tetramer sizing (Fauvet et al. 2012). It is well accepted that α-syn native state is dynamic under both normal and pathological conditions. Its conformation and state of aggregation depends on several factors including relationship to membranes, post-translational modifications, concentrations, oxidative state and the presence of chaperones and toxins.

The spread of α-syn

Distribution and spread of α-syn and Lewy bodies throughout the brain has only recently been investigated. Braak and colleagues assessed the regional distribution of α-syn in the brains of patients with PD and developed a staging scheme. The Braak staging scheme (Braak model) suggests that the disease begins in the lower brain stem and olfactory bulb. The disease then ascends through the dorsal motor nucleus of the vagus nerve through several regions of the brain, before eventually reaching the cerebral cortex (Braak et al. 2003). This is consistent with PD patients having cortical atrophy in olfactory-related brain regions as well as general olfactory dysfunction (Doty et al. 1988; Ward et al. 1983; Wattendorf et al. 2009). The Braak model is dependent on Lewy body pathology not being random, which Braak and colleagues have supported by describing neurons which are susceptible to forming Lewy bodies (Braak and Braak 2000). The Braak model also makes the suggestion that the pathogenic process of α-syn starts with environmental insults that enter the central nervous system (CNS) through the gastric system. Again, similar to olfactory dysfunction, gastrointestinal dysfunction and Lewy body pathology have been observed in patients with PD (Braak et al. 2006; Lebouvier et al. 2008; Pfeiffer 2003; Shannon et al. 2012). One of the larger implications of the Braak model is that α-syn maybe functioning as a prion. In the 90's, several PD patients received fetal ventral mesencephalic transplants (fetal nigral transplant), to mitigate the loss of striatal dopamine. Over the course of the study, patients who received the transplant had an increase in striatal dopaminergic activity, however, approximately half the patients developed dyskinesia (Freed et al. 2001; Olanow et al. 2003). Further, in some patients who passed away years after the procedure, Lewy body like pathology was found in the grafted neurons; suggesting that α-syn had spread to the transplanted region (Kordower et al. 2008; Li et al. 2008).

Several *in vitro* and *in vivo* studies have given further support to the theory of α-syn acting as a prion. One *in vitro* study demonstrated that fibrils and not monomeric α-syn, when introduced *in vitro,* seeded the formation of Lewy body-like inclusions. This study also found that soluble α-syn (monomeric forms) were recruited into inclusion bodies by fibrils, suggesting that fibrillar α-syn can recruit and convert soluble α-syn into a misfolded state, and later growth into inclusion bodies. This effect is not limited to wt α-syn, as it was shown that seeding wt α-syn fibrils with A30P seeds, led wt α-syn to accelerate formation of their fibrils similarly to A30P fibrils (Yonetani et al. 2009). Further, it was demonstrated that α-syn fibrils could transfer from neuron to neuron via axonal transport (Freundt et al. 2012). In an *in vivo* study, Luk et al. found that wt mice given a single instrastriatal inoculation of α-syn had Lewy pathology throughout the brain, and loss of dopaminergic neurons (Luk et al. 2012). In another study using transgenic α-syn mice, brain homogenates were injected from older transgenic mice exhibiting α-syn pathology, into younger transgenic mice. The younger transgenic mice injected with the homogenates formed inclusion bodies faster and had reduced survival (Mougenot et al. 2012). Similarly to the grafting studies performed in patients with PD, when mesencephalic neurons from wt mice were grafted into the striatum of mice overexpressing human α-syn, aggregation of α-syn was found in wt grafted dopaminergic neurons (Hansen et al. 2011). Additionally a recent study found that low dose exposure to a pesticide, rotenone, can cause accumulation of α-syn, which can be taken up and released by other neurons (Pan-Montojo et al. 2010). Interestingly when the same group performed a hemivagotomy and partial sympathectomy, the spread of synuclein was prevented, and dopaminergic cell toxicity was reduced (Pan-Montojo et al. 2012). These studies add further support for the theory that α-syn may act as a prion.

Most recently a Danish epidemiological study has further supported the Braak model. They found that patients who underwent a full truncal vagotomy (division of main

trunk of vagus), had a decreased risk for PD as compared to controls (Svensson et al. 2015). Despite some important limitations to this study, their data suggest that α-syn can act as a prion and spread throughout the brain and form Lewy body like inclusions in *in vivo* models and human brains.

Toxicity of α-syn

One of the most researched and discussed topics in the synuclein field, is which form of α-syn is most toxic, the monomer, oligomer, or fibril? In its native form α-syn does not appear to be toxic, and has a role in synaptic vesicle release as discussed above. Studies suggest that it is possible that post translational modifications, presence of metal ions, oxidative stress, and even dopamine itself may cause α-syn to aggregate (Conway et al. 2001; Hashimoto et al. 1999; Uversky et al. 2001). Although, aggregates and Lewy/inclusion bodies are the pathological hallmark of PD, which may suggest that they maybe involved in the toxicity of α-syn, several studies have demonstrated that they maybe protective. Tanka et al. reported that the presence of α-syn aggresomes protected cells from apoptosis (Tanaka et al. 2004). This maybe the case because through the formation of inclusion bodies, smaller aggregates of α-syn are removed from the presynaptic terminals (accumulation of α-syn is associated with loss of dendritic spines) and the accessible toxic surface of the protein is reduced as compared to smaller aggregates (Kramer and Schulz-Schaeffer 2007). Formation of fibrils/aggresomes/inclusion bodies may also promote the degradation of aggregated proteins through the protein degradation pathway, autophagy (Bieschke et al. 2010; Iwata et al. 2005a; Iwata et al. 2005b; Ravikumar et al. 2002). However, there is other evidence to suggest that α-syn inclusion bodies actually resist degradation via autophagy and may impair the degradation pathway (Tanik et al. 2013).

Although all the modifications listed above may cause synuclein to aggregate and form fibrils, it is interesting that protofibrils/oligomers may be the actual cause of toxicity. *In vitro* studies have demonstrated that oligomeric forms of α-syn can cause cytotoxicity. In one study, one form of α-syn entered cells and seeded intracellular α-syn aggregation, while a second form that did not enter the cell, acted on the cellular membrane and increased intracellular calcium levels. Association with the cellular membrane may alter calcium homeostasis. The second form of α-syn appeared to act at the cellular membrane to increase intracellular calcium levels (Danzer et al. 2007), an effect which has also been observed in transgenic synuclein mice (Reznichenko et al. 2012). Alterations in intracellular calcium homeostasis may be attributed to the ability of profibrils forms of α-syn creating pores in the cellular membrane (Lashuel et al. 2002; Volles et al. 2001; Volles and Lansbury 2002). This is further supported by the fact that the sizes of α-syn fibrils found in the *in vitro* study discussed above were similar to those extracted from patients with multiple-systems atrophy (Pountney et al. 2004). The toxicity of the oligomer is complex, but maybe attributed to stabilization of α-syn. In one study use of the BiFC (bimolecular fluorescence complementation) assay suggested that when α-syn was stabilized, the half-life of the protein and its cytotoxicity increased. Additionally, overexpression of the molecular chaperone HSP70 (which is associated with autophagy and acts on high molecular weight species), protected against stabilized oligomeric α-syn's toxicity in this study (Outeiro et al. 2008). *In vivo* studies of oligomeric α-syn have shown similar results to those *in vitro*. Winner et al. investigated the use of different forms of α-syn, including, wt α-syn, oligomeric mutants and fibrilar forms in mice. Oligomeric forms of α-syn caused a significant increase in dopaminergic cell toxicity, as well as alterations in neuron morphology consistent with axonal pathology seen in PD. The experiments repeated *in vitro* demonstrated a similar result, the oligomeric forms increased toxicity as compared to wt and fibril variants. Additionally, the

oligomeric forms of α-syn formed ring like structures, which were found to associate with liposomes, suggesting association with membranes and further, modulation of calcium homeostasis (Winner et al. 2011). Rockenstein et al developed a mouse model based on the same oligomeric variant as Winner et al. (Rockenstein et al. 2014). Many of the effects observed in this transgenic model recapitulate results in other studies of oligomeric α-syn including association with membranes (and further possible alterations in calcium signaling), and neuronal toxicity. Although several studies have demonstrated the association of oligomers and α-syn toxicity, a recent study has suggested that monomeric synuclein resulting from destabilization of a stable form of synuclein may be the actual cause of toxicity. In mice with the A53T mutation, a decrease in the ratio stable α-syn tetramer (as proposed by the group) to monomer vs. wt α-syn mice was observed. Additionally, Dettmer et al. found that neurons expressing the E64K PD mutation found a larger change in the tetramer/monomer ratio, and increased neuronal toxicity (Dettmer et al. 2015).

α-Syn Degradation

Within the cell there are two primary degradation pathways by which α-syn is processed. The first is the Ubiquitin Proteasome System (UPS). The UPS is responsible for degradation of most proteins in the cells, including those associated with cell growth factors, transcriptional regulators, development, apoptosis, those that have become damaged, mislocated, and misfolded (Hershko and Ciechanover 1998). The UPS is composed of two components the 19S and 20S proteasomes, making up the 26S proteasome, which is responsible for degradation of proteins. The process of degradation by the proteasome begins with proteins being tagged with ubiquitin for degradation. The process of ubiquitination occurs via three ubiquitin activating enzymes, E1, E2, E3 (Hershko et al. 1983). Following ubiquitination, the protein undergoes

proteolysis in the 26S proteasome, and the resulting peptides are released, and ubiquitin is debiquitinated by deubiquitylating enzymes like UCHL1 (Lim and Tan 2007). Monomeric ubiquitin can then reenter the UPS and continue the degradation cycle.

Proteasome dysfunction in genetic cases of PD is well documented. UCHL1 has previously been identified as a susceptibility gene for PD (Facheris et al. 2005; Maraganore et al. 2004). Parkin is an E3 ligase, which has also been implicated as a susceptibility gene for PD as discussed above, however, proteasome dysfunction is not limited to genetic cases of PD. McNaught et al. demonstrated that enzymatic activity of the proteasome is impaired in the SN of patients with PD (McNaught and Jenner 2001). In a later study the same measured the integrity and enzymatic activity of the 26S/20S proteasome in the brains of patients with sporadic PD. They found that the structures of the 26S/20S proteasome were altered in patients with sporadic PD, specifically alterations in the secondary structure that could affect proteolytic activity. In line with alterations in structure of the proteasome, they found a significant decrease in proteolytic activity of the 20S proteasomes (McNaught et al. 2003).

α-Syn appears to have a role in dysfunction of the proteasome. Both monomeric and aggregated forms of α-syn have been found to bind with the 19S proteasome and inhibit the function of the 26S proteasome (Snyder et al. 2003). Further oligomeric forms of α-syn have been found to interact with the 20S proteasome, and cause inhibition of its proteolytic activity (Lindersson et al. 2004). Tanka et al found *in vitro*, that cells expressing mutant α-syn had decreased proteasome activity, and when treated with a sub-toxic concentration of lactacystin (proteasome inhibitor), an increase in markers of apoptosis and inhibition of mitochondrial depolarization occurred (Tanaka et al. 2001). Additionally, Stefanis et al. found that the A53T mutant form of synuclein caused decreased proteasome activity, and increased neuronal toxicity (Stefanis et al. 2001). Chou et al. found that in primary culture a pesticide, ziram, inhibited E1 ligase of the

proteasome, increased protein levels of α-syn, and increased neuronal toxicity in dopaminergic neurons (Chou et al. 2008). Additionally, other pesticides like paraquat and rotenone which have been implicated in PD, have been found to inhibit the proteasome and together with α-syn may increase toxicity (Chou et al. 2010; Yang and Tiffany-Castiglioni 2007). Degradation of α-syn by the proteasome appears to be the first method of degrading the protein, however, after it forms fibrils, it will be degraded by autophagy.

Autophagy is a process that is used by the cell to eliminate misfolded or aggregated proteins, damaged organelles, and intracellular pathogens (Glick et al. 2010). There are several forms of autophagy: chaperone-mediated autophagy (CMA), macroautophagy, and microautophagy. These will be explored in more detail in Chapter II of this thesis. With regards to α-syn and PD, the process of autophagy likely acts upon oligomers and protofibrils of α-syn. Cuervo et al. found that CMA is used for degrading α-syn (Cuervo et al. 2004). Specifically they found that heat shock protein 70 (HSP70), recognizes and binds to α-syn. Once bound to HSP70, α-syn is transported to and binds to the lysosomal-associated membrane protein type 2A (LAMP-2A) at the lysosomal membrane. α-syn is then transported into the lysosome and degraded by proteases. Interestingly the same group found that mutant forms of α-syn (A30P and A53T), were able to bind LAMP-2A stronger, but were not transported into the lysosome, and caused increased toxicity. This is similar to the result reported by Stefanis et al. where A53T caused an increase in autophagosome formation, but also an increase in cell death suggesting lysosomal dysfunction (Stefanis et al. 2001). Further Martinez-Vincente et al. found that oligomeric forms of α-syn and α-syn modified by DA could not be taken up by lysosomes via CMA. In brains of patients with PD, post mortem analysis found autophagic degeneration (condensation of chromatin and an increase in lysosome-like vacuoles, likely autophagosomes) in melanized DA neurons (Anglade et al. 1997).

The Environment and PD.

As discussed above, as much as 10% of PD cases can be attributed to Mendelian genetics. This means that 90% of sporadic cases must be caused by the environment and/or gene-environment interactions. One of the first examples of an neurotoxin causing PD like symptoms was MPTP (1-methyl-4-phenyl-1,2,3,6-tetrahyrdopyridine). In the early 80's several heroin users, used MPTP as a synthetic heroin, which resulted in a Parkinsonian-like state (Smeyne and Jackson-Lewis 2005). Prior to the discovery of MPTP, there were very few animal models for studying the effects of PD. *In vivo*, MPTP causes loss of dopaminergic neurons and alterations in motor behavior (Jenner 2003; Kopin and Markey 1988; Yazdani et al. 2006). MPTP is converted by monoamine oxidase-B (MAO-B) to MPP+, which is taken up by the Dopamine transporter (DAT), the cause of its selectivity for DAergic neurons. MPP+ is an inhibitor of complex-1 cellular respiration, resulting in a decrease in cellular ATP, and an increase in oxidative species (Chan et al. 1991; Nicklas et al. 1985; Przedborski and Jackson-Lewis 1998; Zang and Misra 1993). Identification and understanding of MPTP's mechanism of action was important in finding other environmental compounds that have a similar structure and can increase risk for PD.

For several decades epidemiological studies have suggested a correlation between exposure to pesticides and PD. Studies that have examined both occupational and residential exposure have found that pesticides can increase risk for PD (Ascherio et al. 2006; Fleming et al. 1994; Gatto et al. 2009; Hertzman et al. 1990; Ritz and Yu 2000; Tanner et al. 2009; Tanner et al. 2011; A Wang et al. 2011). Although several of the earlier studies were self-reporting, more recent studies in California have used the pesticide use reporting system and independent physician verification of cases to study the correlation between PD and pesticide exposure. Wang et al. found that individuals

exposed to three pesticides, paraquat, ziram, and maneb at the work place had a three fold increased risk for developing PD, and for residential exposures an 80% increased risk for exposure to those three pesticides (A Wang et al. 2011).

The connection between PD and pesticides has been further strengthened using *in vitro* and *in vivo* models. Many of these models have demonstrated the loss of dopaminergic neurons after treatment with pesticides and alterations in motor behavior in animal models (Betarbet et al. 2000; Chou et al. 2008; Fitzmaurice et al. 2013; Peng et al. 2004; Ryan et al. 2013; Thiruchelvam et al. 2000). The connection between α-syn and pesticides has been further supported by animal models. Betarbet et al. found that animals exposed to the pesticide rotenone had loss of dopaminergic neurons, "parkinsonian behavior", and found cytoplasmic inclusions in nigral neurons, which contained both ubiquitin and α-syn (Betarbet et al. 2000). Additionally, in a rodent model of a α-syn mutant (A53T), exposure to paraquat and maneb resulted in increased α-syn pathology throughout the CNS, specifically aggregation of filamentous α-syn in axon terminals (Norris et al. 2007). The pesticide ziram was found to cause an increase in dopaminergic cell loss, proteasome inhibition, an increase in α-syn protein levels, and motor deficits in mice (Chou et al. 2008).

Studies have suggested a link between pesticide exposure and increased risk for developing PD. It is important to note that not all pesticides cause PD, and on a larger level the use of pesticides is essential for survival especially at the rate of population growth. However, identifying and understanding which environmental toxins, such as pesticides, affect human health is crucial.

Through this dissertation I propose to study the effects of ziram, a pesticide that has been previously identified to increase risk for PD. I will study the mechanisms of ziram's toxicity using a novel *in vivo* model, ZF. Our group has previously used ZF to

study the effects of α-syn overexpression and to study the mechanisms of another dithiocarbamate fungicide that increases risk for PD, benomyl (Fitzmaurice et al. 2013). We previously studied the mechanisms of toxicity of ziram in primary culture (Chou et al. 2008), but there is great need to understand the effects and mechanisms of toxicity of the pesticide on several biological systems simultaneously *in vivo*.

The general and neuronal toxicity of ziram on ZF is examined in chapter 1. We investigate the effects of ziram on catecholaminergic neurons. Additionally, we attempt to determine if the neurotoxic effects of the pesticide are selective for dopaminergic neurons using several transgenic ZF lines, and studying the effects of ziram on motor behavior.

In chapter 2, we focus on the mechanisms of ziram's toxicity *in vivo.* Specifically we investigate whether ZF synuclein can be used to study the effects of ziram in our model, whether the proposed mechanism of ziram's toxicity is conserved in ZF, and finally if ziram's toxicity is mediated by synuclein.

The studies from this dissertation will provide better understanding of the mechanisms of toxicity of ziram in an *in vivo* system, and contribute to the understanding of how environmental toxins can contribute to the development of PD.

Chapter 1:

Introduction

Parkinson's disease (PD) is a neurodegenerative disease that affects seven to ten million people worldwide. Although significant progress has been made in understanding the pathophysiology of PD, the etiology is still not well understood. There does not appear to be one simple cause of PD.

PD and Pesticides

The genetics of PD have been studied extensively, but only account for a small percentage of patients with PD (5-10%), suggesting that environmental factors play an important role in the development of PD (International Parkinson Disease Genomics et al. 2011; Trinh and Farrer 2013). Several epidemiological studies have demonstrated that pesticide exposure correlates with increased risk for PD (Ascherio et al. 2006; Brown et al. 2006; Fleming et al. 1994; Gatto et al. 2009; Goldman 2014; Hertzman et al. 1990; Ritz and Yu 2000; Tanner et al. 2009; Tanner et al. 2011; A Wang et al. 2011).

One of the more recent epidemiological studies examined individuals who live in the central valley of California. This study was unique from other epidemiological studies because self-reporting was not used as a form of reporting. Rather, the group used California pesticide usage reports to determine individuals who lived or worked within 500m of spraying areas and pesticide exposure estimates (A Wang et al. 2011). Additionally, the group had a movement disorder specialist evaluate patients diagnosed with PD from these areas. They focused on three pesticides ziram, maneb, and paraquat, all of which had been previously found to cause dopaminergic cell death, and in the case of maneb and ziram, inhibit the proteasome (Chou et al. 2008; McCormack

et al. 2002; Purisai et al. 2007; Zhou et al. 2004). They found that occupational exposure to all three pesticides increased the risk for PD three fold, while residential exposure increased risk by 80%. Residential and workplace exposure to ziram was found to increase risk for PD three fold, and as high as six fold for early onset cases. This study demonstrated that the pesticide ziram, a known proteasome inhibitor, can increase risk for PD.

Ziram General Information

Ziram (also known as AAprotect, Cuman, Z C Spray, and Zirex) is an agricultural dithiocarbamate fungicide that is used primarily to prevent the spread of fungal infections. Ziram was first registered in the US in 1960, as a broad spectrum fungicide used to control fungus growth on several stone fruits. Since then the pesticide has been approved for use on almonds, apricots, cherries, pecans, and several other agricultural products. For residential and industrial use, ziram is approved as a rabbit repellent, and as an additive for industrial adhesives and latex paint (Agency 2004).

According to the EPA, environmental concentrations of ziram in drinking water are below the threshold of concern. Additionally, food exposure levels of ziram are considered well below levels of concern, and pose no threat to the general public. With regards to occupational and residential exposure, only occupational exposures are listed as a concern to the agency. For residential exposure, the agency recommends using ziram at lower concentrations (in the case of latex pain, reducing the concentration from 3% to 1%), and believes that homeowners who use ziram, will be exposed for less than seven days on average (Agency 2004), and thus should be at acceptable levels. Lastly the EPA specifies that the ecological effects of ziram vary greatly among species. Ziram has low toxicity for mammalian species, moderate toxicity for avian species, and high toxicity for aquatic species.

Although concentrations of ziram used for spraying vary depending on the application, the EPA estimates that for spraying applications related to agriculture, ziram is sprayed at a concentration of 8 mM.

Toxicity of Ziram

The first documented studies of ziram's toxicity, found that it has fungicidal activity at 30 μM. This is the concentration at which ziram inhibited isolated yeast mitochondrial dehydrogenases and caused toxicity (Briquet et al. 1976). *In vitro* ziram was found to cause increased cytotoxicity in rat hepatocytes at 1 mM (Yamano and Morita 1995). Additionally, the same study also found that ziram inhibited microsomal lipid peroxidation at concentrations as low as 10 μM. Chronic toxicity assays for ziram demonstrated that rats fed with low doses of ziram (5mg/kg/day) over a period of one year showed no long-term effects, and no effects were seen in weanlings also receiving the same dose over a 30 day period. Similarly, dogs fed with ziram at a concentration of 5mg/kg/day also showed no harmful effects (Hodge et al. 1956). However, one toxicity study demonstrated that female rats that were fed ziram over a 9-month period had a decrease in antibody formation, while in another study; rats exposed for an unspecified amount of time had poor growth and development (Kamrin 1997). Further, ziram induced single-strand breaks of DNA in the liver in rats (Residues 1996).

Neurotoxicity of Ziram

The number of studies that examine ziram's neurotoxicity remain very limited. One study found that in rats treated with a single high dose of ziram, behavioral effects were observed, and inhibition of brain neuropathy target esterase was observed. In a study conducted in our lab, mice treated with sodium dimethyldithiocarbamate (used

instead of ziram, because of higher solubility), for two weeks altered motor function, similar to mice that have dysfunction of the nigrostriatal pathway (Chou et al. 2008).

Ziram and Dopaminergic Cell Toxicity

To date there is only one piece of primary literature that has examined ziram's dopaminergic cell toxicity *in vitro* and *in vivo*. The study by our group, examined the effect of ziram on dopaminergic neurons, the ubiquitin proteasome system, and alterations in α-syn; the effects on the proteasome and α-syn will be discussed in chapter 2. In the study, rat primary ventral mesencephalic cultures were exposed to ziram at concentrations from 0.1 μM-10 μM. At higher concentrations (5μM and above), ziram was highly toxic to all cells (Chou et al. 2008). At lower concentrations, 0.5 and 1 μM, ziram was found to decrease TH+ cell survival significantly. Surprisingly, the levels of TH were actually found to be elevated after ziram treatment. Additionally, the effect of ziram was found to be specific for TH+ neurons, as determined by NeuN+ staining and compared to a control (proteasome inhibitor) that caused general neurotoxicty.

Zebrafish

In order to study ziram's toxicity further, I propose to use zebrafish (ZF) as a model system. ZF (*Danio rerio*) are a freshwater tropical fish that have been used extensively in research projects for several decades. In the early 1980's ZF were identified as a genetically tractable disease model, and later used for embryonic mutagenesis screens and identification of genes involved with development (Driever et al. 1996; Haffter et al. 1996). Due to the similarity of their genome to the human genome (Howe et al. 2013), and their value as a developmental and genetic model, ZF have allowed for greater understanding of disease across a variety of field. ZF also have several other attributes that make them valuable for studying disease. Once at sexual

maturity it is estimated that the average female gives approximately 100 eggs per clutch. This allows for experiments to be conducted with large sample sizes, and is valuable for genetic/developmental/toxicity/therapeutic screens. Secondly, ZF can be genetically manipulated in a variety of ways. Today there are several techniques to knockdown expression of genes, overexpress genes, and express genes from other species in ZF (as reviewed by (Lieschke and Currie 2007)). Recently, the opportunities for genetic manipulation in ZF have become even greater, as ZF have been found to be an excellent model to use for the CRISPR-Cas system to study human disease (Hwang et al. 2013).

ZF have been used as a model of neurodegenerative disease in several studies (Klionsky et al. 2012; Milanese et al. 2012; Paquet et al. 2009; Ramesh et al. 2010; Sheng et al. 2010; Tomasiewicz et al. 2002; Wen et al. 2008; Williams et al. 2008). ZF are a valuable model for studying the mechanisms of disease of PD as they have a well-formed DA neuronal network similar to that of mammals (Bretaud et al. 2007; Milanese et al. 2012; Schweitzer et al. 2012; Sheng et al. 2010; Wen et al. 2008; Xi et al. 2011a), have many orthologs to human drug targets (Gunnarsson et al. 2008), and alterations in homeostasis of proteins associated with PD have been found to cause similar effects in ZF (Prabhudesai et al. 2012).

Here we utilized ZF to study the toxicity of ziram, a pesticide associated with increased risk for PD, *in vivo*. To study the effects of ziram's toxicity, we conducted studies and found that the pesticide is toxic to ZF at doses well below recommended usage concentrations. Additionally, utilizing a transgenic line labeling neurons expressing vesicular monoamine transporter (VMAT2), we studied the effect of ziram on catecholaminergic neurons. We found that ziram's neurotoxicity not only causes death of neurons in clusters with high populations of dopaminergic neurons, but also that ziram's toxicity was specific for dopaminergic neurons. Finally, we analyzed the effect of ziram

on motor behavior in fish. We found that ziram caused a decrease in motor behavior under dark conditions in a similar manner to the dopamine antagonist haloperidol. This behavioral phenotype was rescued by using the postsynaptic dopamine agonist apomorphine. These studies demonstrate that ziram causes selective dopaminergic toxicity at concentrations lower than those used in the environment.

Methods

Zebrafish

ZF lines (AB unless otherwise stated) were bred and maintained at 28 °C in recirculating water tanks on a regulated 14h light/10h dark cycle and fed twice a day with brine shrimp. All experiments were carried out in accordance with UCLA Animal Research Committee protocols. ZF expressing GFP driven by the vesicular monoamine transporter promoter (VMAT2:GFP) were purchased from the UCLA core facility and used in this study to identify VMAT2 (dopaminergic, (nor)adrenergic, serotonergic) neurons in whole embryos (Wen et al. 2008). Peripheral sensory neurons (trigeminal and Rohon-Beard) were visualized using the Tg(isl1[ss]:Gal4-VP16,UAS:EGFP)^{zf154} transgenic line, which has been referred to as Tg(sensory:GFP), and were obtained from Dr. Sagasti (Sagasti et al. 2005).

Zebrafish Treatments

ZF embryos, 25-35 per treatment in 10 mL of E3 media (15 mM NaCl, 0.5 mM KCl, 1.0 mM $MgSO_4$, 0.15 mM KH_2PO_4, 0.05mM Na_2HPO_4, 1.0 mM $CaCl_2$, 0.7 mM $NaHCO_3$), were reared at 32 °C and exposed to varying concentrations of ziram (98.5% purity, Chem Service, West Chester PA). Embryos were exposed to 1 nM-1 μM (0.01%DMSO) ziram in E3 media at 5 hours post-fertilization (hpf) or 24 hpf in a 6-well plate for 5 days for confocal microscopy and 7 days post fertilization (dpf) for behavior. Embryos treated with ziram at 5 hpf developed notochord defects as previously described (Haendel et al. 2004; Teraoka et al. 2006), so embryos were treated at 24 hpf to avoid this confound unless otherwise stated. The concentrations of ziram used for this study are well below those used for agriculture (Residues 1996) (approximately 8

mM) (Agency 2015), and necessary for fungicidal activity (30 uM) (Briquet et al. 1976).

Behavioral Analysis

ZF embryos (7 dpf) were placed in 10mL of E3 media and kept in the dark to avoid degradation of added chemicals. Drug or vehicle (5 μM apomorphine, 25 μM haloperidol or 0.1% DMSO) were added and incubated for 30-minutes at 28°C prior to behavioral analysis. Twelve fish from each treatment group were transferred to a square 96-well plate and maintained in the dark for 10 minutes prior to behavioral analysis, which consisted of 10-minute alternating cycles of light (100% light as specified by Zebralab, View Point, France) and dark (total 30 minutes in light and 30 minutes in dark). Movements greater than 2 millimeters were collected every two minutes using the Zebralab system and analyzed for distance traveled. Embryos with notochord malformations were excluded for behavioral analysis. Data were normalized to vehicle controls to account for variances between fish clutches from different days. One-way ANOVA was used for statistical analysis.

Western and Native Blots

ZF embryos (5 dpf) were anesthetized as described above, pooled (35 embryos per treatment), de-yolked, lysed, and sonicated in either 1X-SDS buffer or 1X-Native PAGE sample buffer (Life Technologies). Protein concentrations were determined using the BCA protein assay (Thermo-Fisher, Rockford IL). 75μg of protein was loaded onto SDS-PAGE or Native-PAGE gels and transferred using the XCell-II blotting system (Life Technologies). Membranes were probed with TH 1° antibody (1:2500, MAB 318: Millipore) followed by donkey anti-rabbit HRP 2° antibody (1:2500 dilution, Santa Cruz Biotechnology, Dallas TX). Chemiluminescent substrate (Super Signal West Dura,

Thermo Scientific) was used for band visualization. α-Tubulin (1:500, Sigma-Aldrich) was used as a loading control. Student's t-test was used for statistical analysis.

HPLC

ZF embryos (7dpf) were anesthetized as described above, pooled (100 embryos per treatment), de-yolked, lysed, and sonicated in 0.1 M perchloric acid. Samples were alumina gel purified and run on using a Tosoh C18 column. 15μL of samples were injected onto the column for individual runs. After the intial run, samples were spiked with DOPAL, DOPAC, and DOPAMINE to confirm retention times with standards.

Statistical Analysis

Statistical analyses were performed using Student's t-test, log-rank, and one-way ANOVA where appropriate. A minimum significance level was set at $p<0.05$ for all studies.

Results

***Ziram is toxic at low concentrations**:*

In order to determine an appropriate dose for our ziram studies in ZF, we performed a dose response study. Initially we exposed embryos to ziram early in development (5hpf) at concentrations varying from 1 nM to 1 μM. However, we found that embryos treated with doses at 50 nM and above had notochord malformations by 24hpf (Figure 1-1). This notochord malformation effect has previously been described in ZF, when other dithiocarbamates were used (Haendel et al. 2004; Teraoka et al. 2006). In order to determine the toxicity of ziram without this confound, we exposed embryos at 24hpf, a developmental time point at which the notochord is sufficiently developed. When treated at 24hpf no notochord malformation was observed even at the highest doses. Toxicity of ziram was measured over a seven-day period and by 7dpf, reduced survival was observed for ziram treated fish in a concentration dependent manner. An 80% reduction in survival was observed for embryos treated with concentrations of 100 nM or above (Figure 1-2).

Ziram is selectively toxic to dopaminergic neurons

Previous studies from our lab found that ziram was selectively toxic to dopaminergic neurons in rat primary mesecephalic cultures (Chou et al. 2008). Here we wanted to determine if ziram was neurotoxic in our ZF model system, and if ziram is selectively toxic to dopaminergic neurons. We utilized a VMAT2:GFP ZF line that expresses GFP driven by the VMAT2 promoter to monitor aminergic neuronal integrity (Wen et al. 2008). We had previously utilized this line to study the neurotoxicity of

another dithiocarbamate, benomyl, and found that treatment with the pesticide in VMAT2:GFP ZF increased loss of GFP fluorescence in the diencephalic (DC), and telencephalic (TC) neuronal clusters, both of which have large populations of dopaminergic neurons (Fitzmaurice et al. 2013; R. Jeroen Pasterkamp 2009; Rink and Wullimann 2002). For this study we utilized ziram at a concentration of 50 nM, as this was the highest concentration in which no significant degree of lethality was observed. When treated with at 24hpf and imaged by confocal at 5dpf, we found that ziram treated embryos had a 30% reduction and 39% reduction in the number of GFP-labeled neurons in the TC and DC clusters respectively vs. vehicle controls (Figure 1-3). To determine if ziram's neurotoxicity is selective, we measured the integrity of Rohon-Beard neurons after exposure to 50 nM ziram using Tg(sensory:GFP) embryos as previously described (Fitzmaurice et al. 2013; Sagasti et al. 2005). We did not observe a significant change in the number of sensory neurons for ziram treated fish vs. controls (Figure 1-4). We also performed neuron counts on the Raphe Nuclei of the VMAT2 transgenic line, as these are serotonergic neurons, and did not observe a change with ziram treatment (Figure 1-5). Additionally, to further determine if the ziram is selective for dopaminergic neurons, we measured protein levels of tyrosine hydroxylase-1 (TH-1) using immunoblot analysis. A 63% reduction in TH-1 levels was found for ziram treated fish vs. vehicle controls (Figure 1-6). Collectively, these results suggest that ziram is selectively toxic to dopaminergic neurons.

Ziram alters ZF swimming behavior due to DA dysfunction

In light of the decrease in DA neuron number and TH-1 protein levels, we wanted to investigate whether the loss in dopaminergic neurons also caused a behavioral phenotype. As described above, ZF embryos were treated with 50 nM ziram at 24hpf and at 7dpf, swimming was measured. In order to study behavior we used an alternating

light and dark cycle over a one-hour period, and tracked total distance traveled by the embryos over the hour. Previous studies have suggested that ZF are more active in the dark (Burgess and Granato 2007; Farrell et al. 2011). Here we observed a similar effect for vehicle fish, while ziram treated fish swam significantly less in the dark (Figure 1-7). No change in behavior was observed for either group under light conditions. To determine if the behavioral effects observed in the dark were due to dopaminergic neuronal dysfunction, we treated embryos with a dopamine agonist and antagonist. Treatment with the dopamine antagonist, haloperidol, resulted in a significant decrease in swimming distance in the dark in a similar manner to ziram treated fish (once again no difference in distance traveled was observed in the light). When we used the dopamine agonist, apomorphine, we observed a significant increase in distance traveled for embryos (Figure 1-7). This suggests that the effects of ziram are secondary to a presynaptic dopamine loss as apomorphine rescued the behavioral phenotype of ziram treated fish. These results demonstrate the toxicity of ziram on dopaminergic neurons alters motor behavior in ZF, an effect that can be reversed using apormorphine, a drug used to treat movement dysfunction in PD patients.

Ziram does not alter levels of DA and DOPAC as measured by HPLC

Because we observed a decrease in the total amount of dopaminergic neurons and altered motor behavior for ziram treated fish, we wanted to measure levels of DA and its metabolites DOPAC and DOPAL in ziram treated fish. Previously we found that benomyl caused alterations in DOPAL levels through ALDH inhibition. DOPAL is a toxic intermediate of dopamine synthesis, and maybe the reason why ALDH inhibiting pesticides like ziram and benomyl, cause selective dopaminergic cell loss and increase risk for PD. We attempted to measure DOPAL levels in embryos but were unsuccessful.

We were able to measure DA and DOPAC levels, but did not observe any difference in levels of either DA or DOPAC for ziram treated fish vs. controls (Figure 1-8).

Discussion

The link between pesticide exposure and PD has become more evident in recent years. The identification of specific toxins that increase PD risk such as paraquat, rotenone, ziram and maneb (Gatto et al. 2009; Tanner et al. 2009; Tanner et al. 2011; A Wang et al. 2011), have facilitated mechanistic studies. Ziram has been shown to inhibit both the UPS and aldehyde dehydrogenase (ALDH) (Chou et al. 2008; Fitzmaurice et al. 2013; Fitzmaurice et al. 2014) but a direct link between these activities and neuronal toxicity *in vivo* is still lacking. In this study, we used a ZF model to study environmental toxins relevant to PD and found that ziram caused selective DA neuron damage with behavioral consequences.

Ziram is toxic to ZF at low dose concentrations

Initial toxicity studies for ZF were performed at 5 hours post fertilization (hpf). After 24 hours of exposure we observed an altered morphology for the treated fish. Fish treated with low doses of ziram (50 nM) and below, all had notochord distortion. Other groups using dithiocarbamates (DTCs) similar to ziram have observed a similar phenotype (Haendel et al. 2004; Teraoka et al. 2006). Haendel et al. reported notochord distortion by 24hpf for embryos treated with Sodium Metam at 4hpf, at a concentration of 0.8μM. This effect may be related to the metals of DTCs interacting with Cu/Zn superoxide dismutase, as common metabolites of DTCs like CS_2 did not cause notochord distortion at low doses (Tilton et al. 2006). We continued our studies at 5hpf, looking at alterations in dopaminergic cell count and behavior. This again was problematic as the notochord distortion caused a lack of movement due to severe body curvature. Additionally, this morphological confound presented problems for VMAT2 cell

counts, as more than 50% of fish had died with treatments of 50 nM ziram and above and surviving fish appeared very sick (data not shown). As a result of these issues we began dosing ZF embryos with ziram at 24hpf, a time point at which the notochord had developed sufficiently, and previous studies using DTCs did not result in notochord distortion (Haendel et al. 2004). As a result, all future studies were conducted at this time point. In order to find an appropriate dose for our studies, we treated embryos at 24hpf with five different doses of ziram (n=50 per treatment). We found that ziram caused toxicity in a dose dependent manner. By 5dpf, an increase in death was seen for fish treated with doses greater than 100 nM and by 7dpf both treatments over 100 nM had greater than 80% death. Toxicity for embryos treated with 1 nM and 10 nM was consistent with death seen in the vehicle control group. Based on this survival curve and the survival of embryos treated at 5hpf, we decided to utilize 50 nM ziram for all future studies.

Ziram causes selective dopaminergic cell toxicity

In order to study the effects of ziram on dopaminergic neurons, we utilized a transgenic line in which ZF express GFP driven by the monoamine transporter (VMAT2) promoter. Wen et al. had previously characterized this transgenic line and found that the neurotoxin MPTP caused selective loss of dopaminergic neurons in the diencephalon, hypothalamus, and pretectum (Wen et al. 2008). Additionally, the group observed a selective loss of TH, as neurons in the locus coeruleus remained GFP positive, but a reduction in TH levels was observed in these neurons. We had previously published a study examining the effects of another dithiocarbamate, Benomyl, on catecholaminergic neurons using the same transgenic VMAT2 line. We found that treatment with Benomyl caused loss of VMAT2 neurons from clusters that primarily contain catecholaminergic neurons (Fitzmaurice et al. 2013). In this study we tested ziram at a concentration 50 nM

(as discussed above) and used confocal microscopy at 5dpf to evaluate neuronal integrity. We observed a significant loss in the number of GFP positive neurons in both the diencephalic and telencephalic clusters after ziram treatment. In order to determine if this toxicity was selective to aminergic neurons, we measured the integrity of Rohon-Beard sensory (RB) neurons after exposure to 50 nM ziram using the Tg(sensory:GFP) embryos. These sensory neurons have previously been characterized extensively by several groups, and were utilized by our group to determine the specificity of benomyl for dopaminergic neurons in our previous study (Palanca et al. 2013; Patten et al. 2007; Sagasti et al. 2005). Here we found that ziram treatment did not change the number of sensory neurons for ziram treated fish vs. controls. To further characterize the specificity of ziram for catecholaminergic neurons, we performed neuron counts on the Raphe nuclei neuronal cluster (serotonergic neurons), using the VMAT2 transgenic line (Ogawa et al. 2012; Wen et al. 2008). Similar to the RB neurons, no significant difference was observed for fish treated with 50 nM ziram vs. controls. Thus we conclude that ziram's neurotoxicity is relatively specific for catecholaminergic neurons.

It is possible that the loss of GFP signal in fish treated with ziram does not reflect neuronal loss, but rather injury to the cells or loss of VMAT expression. In several animal models of PD, loss of dopaminergic neurons is associated with reduction in TH (Feany and Bender 2000; Masliah et al. 2000; Pan-Montojo et al. 2012). To determine if ziram's toxicity is specific to dopaminergic neurons, we utilized immunoblot analysis to examine the effect of ziram on TH-1 levels. We observed a significant reduction in TH protein levels for ZF treated with ziram. It is important to note that TH has been found to express in noradrenergic neurons, and thus it is possible that the decrease observed by immunoblot may not be representative of alterations in TH in only dopaminergic neurons (Holzschuh et al. 2001). However, the loss of GFP fluorescence in the diencephalic and telencephalic VMAT2 clusters combined with decreased TH protein levels, suggests that

some of this loss can be attributed to cell death. Another way to evaluate the specificity of ziram's toxicity for dopaminergic neurons is to determine the effect of the pesticide on the dopamine transporter (DAT). The sodium-dependent dopamine transporter is involved with reuptake of dopamine, and thus is involved with regulation of dopamine receptor stimulation (Ciliax et al. 1995). DAT is found throughout the brain and is found in regions of dopamine cell groups as confirmed by TH staining. In patients with PD, levels of DAT can be reduced by at least 30-50% (Ma et al. 2002; Ribeiro et al. 2002). DAT has been directly implicated in MPTP's toxicity (a toxin that causes parkinsonian like symptoms), as it is involved with uptake of transporting the toxic metabolite, MPP+ into the neuron (Chan et al. 1991; Kopin and Markey 1988; Nicklas et al. 1985; Przedborski and Jackson-Lewis 1998; Smeyne and Jackson-Lewis 2005; Zang and Misra 1993). Alterations in DAT can serve as a marker of dopaminergic cell health and in ZF can distinguish dopaminergic neurons from other catecholaminergic neurons (Holzschuh et al. 2001). There are methods to monitor DAT levels in ZF including transgenic lines, immunohistochemistry, and immunoblot (Holzschuh et al. 2001; Wen et al. 2008; Xi et al. 2011b). I hypothesize that if ziram causes specific dopaminergic cell toxicity, a reduction in DAT levels will be observed via immunoblot and immunohistochemistry. Examining alterations in DAT levels after ziram treatment may provide further evidence that ziram's toxicity is specific for dopaminergic neurons.

We used HPLC to determine if the change in TH and loss of GFP fluorescence in VMAT ZF correlated with alterations in DA levels. We did not observe a change in DA levels between ziram-treated fish and vehicle controls as measured by HPLC. This lack of change may result from compensation of the remaining dopaminergic neurons in ziram treated fish. In many reviews of PD, it is has been suggested that motor symptoms of PD first appear when about 50-70% of substantia nigra dopaminergic neurons are lost, although it maybe as low as 31% (Dauer and Przedborski 2003; Lang and Lozano

1998; Marsden 1990; Ross et al. 2004). In this study we observed a 30-40% decrease in VMAT2 neurons in the telencephalic and diencephalic clusters, which may not have been high enough to cause a change in total DA levels.

Overall, the findings that a decrease in TH and the loss of GFP fluorescence in VMAT2 clusters composed largely of dopaminergic neurons after ziram treatment, suggest that ziram's neuronal toxicity is specific to dopaminergic neurons.

Ziram alters ZF motor behavior

To further study the effects of ziram on dopaminergic neurons, we analyzed behavior of embryos treated with ziram at 24hpf. Initially we attempted behavioral studies at 5dpf, as several groups have utilized ZF at this time point and earlier. However, the swim bladder of ZF does not inflate until 5dpf, and may actually inflate several hours later for individual embryos. As a result, we moved behavioral analysis studies to 7dpf. Utilizing a light/dark cycling scheme, we monitored the distance traveled by ZF larvae over a one-hour period. Additionally, we utilized a dopamine antagonist, haloperidol, and an agonist, apomorphine, as controls to determine if the effects of ziram were presynaptic or postsynaptic. We found that ziram significantly decreased locomotion in the dark but not in the light similar to treatment with haloperidol. This decrease in activity was reversed by apomorphine suggesting that the behavioral phenotype was due to a presynaptic dopamine deficiency. These results are consistent with the apparent loss of VMAT2:GFP neurons. Less specific neurotoxins decrease locomotion in both the light and the dark and would not be expected to be completely reversed by a dopamine agonist. For future studies it will be interesting to see if clinical drugs, such as levodopa (converted into dopamine within the brain), which is used to treat the motor symptoms of PD can reverse the behavioral effects seen with ziram (Henry and Scherman 1989). A recent study used a 6-hydroxydopamine (6-OHDA),

which was previously found to cause dopaminergic cell loss (Parng et al. 2007), to study effect of the drug on ZF locomotor activity. Treatment of ZF embryos with 6-OHDA caused alterations in locomotor activity, which were reversed using the clinical drug sinemet (carbidopa-levidopa (Feng et al. 2014). If levodopa were unable to reverse the behavioral effects observed in our study, this would further suggest that the effects of ziram are presynaptic. Another way to study if the effects of ziram are presynaptic, is to use the antipsychotic drug reserpine. The drug acts by irreversibly blocking VMAT and has previously been found to cause a parkinsoninan-like phenotype in rats, and alter behavior in adult ZF (Barcelos et al. 2011; Fumagalli et al. 1999; Henry and Scherman 1989). If reserpine acts similarly in larval ZF to inhibit VMAT uptake (preventing dopamine release), we should simulate the loss of presynaptic neurons, and observe a similar behavioral phenotype to that seen with ziram. It is possible that reserpine will have off target effects on non-dopaminergic neurons as VMAT is expressed throughout the CNS, causing other changes in motor behavior (and possible survival).

Here we have demonstrated that ziram, a pesticide that has been associated with increased risk for PD, is toxic to ZF at low doses. Further we have shown that ziram's neuronal toxicity is specific for catecholaminergic and likely dopaminergic cells, an effect that can be seen in altered motor behavior of fish treated with the pesticide. Although ZF offer several advantages over other animal models when studying environmental toxins, there are a number of limitations that need to be considered. In all of our studies, we used developing embryos whereas PD is a disease of aging. Embryos were exposed at 24 hpf and formation of the blood-brain barrier begins at approximately 3 dpf (Fleming et al. 2013). Additionally, the metabolism of ziram might be different in ZF embryos compared to mammals since absorption at this early age may occur orally, dermally, or through the yolk. Despite these limitations, we believe our model is valid because the results are consistent with previous *in vivo* studies where ziram and maneb

have been shown to cause selective DA-cell loss (Chou et al. 2008; Thiruchelvam et al. 2000).

Understanding the mechanisms by which ziram causes dopaminergic cell toxicity will be invaluable for further understanding the etiology of PD. Previous studies from our lab have found that ziram inhibits E1 ligase of the ubiquitin proteasome system (Chou et al. 2008). Inhibition of the proteasome has been found previously in patients with PD (McNaught and Jenner 2001; McNaught et al. 2003), and has also been implicated in homeostasis of α-syn (Lindersson et al. 2004; McNaught et al. 2004; Stefanis et al. 2001; Tanaka et al. 2001). Several studies have suggested that pesticides can alter α-syn homeostasis *in vivo* and our group previously reported that ziram can cause α-syn levels to increase in dopaminergic neurons (Betarbet et al. 2000; Chou et al. 2008; Pan-Montojo et al. 2012; Zharikov et al. 2015). This increase in α-syn levels via proteasome inhibition, may lead to further issues with autophagy, another degradation pathway in the cell. Changes in autophagic activity have also been implicated in PD, and studies have suggested that inhibition of this pathway can lead to neuronal toxicity (Boya et al. 2005; Cuervo and Dice 1996; Cuervo et al. 2004; Gitler et al. 2008; Martinez-Vicente et al. 2008; Ravikumar et al. 2002; Tanik et al. 2013; Winslow and Rubinsztein 2011; Wu et al. 2015). It is possible that alterations in synuclein may account for the specificity of ziram's neuronal toxicity. Additionally, dithiocarbmate fungicides like ziram and benomyl have been found to cause dopaminergic cell toxicity through inhibition of aldehyde dehydrogenase (ALDH) and increase risk for PD (Fitzmaurice et al. 2013; Fitzmaurice et al. 2014). It is likely that ziram affects several different pathways within the cell, all of which when stressed can lead to cell death. For future studies, I propose to study the effect of ziram on protein degradation pathways and to determine if ziram's toxicity is mediated via synuclein.

The implications of the studies above go far beyond understanding the etiology of PD. Ziram is still actively used in the central valley of California, and yet studies of its toxicity (specifically neurotoxicity) and regulation of the pesticide remains limited. It will be important for future studies to further characterize the mechanisms and associations by which the pesticide may increase risk for PD. On a regulatory level it will be important for regulatory agencies to update toxicity labels and to update PPE guidelines for ziram, so that the general public is more aware of the possible health risks associated with the pesticide.

Figure 1-1: Treatment with ziram at 5hpf results in notochord malformation

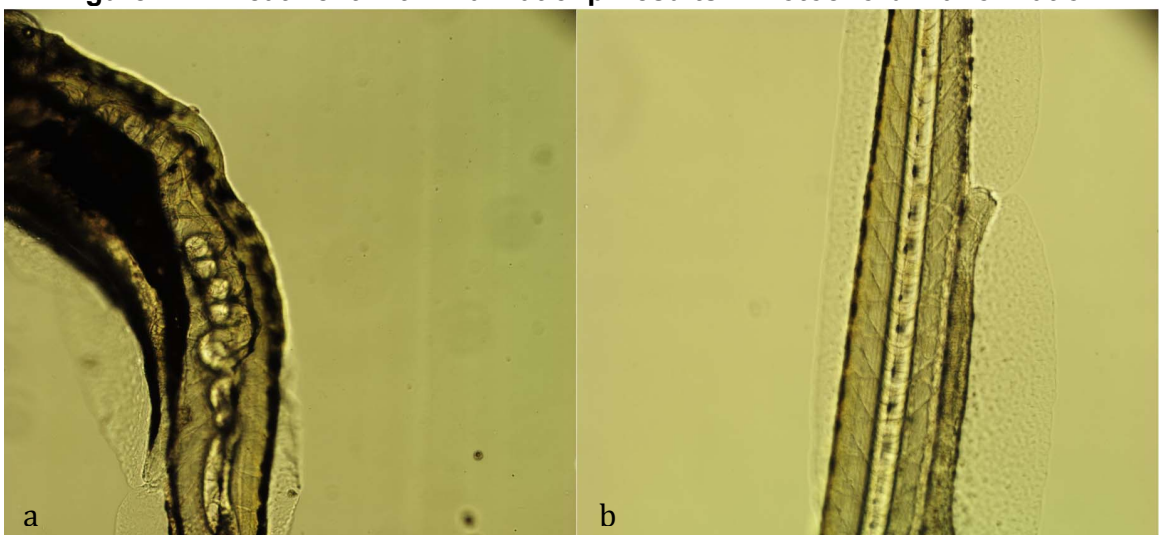

Figure 1-1: Treatment with ziram at 5hpf results in notochord malformation: For embryos treated with ziram at 5hpf, notochord malformation was observed by 24hpf(a). Vehicle treated embryos did not have this confound (b).

Figure 1-2: Ziram is toxic in a concentration dependent manner

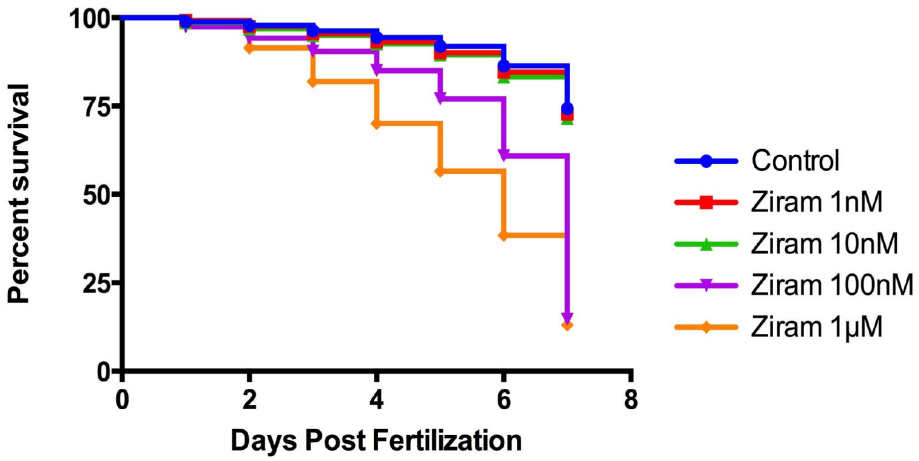

Figure 1-2: Ziram is toxic in a concentration dependent manner: ZF embryos (n=50) were treated with ziram at 24hpf, and survival was recorded over a 7-day period. For embryos treated with ziram at concentrations greater than 100 nM, survival was reduced by 80%. Log-Rank test was used for statistical analysis, $p<.0001$

Figure 1-3: Ziram is selectively toxic to aminergic neurons

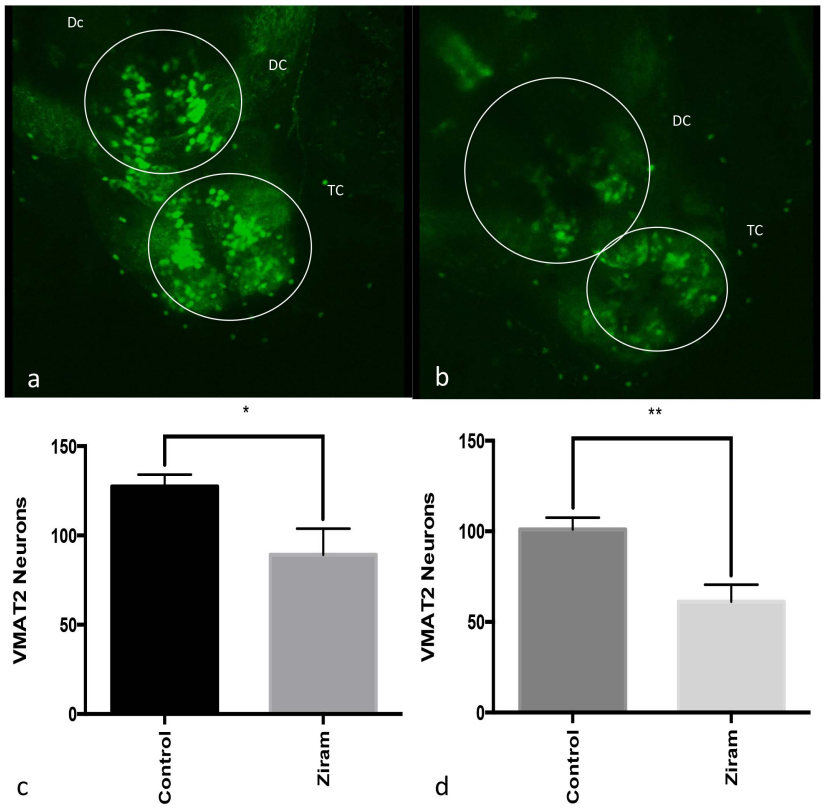

Figure 1-3: Ziram is selectively toxic to aminergic neurons
In order to study ziram's neurotoxicity in ZF**,** VMAT2 ZF embryos were exposed to vehicle (a) and 50 nM ziram (b) at 24hpf. Embryos were imaged at 5dpf via confocal microscopy, and a blinded reviewer conducted neuronal counts. A 30% decrease in telencephalic (c) and a 39% decrease in diencephalic neurons (d) were observed in ziram treated fish. n=5 per treatment. Scale bar = 500 μm. Two-tailed student t-test. *p<.05, **p<.01

Figure 1-4: Ziram is not toxic to sensory neurons

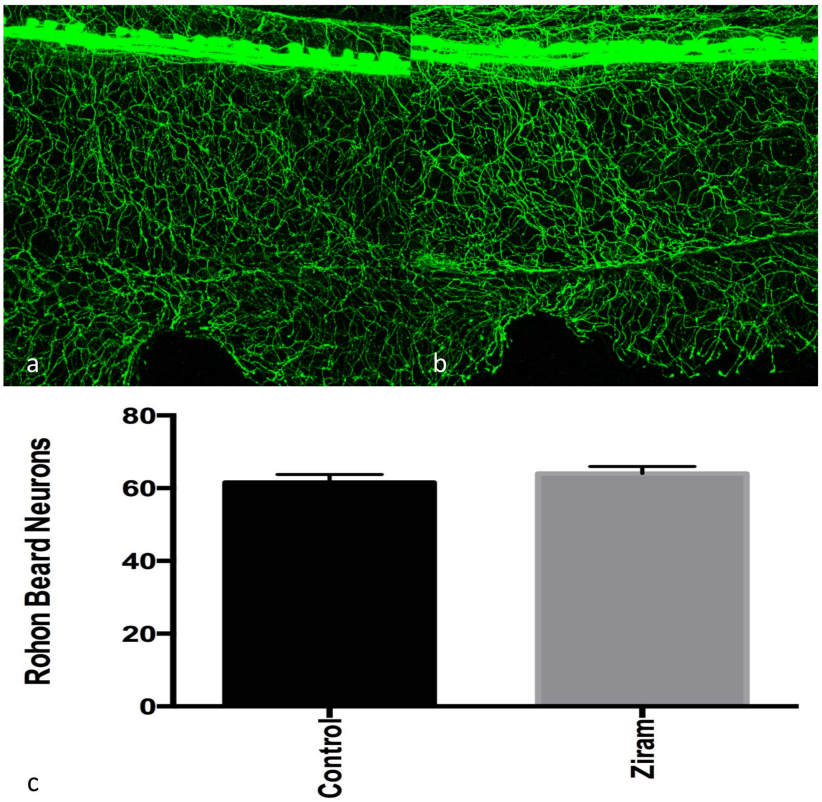

Figure 1-4: Ziram is not toxic to sensory neurons
In order to determine if ziram is selectivity toxic to aminergic neurons, we studied the effect of ziram on Rohon-Beard sensory neurons using Tg(sensory:GFP) ZF. Embryos were exposed to vehicle (a) and 50 nM ziram (b) at 24hpf. Embryos were imaged at 5dpf via confocal microscopy, and a blinded reviewer conducted neuronal counts. No significant difference in the number of sensory neurons was observed for ZF treated with ziram vs. vehicle controls. n=7 per treatment. Scale bar = 500 μm. Two-tailed student t-test.

Figure 1-5: Ziram is not toxic to serotonergic neurons

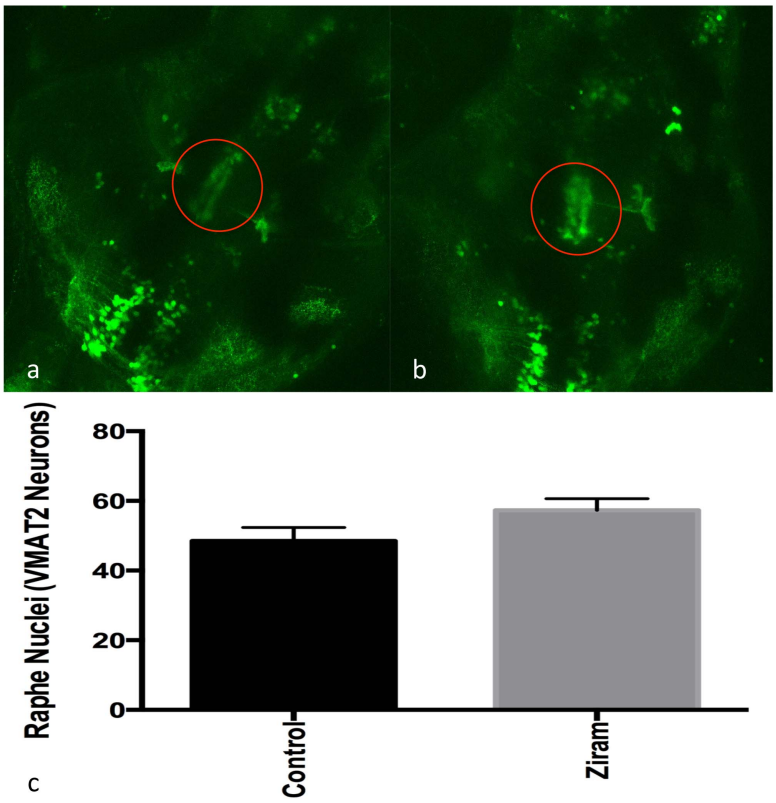

Figure 1-5: Ziram is not toxic to serotonergic neurons
To determine if ziram is selectively toxic to dopaminergic neurons, we studied the effect of ziram on the Raphe Nuclei (serotonergic neurons) in VMAT2:GFP ZF. Embryos were exposed to vehicle (a) and 50 nM ziram (b) at 24hpf. Embryos were imaged at 5dpf via confocal microscopy, and a blinded reviewer conducted neuronal counts. No significant difference in neuron counts was observed for the Raphe Nuclei for ZF treated with ziram vs. vehicle controls. n=5 per treatment. Scale bar = 500 μm. Two-tailed student t-test.

Figure 1-6: Ziram treatment results in reduction of TH-1 levels

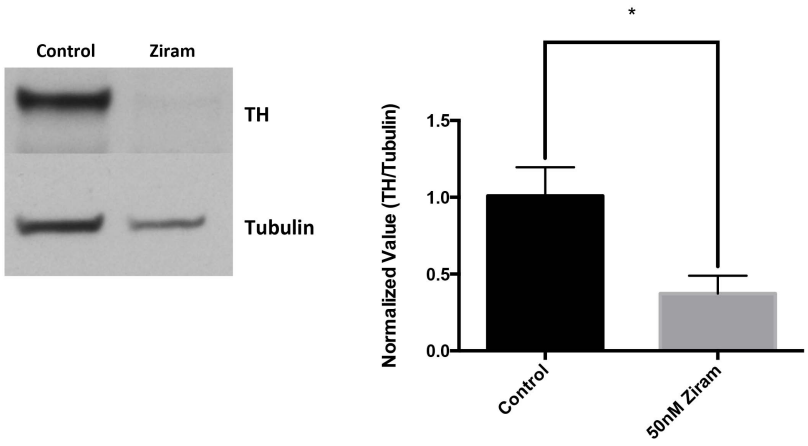

Figure 1-6: Ziram treatment results in reduction of TH-1 levels
Using western blot analysis, the effect of ziram (50 nM) on TH-1 levels was investigated. Embryos were exposed to vehicle (a) and 50 nM ziram (b) at 24hpf and protein measurements were taken at 5dpf. A 63% (*p-value = .03) reduction in TH-1 was observed for embryos treated with 50 nM ziram vs. controls (n=4). two-tailed student t-test. *p<.05

Figure 1-7: Ziram causes alterations in ZF motor behavior

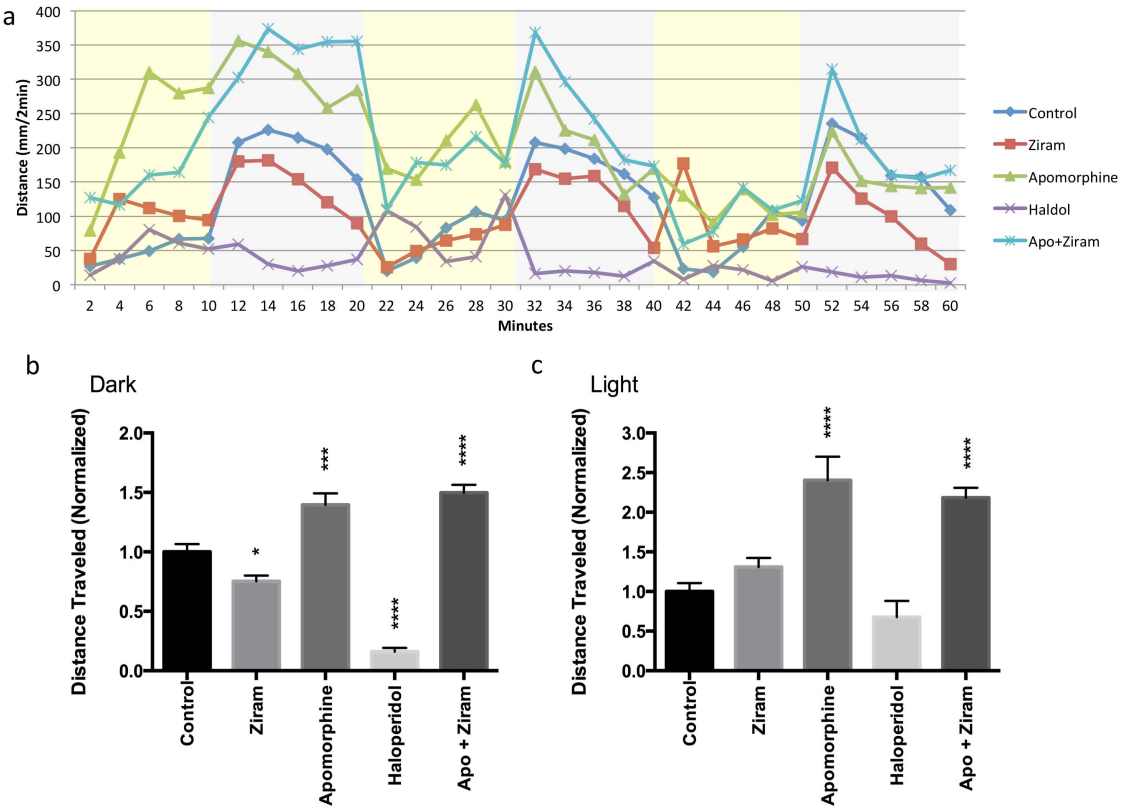

Figure 1-7: Ziram causes alterations in ZF motor behavior
ZF were treated with 50 nM ziram or vehicle at 24hpf. Movement was tracked for ZF at 7 dpf. Distance's greater than 2 mm were tracked under an alternating light (yellow)/dark cycle (grey) (a). A 24.7% decrease ($p<.05$) in distance traveled during periods of dark was observed in ziram-treated ZF relative to vehicle-treated ZF(b) but no significant difference was observed in the light (c). A similar pattern of swimming, less in the dark but no difference in the light, was measured when ZF were treated with the dopamine antagonist haloperidol (b and c). The dopamine agonist apomorphine increased swimming to a similar degree in the ziram-treated and control ZF suggesting that the post-synaptic dopaminergic system remains intact. No significant difference in motor behavior was observed for ziram + apomorphine vs. apomorphine alone for light or dark conditions. All treatment groups were compared to vehicle control for statistical analysis. n=24 per treatment. *$p<.05$, ***$p<.001$, ****$p<.0001$, one way ANOVA.

Figure 1-8: Ziram does not alter levels of DA and DOPAC

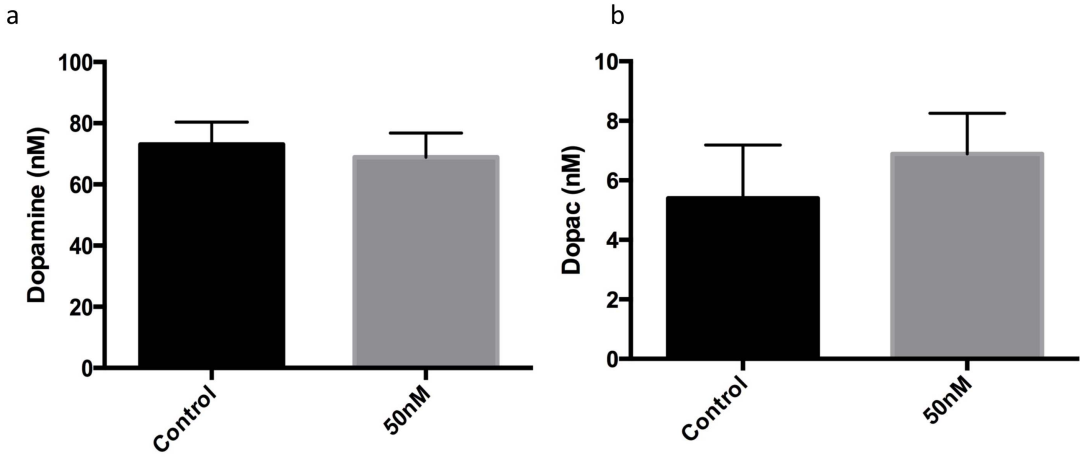

Figure 1-8: Ziram does not alter levels of DA and DOPAC
We measured levels of dopamine and DOPAC by HPLC for fish (100 fish per treatment group) treated with 50 nM ziram and vehicle at 24hpf. No significant differences in levels of DA or DOPAC were observed for ziram-treated fish vs. vehicle-treated fish. n=6. Two-tailed student t-test.

Chapter 2

Introduction

The general function of α-syn is not well understood but it appears to have a prominent role in Parkinson's disease. Several studies have examined the toxicity of α-syn *in vitro* and *in vivo* and found that oligomeric forms of the protein can be toxic to neurons. Understanding how pesticides alter synuclein homeostasis and affect cell health is important to understanding the etiology of PD and producing therapeutics.

α-syn and Pesticides:

The role of α-syn in PD is not well understood and the connection between pesticides and α-syn is even less understood. Although small, the number of epidemiological studies implicating pesticides as a risk factor for PD are strong and have continued to grow. A recent study examined a population of individuals with different mutations in the REP1 promoter (previously associated with higher risk for PD), and found that individuals with SNCA REP1 genotype (259) had an increased risk for developing PD when exposed to high levels of paraquat (Gatto et al. 2010; Hadjigeorgiou et al. 2006; Maraganore et al. 2006; Myhre et al. 2008; Rajput et al. 2009). This was one of the first epidemiological studies to show a correlation between pesticide exposure and a known α-syn mutation. A study prior to this had suggested that there was no correlation between pesticide exposure and mutations in REP1(Brighina et al. 2008), however, their data was based on self reporting for pesticide exposure, vs. the Gatto study which utilized pesticide use reports to calculate exposure data.

In vitro and *in vivo* studies have added further support for alterations in α-syn homeostasis as one of the mechanisms of neurotoxicity of pesticides. One of the first studies to demonstrate this used the pesticide rotenone *in vivo*. Betarbet et al. examined the effect of infusing rats with rotenone at doses varying from 1 to 12mg/kg. For rats exposed to rotenone, the group observed a significant loss of TH stained cells in the substantia nigra, but not the ventral tegmental area, similar to what is observed in idiopathic PD. Most interestingly, for rats that had dopaminergic degeneration, cytoplasmic inclusions were observed in nigral neurons. Further, these inclusion bodies contained ubiquitin and α-syn, the latter of which had a granular appearance similar to α-syn inclusion bodies observed in trarsngenic α-syn mice (Betarbet et al. 2000). Several studies after the Betarbet study have shown a similar effect of pesticides on α-syn homeostasis. Mice expressing the A53T mutant of α-syn (M83) and treated with paraquat and maneb were found to have an increase in α-syn pathology, specifically the amount of inclusion bodies in the brain stem, striatum, and thalamus was higher vs. transgenic mice treated without paraquat and maneb. Additionally, an increase in the amount of α-syn fibrils in axon terminals was observed for mice treated with the pesticides (Norris et al. 2007).

Another *in vivo* study found that low dose chronic exposure to rotenone caused an increase in selective dopaminergic degeneration in the substantia nigra. Similar to previous rotenone studies in rodent models, chronic exposure to rotenone at low doses resulted in cytoplasmic aggregation of α-syn in nigral neurons (Sherer et al. 2003). Most interestingly, two recent studies have suggested that chronic low dose exposure to rotenone not only induces accumulation of α-syn synuclein, but that α-syn is then released and taken up by other neurons, further suggesting that α-syn acts as prion (Pan-Montojo et al. 2010; Pan-Montojo et al. 2012). Further hemivagotomy and partial sympathectomy prevented the spread of synuclein and protected against dopaminergic

cell death in mice (Pan-Montojo et al. 2012). The implications of these studies are that environmental toxins act as an insult on the system, altering α-syn homeostasis, which can then spread as a prion and cause staging similar to the Braak model. Further this suggests that environmental toxins, specifically pesticides maybe directly causal for the spread of a toxic protein implicated in PD.

Pesticides, α-syn, and protein degradation:

Although *in vivo* and epidemiological studies have suggested that pesticides may alter α-syn homeostasis, how this occurs and why α-syn aggregates remains unclear.

The ubiquitin proteasome system (UPS) is one of the degradation pathways within the cell that is responsible for degrading misfolded proteins like α-syn. The process of degradation via the proteasome begins with ubiquitination of proteins. Ubiquitin is attached to the protein to be degraded (substrate) via several enzymes. E1,E2, and E3 (also known as Parkin) ligase(s), are involved with activation of ubiquitin via ATP reactions and for transferring ubiquitin to the substrate. E1 ligase is responsible for activating ubiquitin via an ATP reaction, generating a high-energy thiol ester intermediate as reviewed by (Ciechanover and Iwai 2004). E2 ligase then transfers the activated ubiquitin from E1 via another thiol ester intermediate to E3 ligase, which is bound to the substrate. In the final step of the reaction, E3 catalyzes the conjugation of ubiquitin to the substrate. In some cases, E4 another ligase, is involved with elongating the ubiquitin chain to a substrate. Following conjugation with ubiquitin the substrate is transferred to the 26S proteasome for degradation.

The 26S proteasome is composed of two components, the 20S, which is involved with the catalytic activity of the proteasome. The 19S proteasome is involved with regulation. The 19S recognizes ubiquinated protein and is involved with allowing the substrate entrance into the proteolytic chamber (Ciechanover and Iwai 2004). Before

degradation proteins are unfolded by a variety of ATPases and then transported into the proteolytic chamber to be cleaved in smaller peptides as reviewed by (Ravid and Hochstrasser 2008). Following degradation, ubiquitin is recycled by several enzymes and can be reused for the degradation process.

Studies from our lab have shown that several pesticides can inhibit the UPS. Benomyl, rotenone, ziram, and several other pesticides were found to inhibit the proteasome at 10uM (and at 1uM for both ziram and rotenone) (Wang et al. 2006). Another study by our group examining the mechanisms of toxicity of ziram, found that *in vitro,* ziram causes dopaminergic cell death via inhibition of E1 ligase of the proteasome. Ziram caused selective dopaminergic cell toxicity in primary culture, and western blot analysis found that cells treated with ziram had a decrease in total ubiquination vs. cells treated with lactacystin (inhibition of 20S UPS) and rotenone. This suggests that ziram acts by inhibiting E1 ligase of the proteasome, which as discussed above is involved with activating ubiquitin. Further, in addition to inhibition of E1 ligase of the proteasome, α-syn levels were increased in TH+ neurons, further suggesting that ziram alters α-syn homeostasis by disrupting the UPS.

Although the evidence for pesticides increasing risk of developing PD via proteasome inhibition is small, alterations in α-syn homeostasis leading to increased neuronal toxicity is not. Increased cellular levels of α-syn have been found to be toxic through a variety of studies but the exact cause of their toxicity is not well understood. What has been suggested is that the degradation systems (the UPS and Autophagy) of the cell are overworked, or in the case of pesticides inhibited or rendered ineffective. Inability of the degradation systems to compensate for an increase in cellular levels of α-syn is one problem, but studies have demonstrated that α-syn itself can inhibit the UPS and autophagy, further taxing the cell and potentially causing toxicity.

As discussed earlier, decreased proteasome function has been observed in patients with PD (McNaught and Jenner 2001). Further *in vitro* studies have supported this finding. In PC12 cells, expression of human wt α-syn or mutant α-syn caused a decrease in chymotryptic-like, tryptic-like, and postacidic activities (Tanaka et al. 2001). Additionally, treatment with the proteasome inhibitor lactacystin and overexpression of α-syn resulted in an increase in apoptotic cell death. A similar effect of proteasome inhibition and alterations in α-syn has been observed *in vivo*. In rats exposed to proteasome inhibitors over a two-week period, depletion of striatal dopamine, an increase in dopaminergic cell death, and neuro-inflammation were observed. Most interestingly, in rats treated with proteasome inhibitors, intracellular protein accumulation and intracytoplasmic inclusions were observed in neurons of the substantia nigra (McNaught et al. 2004). Immunoreactivity studies on the inclusion bodies, stained positive for α-syn and ubiquitin. Additionally, these inclusion bodies stained positive for thioflavin-S, indicating the presence of β-pleated sheets, similar to Lewy bodies found in PD patients. It is likely that inhibition of the proteasome leads to aggregation of α-syn, after which oligomeric and aggregated forms of α-syn may inhibit the proteasome further. Lindersson et al found that both oligomeric and filamentous α-syn can inhibit the 20S proteasome (Lindersson et al. 2004). Specifically, filamentous α-syn forms β-pleated sheets and was found to inhibit chymotrypsin activity by as much as 60%. Similarly oligomeric forms of α-syn were also found to inhibit chymotrypsin activity of the proteasome. Interestingly, heat shock protein 70 (HSP70), which is also involved with the degradation of proteins via chaperone mediated autophagy, was found to attenuate the toxicity of filamentous α-syn.

Autophagy

Autophagy is a degradation process within the cell by which proteins (insoluble), misfolded proteins, and organelles are degraded. There are three different types of autophagy, chaperone-mediated autophagy, macroautophagy, and microautophagy. Dysfunction of autophagy in PD has been suggested by post mortem examination of patients with PD, as increases in the number of lysosome-like vacuoles have been found in DA neurons of patients (Anglade et al. 1997). The role of autophagy in PD is unclear, but both macroautophagy and CMA are involved in degradation of α-syn (Cuervo et al. 2004; Huang et al. 2012; Martinez-Vicente et al. 2008; Stefanis et al. 2001; Tanik et al. 2013; Vogiatzi et al. 2008; Webb et al. 2003; Winslow and Rubinsztein 2011) and may have a greater role in clearance of aggregates than the proteasome (Petroi et al. 2012).

Chaperone-mediated autophagy

Chaperone-mediated autophagy (CMA) degrades proteins after transporting them to the lysosomal membrane. All proteins degraded via CMA (substrate), have the peptide-targeting sequence (KFRERQ), which is recognized by heat shock proteins (HSP; specifically HSP-70) acting as chaperones. Following binding of the chaperone to the substrate, the complex is transported to and interacts with the lysosomal-associated membrane protein type 2a (lamp2a) (Cuervo and Dice 1996). Once bound to lamp2a, the targeted protein is transported into the matrix of the lysosome, and degraded by lysosomal proteases (Cuervo and Dice 2000). Previous studies have suggested that CMA is the primary method of autophagy for degrading α-syn, although mutated forms of α-syn have been found to inhibit CMA. In one study, both wt, A30P and A53T variants of α-syn were found to bind with lamp2a, however, only wt α-syn was taken into the lysosome and degraded. Both mutant variants of α-syn bound lamp2a stronger than wt α-syn, but were not translocated into the lysosomal lumen for degradation (Cuervo et al. 2004). Interestingly, the structure of synuclein can alter whether CMA can degrade the

protein. In a study looking at the degradation of monomer, dimer, and oligomeric forms of α-syn via CMA, only the monomer and dimer were translocated into the lysosomal matrix for degradation (Martinez-Vicente et al. 2008). Additionally, in the same study increases in intracellular dopamine were found to inhibit CMA, and increase activity of another autophagy pathway, macroautophagy.

Macroautophagy

Macroautophagy is another autophagy pathway by which α-syn can be degraded. In macroautophagy, substrates are sequestered into autophagosomes (double membrane vesicles). Once the proteins/organelles for degradation are sequestered in the autophagosome, the complex is translocated to the lysosome. The autophagosome then fuses with the lysosome, and releases the inner single membrane into the lysosome for degradation. Many of the early studies on macroautophagy were performed in yeast. Use of this model led to the discovery of several autophagy related genes/proteins (Atg; 31 have been identified to date), which are important throughout the formation of the autophagosome and eventual degradation within the lysosome. Many of the Atg proteins are part of subgoups that are involved with individual components of the autophagosome. For example, Atg 2,9, and 18 are involved with membrane delivery to the developing phaophore, while Atg 3,4,5,7,8,10,12, and 16 are involved with expansion of the autophagosome. For studies conducted in this dissertation, we will focus on Atg8, as this has been used and developed as a marker of autophagy. Atg8 proteins are essential for macroautophagy, however their exact role in autophagy is not well understood. Atg8 appears to have a role in biogenesis of the autophagosome as well as recruitment of cargo into the autophagosome as reviewed by (Shpilka et al. 2011). With regards to autophagosome biogenesis, studies of Atg8 in yeast, suggested that the protein is involved with determining the size of autophagosomes, specifically by

regulating elongation of the autophagosome membrane and also indirectly regulating levels of autophagy (H Abeliovich et al. 2000; Nakatogawa et al. 2007; Xie et al. 2008). Additionally, because Atg8 is the only Atg protein associated with both immature and mature autophagosomes, it is used as a marker of autophagosome formation and general marker of autophagic flux. Specifically, one of the subfamilies of Atg8, microtubule-associated protein 1 light chain 3 (LC3) is used widely in the autophagy field as a marker. There are two forms of LC3 found in the cell, LC3-I and LC3-II, which are formed by cleavage of proLC3, the full-length precursor protein. LC3-I is a 18kDa protein found with in the cytoplasm of cells, while LC3-II is a 16kDa protein found in the membrane of the autophagosome, and at least partially on the surface of the autophagosome (Kabeya et al. 2000). For *in vitro* studies, under starvation conditions, levels of LC3-II increased significantly, and an increase in the number of autophagosomes was observed, suggesting that levels/amount LC3-II can be used as a marker of autophagy. Because of this, LC3 has been fused with GFP to serve as a marker of autophagic flux (Kabeya et al. 2000; Mizushima et al. 2004). In this dissertation we utilize LC3 to study alterations in autophagic flux that may result from pesticide treatment.

Macroautophagy and α-syn

Although CMA has been suggested as the primary mechanism of autophagy for degrading α-syn, recent studies have suggested that macroautophagy may also have a significant role in degradation of α-syn (especially for those forms which cannot be degraded by CMA). Webb et al. demonstrated that α-syn can be degraded by the proteasome and macroautophagy *in vitro* by using several inhibitors and activators of the degradation pathways. Further they showed that mutant and aggregated forms of α-syn detected within lysosomes can be degraded via macroautophagy after using rapamycin,

an inducer of autophagy (Webb et al. 2003). Although limited, studies have demonstrated that while macroautophagy can clear α-syn, the protein itself can also inhibit macroautophagy. Overexpression of α-syn *in vitro* was found to decrease both LC3-II protein levels and the number of vesicles and was rescued by knocking down α-syn (Winslow and Rubinsztein 2011). *In vivo* a similar effect was observed in mice overexpressing α-syn levels, as LC3-II were decreased in a α-syn dose dependent manner. Additionally, it was found that α-syn and knockdown of Rab1a, which is involved with endoplasmic reticulum to golgi trafficking and was previously found to be altered by α-syn (Gitler et al. 2008), affected the formation of the omegasome (a precursor to the autophagosome), through mislocalization of Atg9 (Winslow and Rubinsztein 2011). Similar to previous studies that suggested that aggregated forms of α-syn were not translocated into the lysosome via LAMP2A, Tanik et al. found that aggregated forms of α-syn, did not co-localize with Lamp1. Even when the autophagy pathway was induced using rapamycin, no change in aggregated synuclein was observed, although α-syn inclusions were found to associate with autophagy machinery and an increase in LC3-II was observed. To determine whether the increase in LC3-II was from an increase in synthesis of autophagosomes vs. a lack of degradation of autophagosomes, inhibitors of lysosomal degradation were utilized (Tanik et al. 2013). Interestingly, α-syn did not inhibit the formation of autophagosomes, but rather appeared to interfere with their clearance.

Several studies have found that pesticides can alter α-syn homeostasis as discussed above, but very few studies have examined the effect of pesticides on autophagy in neurodegenerative disease. A recent study looked at the effects of Rotenone on autophagic flux both *in vitro* and *in vivo*. Dopaminergic neurons treated with rotenone were found to have an increase in accumulation of α-syn, double membrane structures (presumed to be stalled autophagosomes), and an increase in

LC3-II protein levels (Wu et al. 2015). Additionally, lysosomal dysfunction was observed for neurons treated with rotenone, specifically a reduction in lysosomal integrity. This was one of the first studies to examine the effect of a pesticide known to alter α-syn homeostasis, and demonstrate that pesticides may directly alter autophagy, a pathway associated with neurodegenerative disease.

Zebrafish as a model to study the effects of pesticides on synuclein homeostasis

As discussed previously, zebrafish (ZF) are an excellent model for studying neurodegenerative disease because of the similarity of their nervous system to humans, utility as genetic model, transparency during development, and ability to do studies with large sample sizes. Previous studies from our lab have examined the effect of overexpessing human α-syn in ZF. We found that α-syn overexpression in developing ZF caused α-syn to aggregate and resulted in neuronal toxicity and reduced survival by 3 days post fertilization (Prabhudesai et al. 2012). Here we propose to use ZF as a model to study the effects of ziram, a pesticide associated with increased risk for PD, on endogenous ZF synuclein homeostasis.

Zebrafish Synuclein

ZF have three different types of synuclein: γ1, γ2, and β, however, ZF do not have an orthologue of α-syn. All ZF synucleins (zSyns) have sequence similarity to the corresponding human synucleins. Based on synteny maps, it appears that both γ synucleins and β synuclein in ZF and humans are derived from a common ancestral locus. zSyn γ1 and γ2 are very similar, and likely arose from a duplication event of an ancestral locus (Milanese et al. 2012). Sequence analysis of zSyns found that zSyn β is 82% similar to human β synuclein, whereas zSyn γ1 is 47% similar to human γ syn, and zSyn γ2 is 50% similar to human γ syn (Sun and Gitler 2008). One of the differentiating

factors of α-syn from other human synucleins is a 12 residue hydrophobic region, however, this motif is not found in any of the zSyns. Where the zSyns are expressed varies throughout the development of the ZF. zSyn γ1 begins expressing at 26hpf and is found in the spinal cord neurons, the hind brain, and cranial ganglia (Milanese et al. 2012; Sun and Gitler 2008). zSyn γ2 expression begins earlier than γ1 but its expression is restricted to the notochord. zSyn β is the earliest expressed zSyn and is found throughout the diencephalon, olfactory, cranial ganglia, and ventral tegmentum. In areas where cathetcholaminergic (specifically dopaminergic) neurons are found including the telencephalon, diencephalon, and hindbrain, both zSyn β and γ1 are co-expressed (Milanese et al. 2012).

In a study where both zSyn β and γ1 were either individually or knocked down together, ZF embryos were found to develop normally but were found to have abnormal neurobehavior (Milanese et al. 2012). Further, in ZF in which Syn β and γ1 were knocked down, a decrease in the number of dopaminergic neurons was observed. Interestingly when α-syn was expressed in these knockdown fish, the number of dopmaniergic cells was similar to controls. This data suggests that zSyn β and γ1 are essential for the development and differentiation of dopaminergic neurons in ZF, and may have a similar function to α-syn.

In this study we investigate the role of ZF γ1 in ziram's neuronal toxicity. We demonstrate for the first time that ZF γ1, a functional homologue of human α-syn, is able to aggregate and form fibrils similar to α-syn *in vitro* and can aggregate and act as an amyloidogenic protein *in vivo*. Further we demonstrate that ziram's proposed mechanism of toxicity, inhibition of the proteasome, is conserved in our ZF model, and that treatment with ziram alters levels of ZF γ1 *in vivo*. Finally, using anti-sense technology and a pharmaceutical intervention, we demonstrate that ziram's toxicity is mediated via ZF γ1.

These studies demonstrate that ziram, a pesticide that has previously been implicated as a toxin that increases risk for PD, mediates its toxicity through synuclein.

Methods

Zebrafish

ZF lines (AB unless other wised stated) were bred and maintained at 28 °C in recirculating water tanks on a regulated 14h light/10h dark cycle and fed twice a day with brine shrimp. All experiments were carried out in accordance with UCLA Animal Research Committee protocols. ZF expressing GFP driven by the vesicular monoamine transporter promoter (VMAT2:GFP) were purchased from the UCLA core facility and used in this study to identify VMAT2 (dopaminergic, (nor)adrenergic, serotonergic) neurons in whole embryos (Wen et al. 2008). Peripheral sensory neurons (trigeminal and Rohon-Beard) were visualized using the Tg(isl1[ss]:Gal4-VP16,UAS:EGFP)^{zf154} transgenic line, which has been referred to as Tg(sensory:GFP), and were obtained from Dr. Sagasti (Sagasti et al. 2005).

A ZF γ1-synuclein expression construct (γ1-DsRed) composed of a T2A bicistronic configuration, driven by the *HuC* neuronal promoter and expressing monomeric DsRed, was used as previously described (Prabhudesai et al. 2012). The T2A sequence is cleaved after translation generating two proteins from a single open reading frame and resulting in stoichiometric expression of the gene of interest and the fluorescent reporter (Tang et al. 2009). ZF embryos were injected with *HuC*-ZFγ1-T2A-DsRed or *HuC*-DsRed (control) cDNA (50ng/μL) at the single cell stage.

A CMV:GFPu (degron) expression construct that has previously been characterized *in vitro,* was used here to monitor changes in proteasome inhibition after ziram treatment.

High expression of GFP was observed 24 hours post injection, suggesting that proteasome machincery had not matured/developed to a point where degradation of the degron could occur. By 48hpf, GFP fluorescence was reduced almost completely. In order to study the possible effects of proteasome inhibition we waited until 48hpf and screened for embryos in which GFP fluorescence was absent. Embryos were then treated with ziram or vehicle at concentrations described above and images at 72hpf for GFP positive cell counts.

Morpholinos (Gene Tools LLC, Philomath OR) were injected (0.1mM) at the single-cell stage for ZF γ1 (CATTAGAACATCCATCCTGGACGCT, translational blocking) or non-targeting/scrambled (CCTCTTACCTCAGTTACAATTTATA), as previously described (Milanese et al. 2012). The molecular tweezers CLR01 and CLR03 were prepared and purified as sodium salts, as described previously (Fokkens et al. 2005; Talbiersky et al. 2008). Specificity of the ZF γ1 morpholino (MO) was validated by SDS PAGE (see Figure 2-2).

Zebrafish Treatments

ZF embryos, 25-35 per treatment in 10 mL of E3 media (15mM NaCl, 0.5mM KCl, 1.0mM $MgSO_4$, 0.15mM KH_2PO_4, 0.05mM Na_2HPO_4, 1.0mM $CaCl_2$, 0.7mM $NaHCO_3$), were reared at 32 °C and exposed to varying concentrations of ziram (98.5% purity, Chem Service, West Chester PA). Embryos were exposed to 1 nM-1 μM (0.01%DMSO) ziram in E3 media at 5 hours post-fertilization (hpf) or 24 hpf in a 6-well plate for 5 days for confocal microscopy and 7 days post fertilization (dpf) for behavior. Embryos treated with ziram at 5 hpf developed notochord defects as previously

described (Haendel et al. 2004; Teraoka et al. 2006), so embryos were treated at 24 hpf to avoid this confound unless otherwise stated. The concentrations of ziram used for the study were well below those used for spraying (approximately 8 mM) (Agency 2015) and necessary for fungicidal activity (30 uM) (Briquet et al. 1976). VMAT2:GFP embryos were co-treated with 10μM CLR01 (Fokkens et al. 2005; Prabhudesai et al. 2012; Sinha et al. 2011) and 50 nM ziram. Log-Rank test was used for statistical analysis.

Confocal Microscopy

3 dpf and 5 dpf VMAT2:GFP embryos were anesthetized using Tricane-S (Western Chemicals Inc., Ferndale WA) at a final concentration 50 μg/mL, fixed in 4% paraformaldehyde (PFA) overnight and mounted in 2% low-melting agarose. Embryos were imaged at 20X using a Zeiss LSM 510 microscope. Approximately 100 1.1 μm optical sections were obtained for each embryo. Section images were stacked and reconstituted into 2D and 3D images using ImageJ (National Institutes of Health). Neuron count analyses were conducted in a blinded manner as previously described (Fitzmaurice et al. 2013). For MO and CLR01 studies, neuron counts for treatment groups were normalized to injection and treatment controls to account for variances in fish clutches between days and for treatment and injection survival. Student's t-test was used for statistical analysis.

Histology

ZF embryos were dechorinated at 2 dpf, fixed in 4% PFA for 24 hours, immersed in 30% sucrose overnight and cryosectioned (10-μm). For thioflavin S (ThS) staining, sections were immersed in 0.5% ThS dissolved in PBS (Sigma-Aldrich, St. Louis MO),

washed with ethanol (80%), and then mounted with Vectashield+Dapi (Vector Laboratories, Burlingame CA).

Polyclonal antibodies specific for ZF γ1 were raised using a C-terminal peptide CDFSHGGMEGGEGGE (Genscript, Piscataway NJ). These antibodies bound specifically to ZF γ1 at the predicted mass (17 kDa) in ZF embryos and to recombinant γ1 (Figure 2-1). Furthermore, the ZF γ1 band in Western blots was markedly reduced in ZF, after pre-absorption with the ZF γ1 peptide used to raise the antibody (Figure 2-1). Anti-ZF γ1 antibodies did not recognize any rodent brain proteins (Figure 2-1).

For immunohistochemistry, sections were blocked in 10% normal goat serum (Jackson Labs, Bar Harbor ME), incubated with anti-ZF γ1 antibody (1:1000) followed by incubation with an anti-rabbit-Alexa-Fluor 568 antibody (1:500, Life Technologies, Grand Island NY). The sections were then mounted with Vectashield+Dapi.

Western and Native Blots

ZF embryos (5 dpf) were anesthetized as described above, pooled (35 embryos per treatment), de-yolked, lysed, and sonicated in either 1X-SDS buffer or 1X-Native PAGE sample buffer (Life Technologies). Protein concentrations were determined using the BCA protein assay (Thermo-Fisher, Rockford IL). 75μg of protein was loaded onto SDS-PAGE or Native-PAGE gels and transferred using the XCell-II blotting system (Life Technologies). Membranes were probed with ZF γ1 1° antibody (1:2500 dilution), or TH 1° antibody (1:2500, MAB 318: Millipore) followed by donkey anti-rabbit HRP 2° antibody (1:2500 dilution, Santa Cruz Biotechnology, Dallas TX). Chemiluminescent substrate (Super Signal West Dura, Thermo Scientific) was used for band visualization. α-Tubulin (1:500, Sigma-Aldrich) was used as a loading control. Student's t-test was used for statistical analysis.

Expression and purification of zebrafish synuclein

Competent BL21 (DE3) E. Coli bacteria were transformed with a plasmid containing the ZF synuclein gene, allowed to grow in 3 L Luria broth to $OD_{600} \approx 0.8$, induced with 0.5 mM isopropyl β-D-1-thiogalactopyranoside and incubated for 3 additional hours. The bacteria were collected by centrifugation for 15 min at 4,690 × *g* and resuspended in 60 mL of lysis buffer containing 0.2 M Tris, 1 mM EDTA, pH 8.0, supplemented with Halt EDTA-free protease inhibitor cocktail (Thermo Scientific). The bacteria then were lysed on ice using a tip sonicator set to 3 KJoule for 3 × 2 min cycles of 3 sec power on and 3 sec power off. The lysate was centrifuged at 31,920 × *g* for 20 min and the supernate was collected. The proteins were precipitated from the supernatant by addition of 0.23g/ml ammonium sulfate. The solution with the ammonium sulfate was stirred on ice for 20 min and centrifuged at 31,920 × *g* for 20 min. The supernatant was discarded and the protein pellets were dried. The pellets were resuspended in 40 mL of 20 mM Tris, pH 8.0, and the resulting solution dialyzed overnight against 4 L of the same buffer. The crude protein mixture was fractionated using ion-exchange Q columns (GE Healthcare, Piscataway, NJ) and a 100 mL gradient ranging from 0 to 1.0 M NaCl in 20 mM Tris, pH 8.0. The protein was purified further by size exclusion chromatography using a 2.15 × 600 mm TSK-gel G3000SW column (Tosoh Biosciences, San Francisco, CA) with elution buffer comprising 100 mM sodium sulfate, 25 mM sodium phosphate, and 1 mM sodium azide, pH 6.5. Finally, the fractions containing purified ZF synuclein were dialyzed against 10 mM sodium phosphate, pH 7.4. The purity of the protein was assessed by SDS-PAGE and Coomassie blue staining.

Thioflavin T fluorescence assays

A concentrated protein solution was thawed on ice and filtered through a 0.2 μm filter prior to the fibril formation assay. Fibril formation assays were performed with 150-

μM ZF γ1 or human α-syn as a positive control in 10 mM sodium phosphate, pH 7.4, and 10 μM thioflavin T (ThT). ThT is used for identification and staining of amyloid fibrils (Biancalana and Koide 2010). For inhibition assays with molecular tweezers, ZF γ1 was used at 100 μM. Stock solutions were made by dissolving CLR01 or CLR03 at 10 mM in 10 mM sodium phosphate, pH 7.4. CLR01 and CLR03 were added at the molar ratios indicated.

All assays were performed in black, Nunc 96-well optical bottom plates (Thermo Scientific). Teflon balls (1/8 inch in diameter) were distributed into each well of the 96-well plate. Then, 200 μL of solution (four replicates per sample) were pipetted into each well. The plate was agitated at 300 rpm with a 3-mm rotation diameter in a Varioskan microplate reader (Thermo Scientific) at 37 °C. Fluorescence measurements were recorded every 10-15 min by using λ_{ex} = 444 nm, λ_{em} = 482 nm, with an integration time of 200 μs.

The ThT fluorescence signal was corrected for the background by subtracting the mean fluorescence signal acquired during the first couple of hours from the start of the assay. The fluorescence signal was normalized by dividing each measurement by the mean signal collected for 2–4 h during which the fluorescent reading had the largest value. If one of the sample replicates had fluorescence reading close to the background, its fluorescence was normalized by dividing it by the mean fluorescence reading of the remaining replicates. The data were smoothed by substituting each data point with the average value calculated using six data points collected before and after the point and the point itself. This is equivalent to central moving average with a sliding thirteen-data-point-wide window. The normalized fluorescence signal of ZF γ1 and CLR01 (ratio 1:1) and ZF γ1 and CLR01 (1:10), and ZF γ1 and CLR03 (1:10) were calculated using the averaged fluorescence signal of maximum fluorescence acquired from the assays of ZF γ1 alone.

Transmission Electron Microscopy (TEM)

Negatively stained specimens for TEM were prepared by applying 5 µL of sample onto hydrophilic, 400-mesh, carbon-coated formvar support films mounted on copper grids (Ted Pella, Inc.). The samples were allowed to adhere for 3 min, rinsed twice with distilled water and stained for 1 min with 1% uranyl acetate. Grids were examined on JEM1200-EX (JEOL) or T12 (FEI) microscopes.

Statistical Analysis

Statistical analyses were performed using Student's t-test, log-rank, and one-way ANOVA where appropriate. A minimum significance level was set at $p<0.05$ for all studies.

Results

ZF γ1 synuclein forms aggregates in vitro and in vivo

Several studies have suggested that α-syn, specifically aggregates and oligomers are central to the pathophysiology of PD. Our group previously found that ziram increased levels of α-syn in dopaminergic neurons in primary culture, likely through inhibition of the proteasome (Chou et al. 2008; Wang et al. 2006). Additionally our group also found that when overexpressed in ZF, α-syn had the propensity to form aggregates and further inhibited the proteasome. In order to study the effect of ziram on endogenous ZF synuclein, we needed to characterize the aggregation potential and potential toxicity of ZF synuclein. However, there are three isoforms of ZF synuclein, (β,γ1, and γ2), all three of which have previously been partially characterized in ZF but none appear to be the exact orthologue to human α-syn (Milanese et al. 2012; Sun and Gitler 2008). Both β and γ1 are expressed widely throughout the developing brain, while γ2 is expressed primarily in the notochord (Chen et al. 2009). Additionally, only β and γ1 are expressed in TH neurons, and thus were of interest to this study. Because γ1 synuclein contains N-terminal repeats and hydrophobic regions similar to that of α-syn, and expression of human α-syn rescues behavioral defects of γ1-deficient ZF embryos (Milanese et al. 2012), we investigated the propensity of ZF γ1's to aggregate and induce toxicity *in vitro* and *in vivo.* Recombinant human α-syn (hSyn) and ZF γ1 were incubated over a 70 h period and monitored for β-sheet formation using ThT fluorescence. Additionally the morphology of each sample was examined at the end of aggregation reactions by TEM (Sinha et al. 2012). The ThT fluorescence in the hSyn samples began to increase following a lag phase of ~10 h and reached a plateau at ~55

h (Figure 3A). In the ZF γ1 samples, the lag phase was shorter, ~7 h, and the kinetics of ThT fluorescence increase was faster, reaching a plateau by ~25 h (Figure 2-3a). Both proteins formed abundant fibrils as determined by TEM though the fibrils differed in length. hSyn formed long fibrils, ≥1 μm in length with a diameter of 10 +/- 1 nm (Figure 2-3b), whereas ZF γ1 formed 20-740 nm long fibrils with a diameter of 9 +/- 2 nm (Figure 2-3c). This difference in length and abundance of the fibrils can be attributed to ZF γ1's shorter nucleation rate, as reflected by the shorter ThT fluorescence lag phase relative to hSyn. Here we demonstrated that ZF γ1 is an amyloidogenic protein that has the ability to form β-sheet-rich fibrils similarly to other amyloidogenic proteins, and most relevantly α-syn.

Because of ZF γ1's ability to form β-sheet-rich fibrils *in vitro*, we sought to study if the protein could aggregate *in vivo* when overexpressed. As discussed above, we previously demonstrated that overexpression of α-syn in ZF neurons led to malformed embryos, intracellular aggregates, and neuronal death (Prabhudesai et al. 2012). Here we overexpressed ZF γ1 in ZF neurons in order to determine if increased levels of endogenous protein induced aggregate formation, and were neurotoxic *in vivo.* In order to study the effects of overexpression of ZF γ1 in ZF, we used the HuC neuronal promoter to drive expression of ZF γ1. We used a similar construct to the one we had used in the past to overexpress α-syn in ZF, except here ZF γ1 was expressed under control of the *HuC* neuronal promoter as a fusion protein with T2A-DsRed. The T2A peptide is post-translationally cleaved releasing native ZF γ1 and the fluorescent DsRed reporter in equal molar concentrations (Prabhudesai et al. 2012). We found the embryos overexpressing ZF γ1 had reduced survival and severe malformations by 72hpf including pericardial edema, shorter body axis, and bent tail compared to embryos overexpressing DsRed (Figure 2-4a,b). This effect was very similar to that seen in embryos where α-syn

was overexpressed (Prabhudesai et al. 2012). To determine if ZF γ1 was able to form aggregates *in vivo* we sectioned injected embryos for immunohistochemistry and used an antibody specific for ZF γ1. We found that embryos overexpressing ZF γ1 had intracytoplasmic aggregates, while those overexpressing DsRed did not (Figure 2-4c,d). To further confirm this finding, we used ThS staining to determine if ZF γ1 was forming β-sheet-rich aggregates. Neurons expressing ZF γ1 stained positively with ThS, while DsRed expressing neurons did not (Figure 2-4e,f). These results further confirm the *in vitro* findings that ZF γ1 has the propensity to aggregate, and potentially cause toxicity.

Ziram inhibits the proteasome *in vivo*

We previously proposed that one mechanism of toxicity for ziram is through inhibition of the proteasome. To study whether the proteasome is inhibited in our ZF model after ziram treatment we utilized a GFP degron system. We utilized the CMV:GFPu construct previously characterized by Bence et al. and previously utilized by our group for *in vitro* studies (Bence et al. 2005; Chou et al. 2010; Wang et al. 2006). In preliminary studies we found that GFP fluorescence 24h after injections was high in all groups, signifying that the proteasome machinery had not yet developed completely and was unable to degrade proteins completely. We conducted our study at 48hpf, after GFP fluoresnce was absent in most fish. 24hours after treatment (72hpf), we imaged embryos and found that ZF treated with ziram had a significant increase in the amount of labeled neurons as compared to vehicle controls (Figure 2-5). Here we demonstrate that an effect of ziram characterized previously *in vitro*, is conserved in our ZF model, and thus relevant for studies of synuclein toxicity.

Ziram treatment decreases protein levels of ZF γ1

As discussed above, our group previously demonstrated that treatment with ziram increased intracellular α-syn levels in primary neuronal cultures. Because ZF γ1 displays many of the same characteristics as α-syn both *in vitro* and *in vivo*, we wanted to study the effects of ziram on ZF γ1. We utilized western blot analysis under denaturing conditions to examine changes in protein levels of ZF γ1 for ziram treated embryos at 5dpf (the time at which we had performed neuronal counts). In preliminary western blot studies using our anti- ZF γ1 antibody, we detected a band at 17kDa (presumed monomer, Figure 2-1a). Western blots for ziram treated fish revealed a significant decrease in intensity of the monomeric band at 17 kDa for embryos with ziram (50 nM) as compared to vehicle-treated controls (Figure 2-6a). Studies have suggested that synuclein under denaturing conditions may behave/present differently than synuclein under native conditions. In order to test this for ZF γ1, we performed western blots using non-denaturing/native conditions. Using this method we observed a major band at 480 kDa and a minor band at 242 kDa (2-6c). This suggests that ziram does not alter the degree of oligomerization at the time point we examined.

Targeting zSyn with a morpholino protects against ziram's neuronal toxicity

In order to further study the role of ZF γ1 in ziram's neuronal toxicity, we performed knocked down studies for ZF γ1. We designed a MO to prevent translation ZF γ1, and confirmed knockdown via western blot (Figure 2-7). For ziram studies, we injected the MO and treated VMAT2 embryos at 24hpf as described above. We found that MO knockdown of ZF γ1 protected against loss of VMAT2 neurons after ziram treatment. An 86.8% and 45.1% increase in GFP labeled neurons, telencephalic and diencephalic respectively, was observed for ziram treated embryos injected with ZF γ1

MO vs. ziram treated embryos injected with scramble MO (control). This result demonstrates that ziram's toxicity is mediated via ZF γ1.

CLR01 inhibits synuclein aggregation *in vitro and protects against ziram's toxicity in vivo*

To further explore the role of ZF γ1 in ziram's neuronal toxicity, we utilized the molecular tweezer, CLR01. CLR01 has previously been found to reduce human α-synuclein toxicity by disrupting α-syn aggregation *in vivo* and *in vitro* (Acharya et al. 2014; Prabhudesai et al. 2012; Sinha et al. 2012). We have previously reported that CLR01 reduced α-syn toxicity in cell-based models and in ZF (Prabhudesai et al. 2012). Here, we found that CLR01 also inhibited recombinant ZF γ1 fibrillation as determined by ThT fluorescence and EM (Figure 2-8). Additionally, utilizing the VMAT2:GFP line, we studied the effect of ziram treatment plus CLR01. We found that fish treated with CLR01 and ziram had a 173% increase in the number of labeled neurons (diencephalic cluster), as compared to fish treated with ziram alone (Figure 2-9). Thus, ziram's neurotoxicity appears to be dependent not only on the total ZF γ1 levels, as suggested by the MO experiment (Figure 2-7), but also on formation of toxic forms of ZF γ1, which can be disrupted by CLR01 (Figure 2-9).

Discussion

It is not completely clear how ziram causes selective DA neuron damage. Previous studies from our group have suggested that the pesticide acts by inhibiting the UPS, and increasing intracellular levels of α-Syn. ZF do not have an orthologue of human α-Syn, but studies have suggested that ZF γ1 is expressed in dopaminergic neurons and may have a similar physiologic function to α-syn. Here we investigate the propensity of γ1 to aggregate *in vitro* and *in vivo*, potential toxicity of the protein *in vivo*, and determine if ziram mediates its toxicity through ZF γ1.

zSyn γ1 aggregates and forms fibrils similar to α-Syn

We investigated the propensity of ZF γ1 to form fibrils *in vitro* and *in vivo*. Previously other studies have suggested that ZF γ1 may function similarly to α-syn (Milanese et al. 2012). Using ThT staining we found *in vitro* that recombinant ZF γ1 formed fibrils with similar kinetics to α-syn. Although the kinetics of fibril formation for ZF γ1 were slightly faster than α-syn, the resulting fibrils formed were nearly indistinguishable by electron microscopy The fact that ZF γ1 was able to form fibrils is not unexpected. It had been previously demonstrated that human γ synuclein is able to aggregate to form oligomers and fibrils with enhanced β-sheet content (Uversky et al. 2002). Additionally, the same study demonstrated that human γ synuclein fibrils were indistinguishable from α-syn fibrils, similar to the result we observed in our study. One difference from the study performed by Uversky et al. and our study is the aggregation

kinetics. In our study we found that γ1 formed fibrils at a faster rate than α-syn, while Uversky et al observed the opposite effect for human gamma synuclein. It is possible that the conditions we were using for our *in vitro* study were effective for inducing aggregation of proteins as other studies have demonstrated as reviewed by (Song 2013). It is also possible that ZF has aggregation properties intermediate between human alpha and gamma synuclein.

To evaluate this further, we overexpressed ZF γ1 in embryos to determine if the protein can aggregate *in vivo*. Our group had previously performed a similar study for studying human α-syn in ZF embryos. In this study we found that α-syn was able to form aggregates in ZF neurons and caused neurotoxicity (Prabhudesai et al. 2012). Similarly, in this study when we overexpressed ZF γ1 via microinjections at the one cell stage, we found that ZF γ1 appeared to aggregate within neurons (as determined by antibody labeling). To confirm the presence of aggregates and β-pleated sheets, we utilized immunohistochemistry (specifically ThS staining). Compared to DsRed controls, we observed a significant increase in thioflavin positive aggregates within neurons expressing ZF γ1. We were surprised to find that ZF γ1 causes neurotoxicity similar to α-syn. We suspect that the neurotoxicity observed within neurons overexpressing ZF γ1 was due to the fact that aggregation of the protein inhibited the proteasome and autophagy, and has previously been shown to increase cell death (Boya et al. 2005; Suraweera et al. 2012).

Ziram inhibits the proteasome in zebrafish

Our group previously found that ziram inhibits the proteasome in primary culture. Here the use of the previously characterized GFPu construct (CMV:GFPu) enabled us to determine if ziram inhibited the proteasome in our ZF model. Initial studies were conducted over three days, where embryos were exposed at 24hpf and imaged at 3dpf

for fluorescent neurons. Although we observed a difference between the ziram treated fish vs. vehicle controls, we could not completely distinguish whether the effect observed was based on inhibition of the proteasome or a result of variations in microinjection efficiency. To remove this confound, instead of treating embryos at 24hpf, we waited until 48hpf for fluorescence to dissipate completely (a result of the proteasome functioning by this time, and degrading the degron). After treatment at 48hpf, we saw an increase in fluorescent neurons for ziram treated fish suggesting that ziram had inhibited the proteasome.. Previously our group investigated how ziram may inhibit the proteasome *in vitro* and found that ziram did not alter chymotryptic activity of the proteasome like other pesticides (Chou et al. 2008). In fact, ziram did not alter 20S proteasome activity at all. Interestingly, ziram did alter polyubiquitin levels of proteins, suggesting that ziram's mechanism of action maybe through interference of the ubiquitination process, specifically interference of ubiquitin ligation of E1 ligase of the proteasome.

ZF have a functional proteasome similar to humans including E1 ligase. We attempted to study whether E1 ligase was essential to dopaminergic neurons in ZF in a knockdown study. We designed a morpholino to block translation of E1 ligase in ZF, and performed neuronal counts on VMAT2 neurons as described previously. We did not observe a change in the number of neurons for ZF with the E1 ligase knockdown vs. controls. It is possible that the E1 ligase we knocked down using morpholinos was not the only E1 ligase, as other studies have suggested that ZF have a second E1 ligase, UBA6 (as reviewed by (Schulman and Harper 2009), which may have compensated for knockdown of only 1 E1 ligase. It is also possible that the morpholino we designed did not completely knockdown expression of E1 ligase completely. Efficacy has been shown to vary among different morpholinos, and thus if the enzyme has been knocked down 90%, the remaining 10% may be enough to compensate for degradation within the

cell (Bill et al. 2009; Eisen and Smith 2008). In future studies efficacy of the morpholino can be measured using immunoblot analysis to measure ubiquitination via E1. We previously demonstrated that ziram decreases ubiquitination of E1 ligase, suggesting interference with ubiquitin ligation. For E1 knockdown or ziram treated embryos we predict that we will see a similar decrease in ubiquinated E1, although the ability to perform this experiment maybe limited by availability of antibodies that can detect E1 ligase in ZF. Another alternative to study knockdown of E1 ligase, would be to design a splice blocking morpholino. This method has been suggested as an alternative to translational blocking morpholinos. Splice blocker morpholinos maybe more appropriate for knockdown vs. translational blocking morpholino as they can be designed to target specific isoforms of a gene (Bill et al. 2009). Using this method would allow us to knockdown all isoforms of E1, and enable us to measure knockdown efficacy via PCR.

Although inhibition of E1 ligase has been proposed as a mechanism of ziram's toxicity, it is likely that this is only one of several pathways altered by the pesticide. Studies from our lab have demonstrated that ziram can also inhibit aldehyde dehydrogenase (ALDH). Inhibition of ALDH has been implicated as a risk factor for PD, and we previously demonstrated that benomyl (a dithiocarbamate fungicide), which inhibits ALDH, can cause dopaminergic cell both *in vitro* and *in vivo* (Fitzmaurice et al. 2013). Additionally, a recent study by our lab demonstrated that ziram can inhibit activity of ALDH and is associated with increased risk for PD (Fitzmaurice et al. 2014). We attempted to investigate the effect of ziram on ALDH activity in our zebrafish model using HPLC. Initially, our focus was to determine alterations in 3,4-dihydroxyphenylacetaldehyde (DOPAL) levels. DOPAL is a toxic intermediate of dopamine metabolism that is normally metabolized by ALDH into a non-toxic metabolite, DOPAC (Casida et al. 2014; Fitzmaurice et al. 2013; Goldstein et al. 2013). Our initial studies focused on studying DOPAL levels using embryos, however we were unable to

detect DOPAL in ZF embryos. Because ALDH inhibition should alter DOPAC levels (we hypothesized that a decrease in DOPAC would be observed if ALDH was inhibited), we attempted to measure levels of DOPAC in ZF. We did not observe a change in total DOPAC levels, which maybe attributed to the fact that there was, increased compensation of dopaminergic neurons not affected by ziram to produce dopamine and its metabolites. The results of this study were inconclusive with regards to changes in alterations in DOPAL/DOPAC levels. For future studies, it will be interesting to look at the effect of ALDH inhibition via knockdown (morpholinos) or by chemical inhibition, to determine if inhibition of the enzyme increases dopaminergic cell toxicity *in vivo*. Specifically, we can use the VMAT2 line characterized in Chapter 1 and below, to study the effect of ALDH inhibition on dopaminergic neurons.

Ziram's toxicity is mediated by synuclein

Previous findings from our group suggested that ziram not only inhibited the proteasome via E1 ligase, but that this directly led to an increase in intracellular α-syn. If the mechanism of toxicity is conserved in ZF, we predicted that ziram would increase ZF γ1 levels as measured by immunoblot and immunohistochemistry. Interestingly for embryos treated with ziram at 24hpf and sacrificed for immunoblot at 5dpf, we actually observed a decrease in protein levels of ZF γ1. We hypothesize that the decrease in ZF γ1 protein levels by 120hpf can be attributed to neuron terminal loss, as is suggested by the reduction of GFP fluorescence in VMAT-2 neurons. Additionally, we did not detect fibril formation with ThS *in vivo* after ziram exposure. The formation of synuclein β-sheets is dependent on several factors including concentration and time. It is possible that ZF γ1 did not reach high enough concentrations, or had enough time to form aggregates as seen in the *in vitro* and overexpression studies discussed above. Even though this might be the case it is possible that ziram alters ZF γ1, which we

hypothesize will result in the formation of toxic prefibrillar oligomers. Previous studies have suggested that Lewy bodies and monomeric forms of α-syn are not the cause of toxicity in neurons, but rather the toxicity is caused by toxic prefibrillar oligomers (Danzer et al. 2007; Winner et al. 2011). In order to test this hypothesis, we studied the effect of a knockdown of ZF γ1 and the use of a molecular tweezer that was previously found to protect against α-syn's toxicity.

In order to determine if ziram's toxicity is mediated via ZF γ1, we created a morpohlino designed to prevent translation of ZF γ1. Knockdown of ZF γ1 prevented the neurotoxicity of ziram in both the telencephalic and diencephalic neuronal clusters. This finding is supported by several others in the field, which have demonstrated that knockdown of synuclein can protect against environmental factors causing neurotoxicity (Tai et al. 2014; Wu et al. 2009; Zharikov et al. 2015). Further a recent study by Zharikov et al, demonstrated that knockdown of α-syn using shRNA, protected against rotenone's (a pesticide previously associated with increased risk for PD) neuronal toxicity (Zharikov et al. 2015). The finding that ziram's toxicity is mediated via ZF γ1 is further supported by the finding that CLR01 also protected against ziram's toxicity in our ZF model. Our group and others have previously demonstrated that CLR01 acts on amyloidogenic proteins and protects against their toxicity both *in vivo* and and *in vitro* (Attar et al. 2012; Prabhudesai et al. 2012; Sinha et al. 2011). CLR01's only known activities are to remodel the self-assembly of amyloidogenic proteins into non-toxic and non-amyloidogenic structures and to facilitate their clearance (Acharya et al. 2014; Attar and Bitan 2014; Prabhudesai et al. 2012). Here we found that CLR01 prevented ZF γ1 from aggregating *in vitro* and prevented neurotoxicity *in vivo*. This again suggests that ziram may cause the formation of toxic prefibrillar oligomers, which CLR01 protected against. One limitation of this study was the treatment protocol, as embryos had to be treated at 5hpf with both CLR01 and ziram (based on previous treatment protocols for CLR01). It is

possible that CLR01 prevented the aggregation of ZF γ1, maintaining the protein in its monomeric forms, which can then be degraded via the UPS. If that were the case, CLR01 would prevent the formation of toxic oligomers within the cells. For future studies we can expose ziram treated embryos with CLR01 at a later developmental time point, to determine if CLR01 can provide protection against preformed/toxic oligomers of ZF γ1.

Most neurodegenerative disorders like PD have a relatively selective pattern of neuronal loss although the mechanisms responsible for this selectivity have remained elusive. Ziram and other DTCs have been shown to inhibit the UPS, but this would not explain the selectivity of neuronal damage. It is possible that ziram's ability to inhibit ALDH in addition to its UPS-inhibiting activity, leads to selective DA damage. ALDH inhibition causes the accumulation of DOPAL in DA neurons, which is toxic (Burke et al. 2008; Casida et al. 2014; Fitzmaurice et al. 2013; Fitzmaurice et al. 2014; Panneton et al. 2010).

The experiments from this study add to the growing evidence that pesticides mediate their toxicity through synuclein. Here we demonstrated that ziram can inhibit the proteasome and its toxicity is mediated via ZF γ1. For future studies, we will examine the effect of ziram on macroautophagy. Alterations in autophagy have previously been implicated in patients with PD (Anglade et al. 1997). Several studies have suggested that impairment of autophagy via several mechanisms (including synuclein itself) can lead to cell death (Boya et al. 2005; Cuervo et al. 2004; Martinez-Vicente et al. 2008; Stefanis et al. 2001; Tanik et al. 2013; Webb et al. 2003; Wu et al. 2015). It will be interesting to examine the effect of ziram on autophagic flux. There are several tools available to measure changes in autophagy in zebrafish. He et al. generated a transgenic GFP-LC3 fish, and were able to image alterations in autophagic flux after inducing autophagy (He et al. 2009). Additionally, the group utilized immunoblot analysis

to examine the autophagy. They were successful in detecting alterations in LC3-I and LC3-II levels using inhibitors and inducers of autophagy. I hypothesize that ziram, which inhibits function of the proteasome, will have a similar effect on autophagy. We can measure alterations in autophagic flux using the transgenic line described above, and by analyzing changes in levels of LC3-I and LC3-II. Further, we can study the effect of knockdown of ZF γ1 on autophagy after treatment with ziram.

Another pathway of interest is the retromer, which has recently been implicated as a risk factor in neurodegenerative diseases such as AD and PD (Follett et al. 2014; Small et al. 2005). The retromer is involved with retrieval of "cargo" from endosomes, and delivery to the trans-Golig network and structurally is composed of two components a trimeric core and a tubulation module (Arighi et al. 2004; Attar and Cullen 2010; Seaman 2004; Small and Petsko 2015). Alterations in vacuolar protein sortin-associate proteins (VPS), specifically VPS35 have been implicated in neurodegenerative disease. In parkinson's disease the exact mechanism of retromer dysfuction is not well understood, but it appears that dysfunction of VPS35 can alter delivery of cathepsin D, an endomsomal-lysosomal protease that is involved with the processing of α-syn (Follett et al. 2014; Miura et al. 2014). Specifically, VPS35 dysfunction has been found to cause an accumulation of α-syn within lysosomes (Miura et al. 2014). ZF have a functional homologue of VPS35, and thus it will be interesting to observe if knockdown of VPS35 alters synuclein homeostasis within ZF. Further, there are antibodies available for VPS35 and thus alterations in levels of the protein can be monitored via immunoblot (although specificity of the antibody for ZF VPS35 needs to be tested). Perhaps most interesting will be to determine the effect of inhibition of multiple degradation pathways such as the UPS and autophagy via ziram on retromer activity.

The studies presented here suggest that ziram, a pesticide previously associated with increased risk for PD, mediates its toxicity via ZF γ1. On a larger level, these

studies give further insight into the role that environmental toxins have in the development of PD, and allow for a greater understanding of the etiology of PD. Perhaps most important is that these studies provide future targets for therapeutic exploitation which may one day help to cure the disease.

Figure 2-1: The polyclonal antibody ZF γ1 is specific for ZF

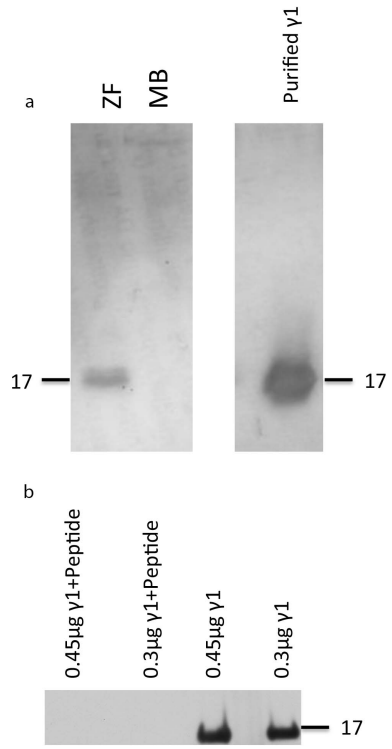

Figure 2-1: The polyclonal antibody ZF γ1 is specific for ZF
Using denaturing conditions/SDS PAGE, a band for γ1 was detected at 17 kDa for ZF adult brain (ZF) and purified ZF γ1 (a). No ZF γ1 signal was detected for mouse brain (MB). Peptide preincubated with the ZF γ1 antibody is shown for SDS PAGE. No band for ZF γ1 was detected after preincubation of γ1 antibody with γ1 peptide (b).

Figure 2-2: Specificity of ZF γ1 Morpholino is validated by SDS PAGE

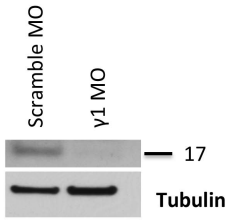

Figure 2-2: Specificity of ZF γ1 Morpholino is validated by SDS PAGE
In order to validate specificity of the morpholino ,we utilized western blot analysis under denaturing conditions. Embryos (n=75) were injected with ZF γ1 MO or scramble (control) and were prepared for western blot analysis. A decrease in the monomer of γ1 was determined via western blot for embryos injected with the ZF γ1 MO.

Figure 2-3: ZF γ1 synuclein aggregates and forms fibrils similarly to human α-synuclein

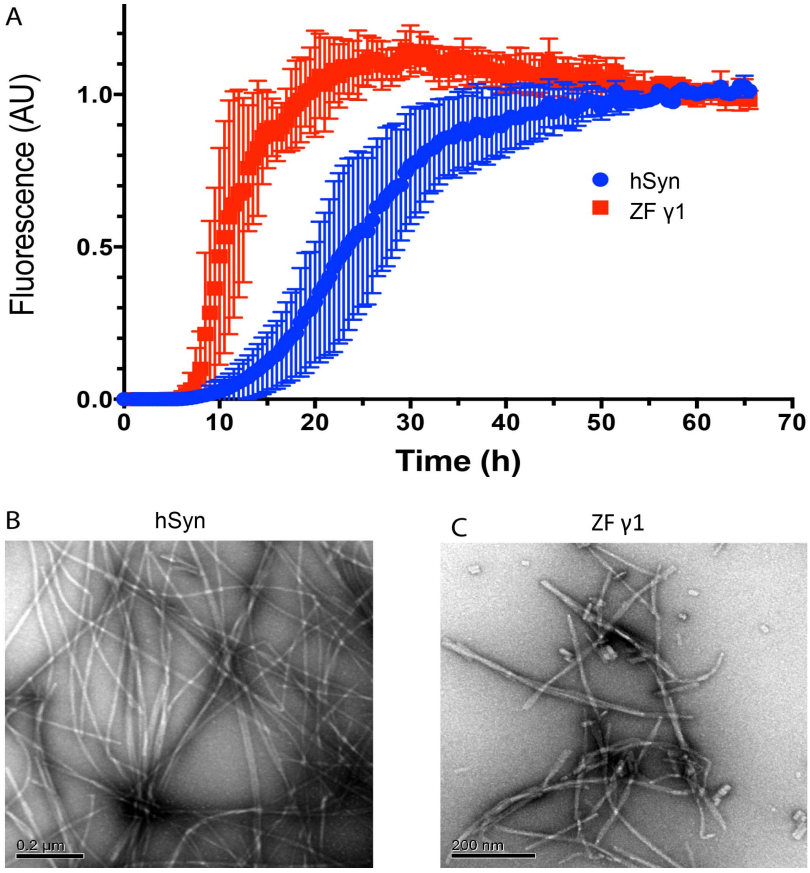

Figure 2-3: ZF γ1 synuclein aggregates and forms fibrils similarly to human α-synuclein. 150µM recombinant hSyn or ZF γ1 were incubated over a 66-hour period and thioflavin T fluorescence was monitored (a). The morphology of hSyn (b) and ZF γ1 (c) was examined at the end of the aggregation reaction using TEM (scale bar = 0.2 µm).

Figure 2-4: Overexpression of ZF γ1 *in vivo* causes intracellular aggregation of synuclein

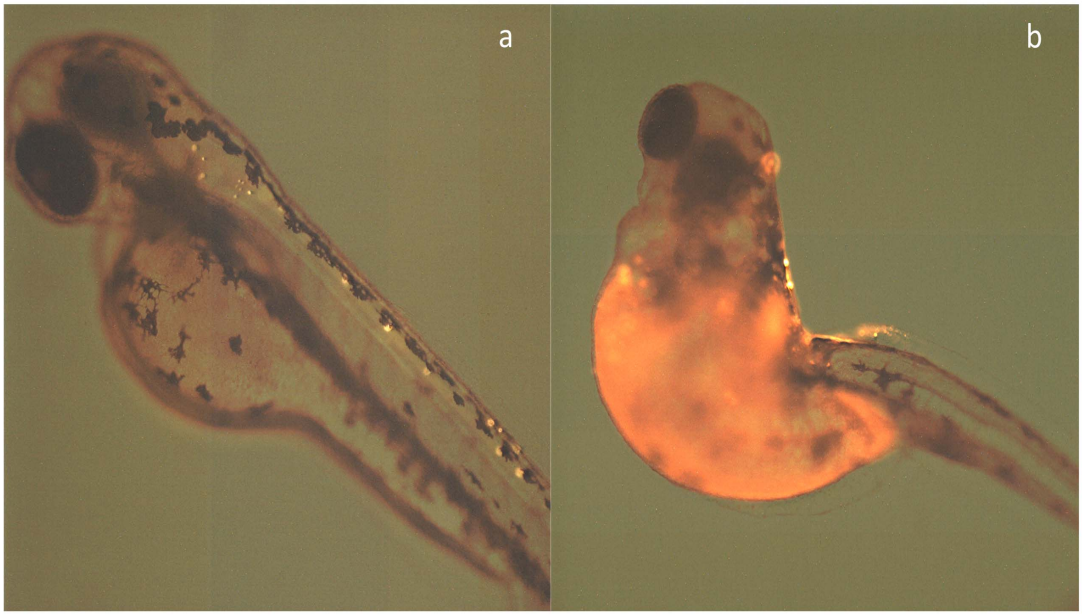

Figure 2-4: Overexpression of ZF γ1 *in vivo* causes intracellular aggregation of synuclein

Embryos were injected with constructs for Huc-T2A-DsRed (a) or Huc-γ1-T2A-DsRed (b), embryos shown at 2 dpf (scale bar = 00 μm). Sectioned embryos were stained with a primary antibody for ZF γ1. HuC-DsRed (c) injected embryos did not have intracellular ZF γ1 aggregates, while embryos injected with HuC-ZFγ1 (d) were found to have intracellular ZF γ1 aggregates (blue arrow) (scale bar = 10 μm). To determine if ZF γ1 formed β-pleated sheets *in vivo*, embryos injected with HuC-DsRed and Huc-γ1-T2A-DsRed were stained with ThS (scale bar = 10 μm). Only neurons overexpressing ZF γ1 (f) were ThS positive (e).

Figure 2-4: Overexpression of ZF γ1 *in vivo* causes intracellular aggregation of synuclein

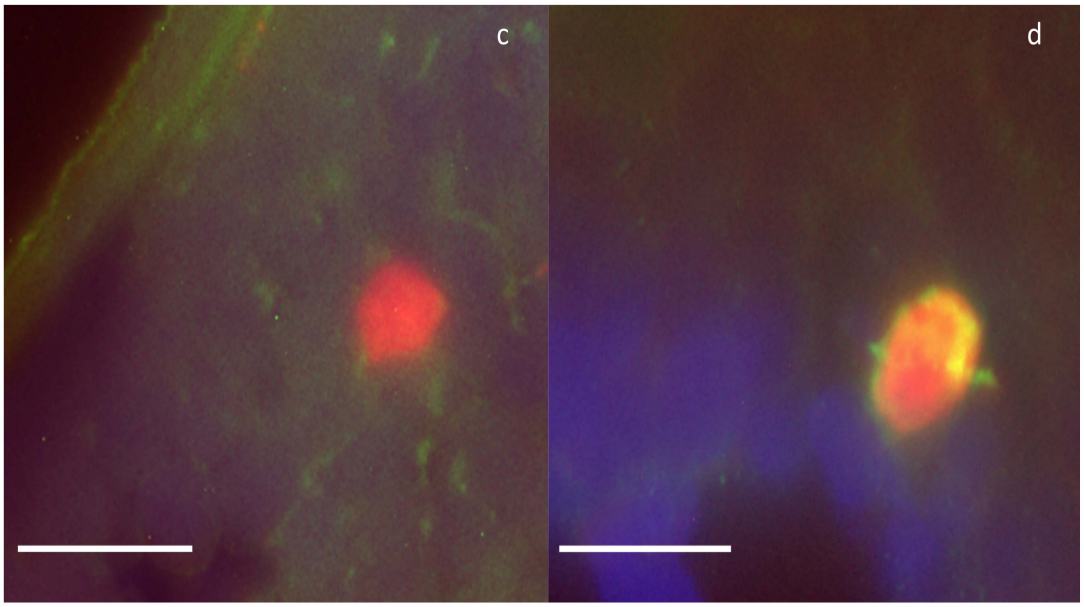

Figure 2-4: Overexpression of ZF γ1 *in vivo* causes intracellular aggregation of synuclein
Embryos were injected with constructs for Huc-T2A-DsRed (a) or Huc-γ1-T2A-DsRed (b), embryos shown at 2 dpf (scale bar = 00 μm). Sectioned embryos were stained with a primary antibody for ZF γ1. HuC-DsRed (c) injected embryos did not have intracellular ZF γ1 aggregates, while embryos injected with HuC-ZFγ1 (d) were found to have intracellular ZF γ1 aggregates (blue arrow) (scale bar = 10 μm). To determine if ZF γ1 formed β-pleated sheets *in vivo*, embryos injected with HuC-DsRed and Huc-γ1-T2A-DsRed were stained with ThS (scale bar = 10 μm). Only neurons overexpressing ZF γ1 (f) were ThS positive (e).

Figure 2-4: Overexpression of ZF γ1 *in vivo* causes intracellular aggregation of synuclein

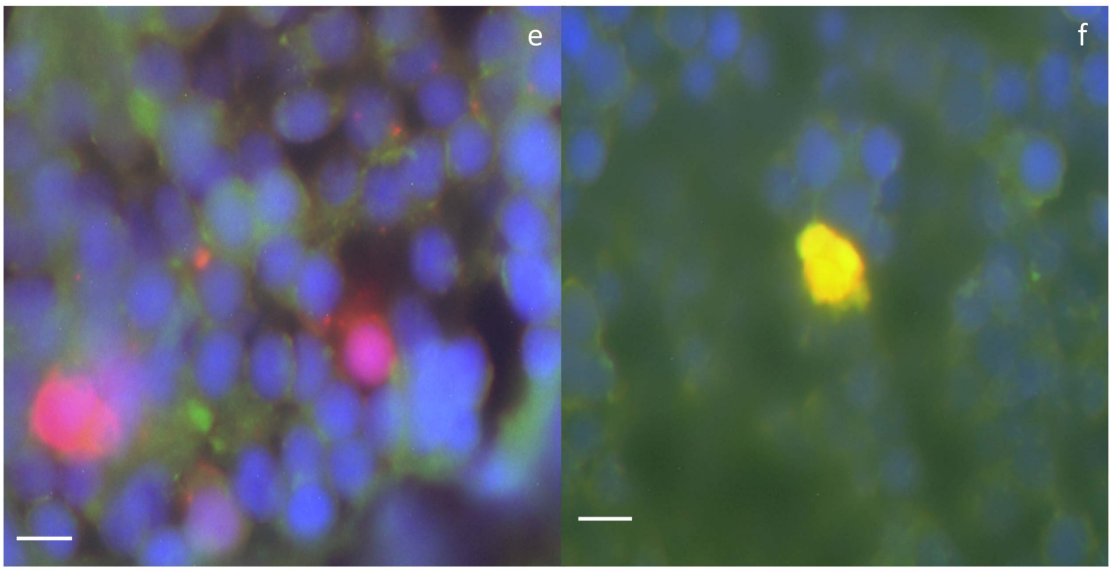

Figure 2-4: Overexpression of ZF γ1 *in vivo* causes intracellular aggregation of synuclein

Embryos were injected with constructs for Huc-T2A-DsRed (a) or Huc-γ1-T2A-DsRed (b), embryos shown at 2 dpf (scale bar = 00 μm). Sectioned embryos were stained with a primary antibody for ZF γ1. HuC-DsRed (c) injected embryos did not have intracellular ZF γ1 aggregates, while embryos injected with HuC-ZFγ1 (d) were found to have intracellular ZF γ1 aggregates (blue arrow) (scale bar = 10 μm). To determine if ZF γ1 formed β-pleated sheets *in vivo*, embryos injected with HuC-DsRed and Huc-γ1-T2A-DsRed were stained with ThS (scale bar = 10 μm). Only neurons overexpressing ZF γ1 (f) were ThS positive (e).

Figure 2-5: Ziram inhibits the proteasome in ZF

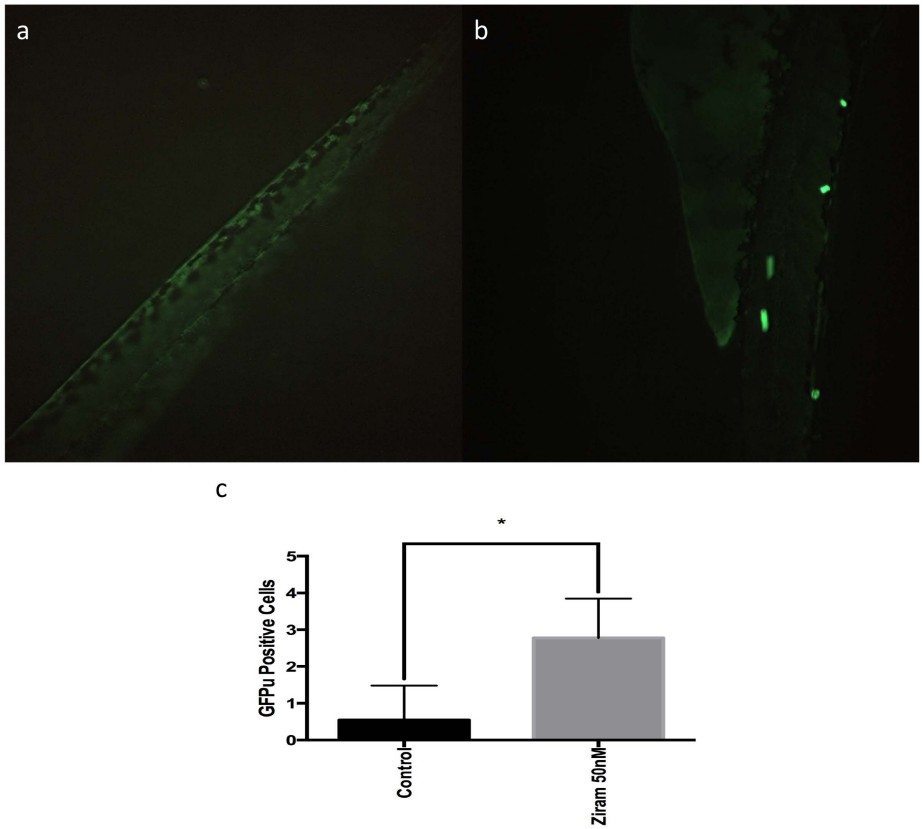

Figure 2-5: Ziram inhibits the proteasome in ZF
We utilized a the CMV:GFPu construct to study whether one of the mechanisms of ziram's toxicity, proteasome inhibition, is seen in ZF. Embryos were imaged at 72hpf, 24h after treatment with 50 nM ziram or vehicle. Ziram-treated embryos had an increase in the number of GFP positive cells vs. vehicle-treated embryos. The average number of positive cells for ziram-treated ZF was higher than for vehicle-treated ZF. n=8-10 per treatment. Two-tailed student t-test. *p<.05

Figure 2-6: Ziram decreases ZF γ1 levels

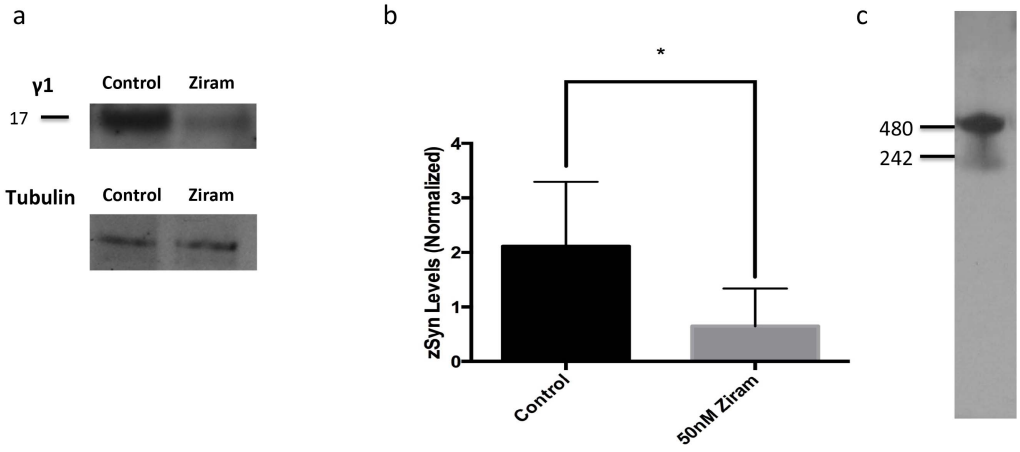

Figure 2-6: Ziram decreases ZF γ1 levels
Embryos were treated with ziram or vehicle and ZF γ1 levels were determined by Western blot analysis at 5dpf (normalized to tubulin). A 69.3% decrease in band density for ZF γ1 was observed for samples treated with 50 nM ziram (a,b, n=4). Using non-denaturing conditions/Native PAGE, a major band for ZF γ1 was detected at 480 kDa and a minor band at 242 kDa (c). n=4 *p<.05 two-tailed student t-test.

Figure 2-7: Ziram's toxicity is ZF γ1-dependent

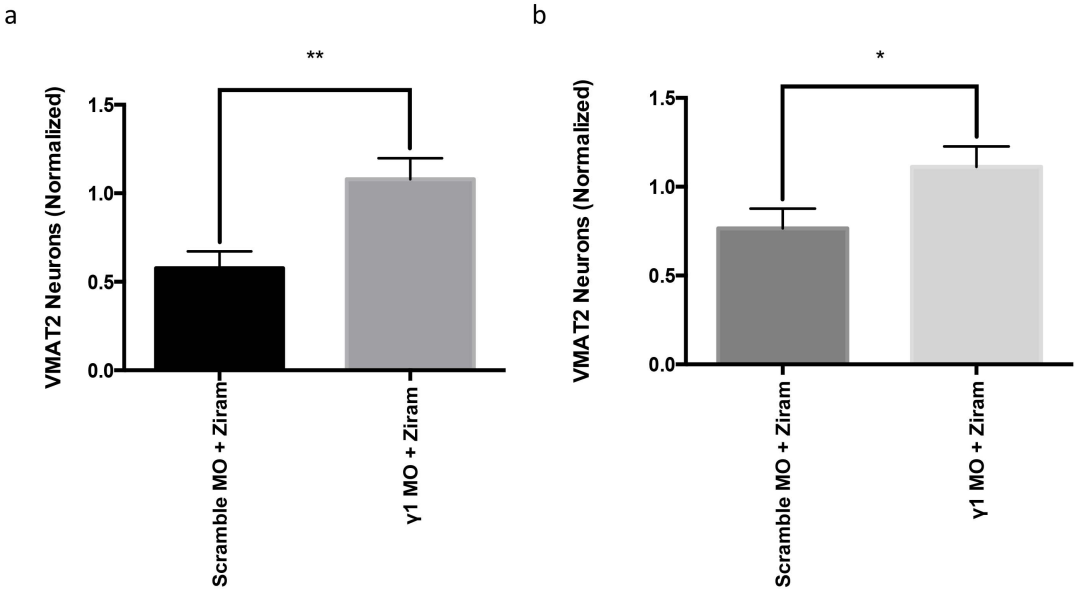

Figure 2-7: Ziram's toxicity is ZF γ1-dependent
ZF γ1 expression was reduced using a specific morpholino (MO) and a scrambled MO was used as a control. Ziram treatment began at 24 hpf. Neuronal counts (normalized to vehicle + scramble/γ1 MO) for γ1 MO injected embryos (n=14). An 86.8% increase in labeled telencephalic (a) and 45.1% increase in labeled diencepahlic (b) VMAT2 neurons at 3dpf was observed for fish treated with ziram + γ1 MO vs. ziram + scramble MO. *p<.05, **p<.01, student t-test

Figure 2-8: CLR01 inhibits ZF γ1 aggregation in vitro

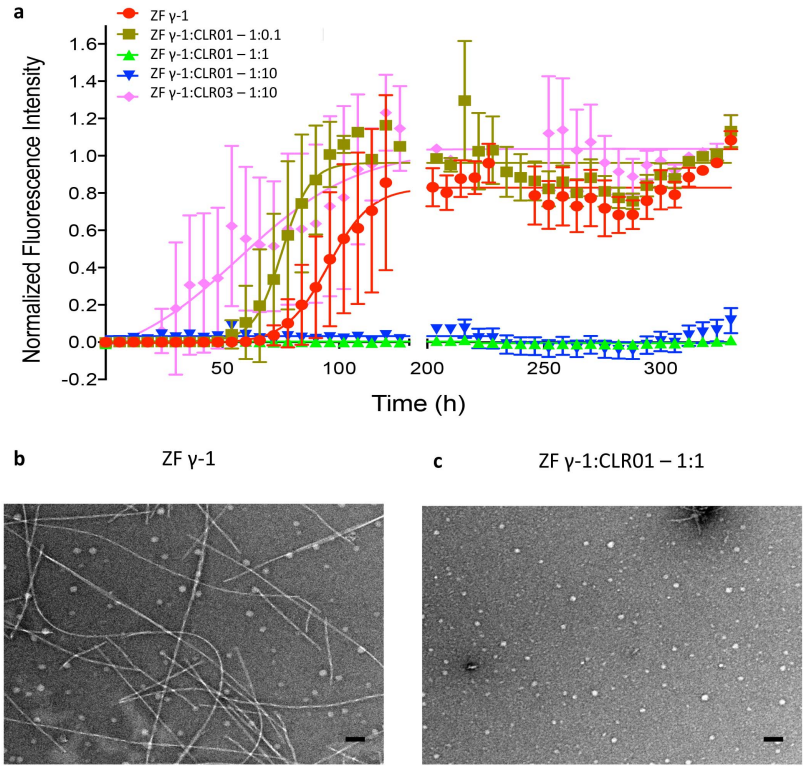

Figure 2-8: CLR01 inhibits ZF γ1 aggregation in vitro
Time-dependent change in normalized ThT fluorescence over 14 days for 100 μM γ1 incubated in the absence or presence of CLR01 (a). The first and last 130 hours are shown. Electron micrographs of ZF γ1 alone (b), and ZF γ1 with CLR01 (c) in equimolar ratio (scale bar = 100 nm) obtained on day 9 or 10 of each reaction. n=4. $p < 0.0001$. ANOVA.

Figure 2-9: CLR01 protects against ziram's toxicity in vivo.

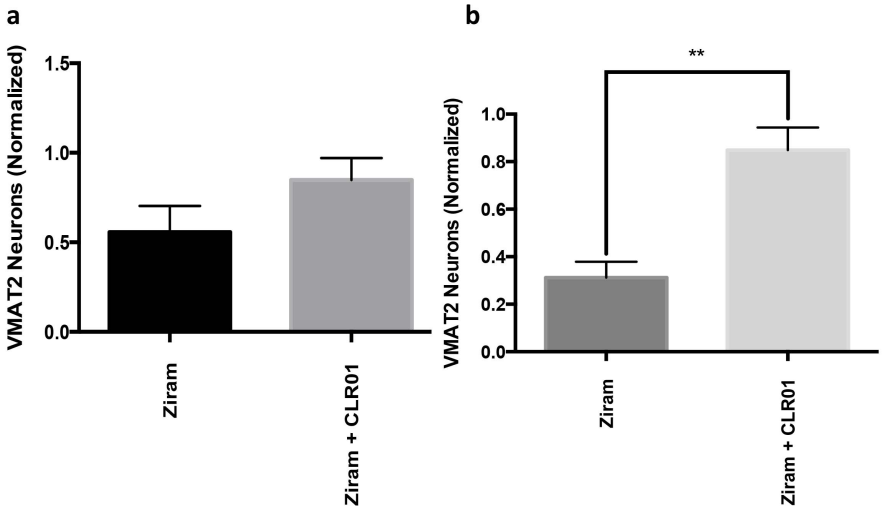

Figure 2-9: CLR01 protects against ziram's toxicity in vivo.
Using the VMAT2 ZF we evaluated whether CLR01 could protect against the toxicity of ziram. When co-treated with 50 nM ziram and CLR01, treatment with CLR01 protected against ziram's toxicity for VMAT2 neurons in the diencephalic cluster (b), but did not reach statistical significance in the telencephalic cluster (a) at 5dpf. n=6. **p<.01, student t-test.

Concluding Remarks

The studies presented here demonstrate that ziram, a pesticide that increases risk for PD, is selectively toxic for dopaminergic neurons and its toxicity is synuclein-dependent in ZF. This dissertation contributes to the growing number of studies in the neuroscience and toxicology fields, implicating environmental toxins in the development of PD. Most importantly this dissertation and the studies in it demonstrate that synuclein a protein that has been implicated directly in the pathogenesis of PD, is directly contributing to dopaminergic cell toxicity after exposure to an environmental toxin. There has been much debate in the field whether or not synuclein is the primary cause of toxicity in dopaminergic neurons in non-genetic forms of PD. Several studies have suggested that environmental toxins like pesticides may cause toxicity through inhibition of complex I, which can lead to alterations in cellular respiration, and creation of reactive oxygen species. This can cause further damage within the cell. In a recent *in vivo* study, knockdown of α-syn protected against dopaminergic cell loss in animals treated with rotenone. Furthermore, it was demonstrated that rotenone can cause dopaminergic cell toxicity *in vivo* and the pesticide triggers the spread of α-syn. Our findings add to the growing evidence that alterations in synuclein homeostasis are central to the pathogenesis of PD despite the etiology.

Additionally, this dissertation has characterized the use of ZF as a model to study the effects of neurodegenerative disease. We have demonstrated that ZF can be used to evaluate the effect of potential environmental toxins on the dopaminergic system, and can be studied using a variety of transgenic lines, genetic manipulation, and behavioral analysis. ZF will be a valuable tool going forward as we attempt to identify other environmental toxins that may increase the risk of developing neurodegenerative

diseases like PD. Also, this model system can be valuable for identifying therapeutics that may protect against the progression or prevent PD.

On a larger level we have provided further evidence *in vivo* that ziram can cause neurotoxic effects that are consistent with pathological changes often seen in PD. It is our hope that studies like this will continue to give insight into the potential toxicity of environmental compounds that are being used. Identifying compounds that can adversely affect human health will be essential for regulation and protection of public health. A better understanding of these processes has the potential to illuminate pathways critical in disease formation, and also highlight targets for future therapeutic exploitation.

Appendices

A. Aldehyde dehydrogenase inhibition as a pathogenic mechanism in Parkinson disease
B. Axon degeneration and PGC-1α-mediated protection in a zebrafish model of α-synuclein toxicity

Appendix A

Aldehyde dehydrogenase inhibition as a pathogenic mechanism in Parkinson disease

Arthur G. Fitzmaurice[a,b,c,d], Shannon L. Rhodes[e], Aaron Lulla[d], Niall P. Murphy[f], Hoa A. Lam[f], Kelley C. O'Donnell[g], Lisa Barnhill[d], John E. Casida[h,1], Myles Cockburn[i], Alvaro Sagasti[g], Mark C. Stahl[a], Nigel T. Maidment[f], Beate Ritz[d,e,j], and Jeff M. Bronstein[a,d,k]

[a]Department of Neurology, David Geffen School of Medicine at UCLA, University of California, Los Angeles, CA 90095; Departments of [b]Cellular and Molecular Neurobiology and [c]Environmental Science and Engineering, California Institute of Technology, Pasadena, CA 91125; Departments of [d]Molecular Toxicology and [g]Molecular, Cell, and Developmental Biology, UCLA, Los Angeles, CA 90095; Departments of [e]Epidemiology and [j]Environmental Health Sciences, UCLA Jonathan and Karin Fielding School of Public Health, University of California, Los Angeles, CA 90095; [f]Department of Psychiatry and Biobehavioral Sciences, Jane and Terry Semel Institute for Neuroscience and Human Behavior, UCLA, Los Angeles, CA 90095; [h]Department of Environmental Science, Policy, and Management, University of California, Berkeley, CA 94720; [i]Department of Preventive Medicine, Keck School of Medicine of University of Southern California, Los Angeles, CA 90089; and [k]Parkinson's Disease Research, Education, and Clinical Center, Greater Los Angeles Veterans Affairs Medical Center, Los Angeles, CA 90073

Contributed by John E. Casida, November 27, 2012 (sent for review October 19, 2012)

Parkinson disease (PD) is a neurodegenerative disorder particularly characterized by the loss of dopaminergic neurons in the *substantia nigra*. Pesticide exposure has been associated with PD occurrence, and we previously reported that the fungicide benomyl interferes with several cellular processes potentially relevant to PD pathogenesis. Here we propose that benomyl, via its bioactivated thiocarbamate sulfoxide metabolite, inhibits aldehyde dehydrogenase (ALDH), leading to accumulation of the reactive dopamine metabolite 3,4-dihydroxyphenylacetaldehyde (DOPAL), preferential degeneration of dopaminergic neurons, and development of PD. This hypothesis is supported by multiple lines of evidence. (*i*) We previously showed in mice the metabolism of benomyl to *S*-methyl *N*-butylthiocarbamate sulfoxide, which inhibits ALDH at nanomolar levels. We report here that benomyl exposure in primary mesencephalic neurons (*ii*) inhibits ALDH and (*iii*) alters dopamine homeostasis. It induces selective dopaminergic neuronal damage (*iv*) in vitro in primary mesencephalic cultures and (*v*) in vivo in a zebrafish system. (*vi*) In vitro cell loss was attenuated by reducing DOPAL formation. (*vii*) In our epidemiology study, higher exposure to benomyl was associated with increased PD risk. This ALDH model for PD etiology may help explain the selective vulnerability of dopaminergic neurons in PD and provide a potential mechanism through which environmental toxicants contribute to PD pathogenesis.

Parkinson disease (PD) is second only to Alzheimer disease as a prevalent neurodegenerative disorder, affecting millions worldwide. Symptoms result from the progressive degeneration of neurons, most notably dopaminergic neurons in the *substantia nigra pars compacta*. More than half of these neurons are lost by the time symptoms manifest themselves (1). Despite the identification of several genetic variants associated with familial as well as idiopathic PD, only a small fraction of total risk can be accounted for genetically (2). Thus, environmental factors almost certainly play an important role in PD. Understanding the relevant mechanisms particularly behind the selective loss of dopaminergic neurons may provide important clues to explain PD pathogenesis so that therapies can be developed to slow or reverse disease progression.

Over the past few decades, epidemiologic studies have consistently reported associations between PD occurrence and rural living, well water consumption, farming occupations, and pesticide exposure (3–12). Pesticides include diverse chemotypes that differ greatly in structures and mechanisms through which they act on target pests or produce chronic low-level exposure effects more relevant to human disease. Fungicides are among the pesticide classes warranting further investigation as potential contributors to PD pathogenesis (13); therefore, benomyl was selected for the present study.

Benomyl was widely used for three decades until accumulating toxicological evidence in laboratory mammals of liver tumors, brain malformations, reproductive effects, and possible carcinogenesis led the US Environmental Protection Agency to cancel its registration in 2001 (14), although some countries continue to use this fungicide. Several relevant mechanisms suggest benomyl may also contribute to PD pathogenesis. The fungicidal action of benomyl is thought to result from microtubule assembly impairment (15), a mechanism that has been implicated in PD (16). Microtubule inhibitors disrupt the ubiquitin-proteasome system (UPS) (17) and cause selective dopaminergic cell damage and aggregation of α-synuclein, the predominant component of an intracytosolic Lewy body, which is the pathologic hallmark of PD (16). Furthermore, benomyl inhibits aldehyde dehydrogenase (ALDH) activity in liver and brain mitochondria (18, 19), although ALDH inhibition has not been measured directly in brains in vivo. The mitochondrial-associated ALDH2 is of particular interest because it metabolizes toxic aldehydes in brain tissue, including the dopamine (DA) metabolite 3,4-dihydroxyphenylacetaldehyde (DOPAL) (Fig. 1). DOPAL has been shown to be neurotoxic and has been suggested to contribute to PD pathogenesis (20–23), although a link with an environmental toxicant has not been established. The accumulation of DOPAL resulting from ALDH inhibition offers potential relevance to the preferential loss of dopaminergic neurons observed in PD.

Benomyl decomposes spontaneously, creating a reservoir for slow release of carbendazim and butyl isocyanate (BIC) (Fig. 1). We previously showed that benomyl inhibits ALDH activity in vivo with indirect evidence in brains as elevated acetaldehyde levels upon ethanol challenge (18). The ALDH inhibitory activity is caused by BIC and its downstream metabolites including *S*-methyl *N*-butylthiocarbamate (MBT), which is further converted by cytochrome P450 (CYP) enzymes to MBT sulfoxide (MBT-SO), a very potent ALDH inhibitor (18). We have also shown that benomyl is an inhibitor of 26S UPS activity (24), but here we find that this occurs at micromolar concentrations. The present study shows that nanomolar concentrations of benomyl metabolite(s) inhibit ALDH activity, resulting in accumulation of toxic aldehydes (e.g., DOPAL) and dopaminergic neuronal loss in vitro and in vivo. Furthermore, we report an association between benomyl exposure and PD occurrence in a human population. This investigation integrates cellular and in vivo models with human patients and environmental exposure data in the study of PD. These findings identify ALDH dysfunction as a plausible pathway

Author contributions: A.G.F., S.L.R., J.E.C., B.R., and J.M.B. designed research; A.G.F., S.L.R., A.L., N.P.M., H.A.L., K.C.O., and M.C.S. performed research; J.E.C., M.C., and A.S. contributed new reagents/analytic tools; A.G.F., S.L.R., N.P.M., L.B., and N.T.M. analyzed data; and A.G.F., S.L.R., J.E.C., and J.M.B. wrote the paper.

The authors declare no conflict of interest.

[1]To whom correspondence should be addressed. E-mail: ectl@berkeley.edu.

This article contains supporting information online at www.pnas.org/lookup/suppl/doi:10.1073/pnas.1220399110/-/DCSupplemental.

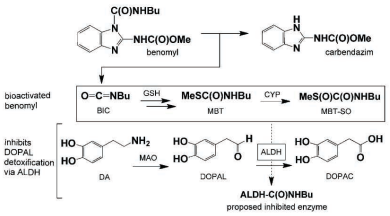

Fig. 1. ALDH inhibition as the proposed mechanism of benomyl-induced Parkinson disease. Benomyl is efficiently metabolized to potent ALDH inhibitors—BIC, MBT, and particularly MBT-SO—so exposure leads to the accumulation of the toxic dopamine metabolite DOPAL. This offers a possible explanation for the selective toxicity to dopaminergic neurons observed in PD pathogenesis. GSH, glutathione.

in PD pathogenesis and potential therapeutic target for developing disease-modifying therapies.

Results

ALDH Inhibition in Primary Neurons and Mitochondrial Preparations. We previously reported that benomyl inhibits ALDH activity in mouse mitochondria (18); we extend the study here to direct measurement in primary neurons using a cell-based assay in which fluorescence increases with ALDH activity. Exposure of ex vivo suspensions of nigral neurons to benomyl for 30 min resulted in concentration-dependent ALDH inhibition (Fig. 2*A*). ALDH activity was inhibited by 19 ± 0.4% ($P = 4.6 \times 10^{-7}$, $n = 3$) at the lowest concentration tested (0.1 μM), progressively increasing to 35 ± 0.6% inhibition at the highest concentration tested (20 μM; $P = 2.7 \times 10^{-20}$, $n = 10$). MBT exposure (10 μM) inhibited ALDH activity by 12 ± 1% ($P = 2.9 \times 10^{-5}$, $n = 5$). In contrast, carbendazim was ineffective at concentrations up to 20 μM (Fig. 2*A*). We also quantitated the ALDH IC_{50} values of benomyl and its metabolites using mitochondria isolated from rat liver (Fig. 2 *B* and *D*). Benomyl and BIC were essentially equipotent with IC_{50} values of 0.12–0.14 μM. MBT had an IC_{50} of 1.3 μM, whereas carbendazim did not inhibit ALDH activity (Fig. 2 *B* and *D*). These results are consistent with those of Staub et al. for hepatic mitochondria prepared from mice (18).

UPS Inhibition. We previously reported that benomyl is a UPS inhibitor (24), but the inhibiting moiety was not determined. Benomyl inhibited the 26S UPS with an IC_{50} of 5.7 μM after a 48-h exposure in an SK-*N*-MC neuroblastoma cell line (Fig. 2 *C* and *D*). Carbendazim had the same effect (IC_{50} = 5.7 μM), whereas MBT did not inhibit the UPS, suggesting that the carbendazim moiety is responsible for benomyl's inhibition of the UPS at micromolar concentrations.

Selective Dopaminergic Neurotoxicity in Vitro. Immunocytochemistry against tyrosine hydroxylase (TH^+) and neuronal nuclei ($NeuN^+$) was conducted on primary mesencephalic cultures to determine the toxicities of benomyl and metabolites on dopaminergic and total neurons (Fig. 3 *A* and *B*). Benomyl was selectively toxic to dopaminergic neurons, resulting in a 24 ± 6% decrease in TH^+ cells at 0.1 μM and a 35 ± 4% decrease at 1 μM after 48-h exposures (Fig. 3*C*) with no significant loss of total $NeuN^+$ neurons at either concentration (e.g., 1 μM, 3 ± 14% change, $P = 0.79$), demonstrating the selective toxicity of benomyl. The total number of $NeuN^+$ neurons (i.e., total neurons) did not significantly change despite the loss of TH^+ neurons because TH^+ cells only contributed on the order of 1% of total neurons counted. MBT exposure (1 μM) resulted in a 27 ± 6% decrease in TH^+ cells (Fig. 3*C*), comparable to benomyl exposure, and similarly had no effect on $NeuN^+$ cells. In contrast, carbendazim exposure alone had no significant effect on TH^+ or $NeuN^+$ neuron counts, and there was no synergistic effect when cells were exposed simultaneously to MBT and carbendazim. These results suggest that benomyl's neurotoxicity is due to MBT, and therefore ALDH inhibition, at the concentrations tested.

ALDH Inhibition as a Neurotoxic Mechanism. We hypothesized that benomyl's selective toxicity to TH^+ neurons was caused by its effects on DA metabolism. DA is oxidized by monoamine oxidase (MAO) to form DOPAL, which is then further oxidized to 3,4-dihydroxyphenylacetic acid (DOPAC) by ALDH (Fig. 1). We were unable to measure DOPAL concentration ([DOPAL]) directly because of its instability and very low concentrations in cultures, so we measured [DA] and [DOPAC] to determine if DA homeostasis shifted with benomyl treatment. A subset of primary cultures treated with benomyl was sacrificed at 3 h. [DOPAC] was 42 ± 11% less in benomyl-treated cultures ($P = 0.034$, $n = 16$), and [DA] remained relatively unchanged (1% decrease, $P = 0.44$), so [DOPAC]/[DA] was 38 ± 13% less ($P = 0.035$), consistent with ALDH inhibition in these neurons. To test if accumulation of ALDH substrates (i.e., DOPAL) caused benomyl's neurotoxicity, DOPAL formation was inhibited with the MAO inhibitor pargyline. TH^+ neuronal loss was attenuated by 30 ± 9% ($P = 0.14$, n = 13–14; Fig. 4) in cultures cotreated with pargyline (200 μM) and benomyl (1 μM). Pargyline completely prevented neurotoxicity in cultures treated with MBT (1 μM), a less potent ALDH inhibitor ($P = 0.011$, n = 14–15). Pargyline alone had no effect on TH^+ neuronal counts at this concentration.

α-Synuclein Levels. The major pathologic hallmark of PD is the formation of Lewy bodies which are comprised primarily of α-synuclein aggregates. α-Synuclein levels measured using immunocytochemistry in surviving dopaminergic neurons did not change significantly in TH^+ neurons exposed to benomyl, MBT, carbendazim, or a combination of MBT and carbendazim.

Selective Aminergic Neurotoxicity in Vivo. Zebrafish have been used in developmental toxicology studies, and they are now being used

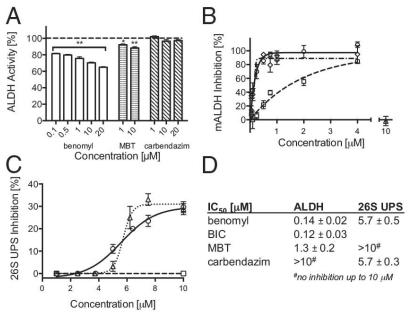

Fig. 2. Inhibitory actions of benomyl and its metabolites. (*A*) Exposure to benomyl or MBT, but not carbendazim, inhibited ex vivo ALDH activity in mesencephalic neurons dissociated from 2-d-old rat pups (n = 3–11). (*B*) Benomyl, BIC, and MBT inhibited in vitro mitochondrial ALDH activity (n = 2–8 at each concentration tested). Carbendazim did not significantly inhibit mALDH activity at up to 20 μM (n = 4). (*C*) Benomyl and carbendazim inhibited 26S UPS activity in SK-*N*-MC neuroblastoma cells (n = 4–14 at each concentration tested), whereas MBT exposure up to 10 μM had no effect (n = 5). (*D*) Benomyl/BIC/MBT inhibit ALDH activity at lower concentrations than benomyl/carbendazim inhibit the 26S UPS. Data are expressed as percent relative to vehicle controls (0.01% DMSO), except for 26S UPS inhibition which is relative to treatment with the 26S UPS inhibitor lactacystin (5 μM). *$P < 0.01$, **$P < 0.0001$; benomyl (○), BIC (◇), MBT (□), carbendazim (△). mALDH, mitochondrial aldehyde dehydrogenase; 26S UPS, ubiquitin-proteasome system.

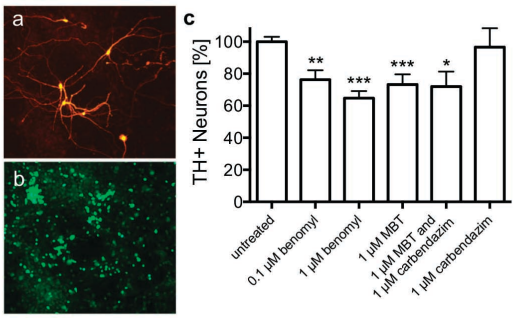

Fig. 3. Dopaminergic neuronal damage in primary mesencephalic cultures exposed to benomyl or its metabolites. Representative field of view (20×) shows untreated immunoreactive (*A*) dopaminergic neurons (TH^+) and (*B*) neuronal nuclei ($NeuN^+$). (*C*) Benomyl neurotoxicity was recapitulated by MBT exposure, whereas carbendazim was not toxic to TH^+ neurons at 1 μM. $NeuN^+$ counts were unaffected by any treatment. Because MBT is either the proximal or penultimate benomyl metabolite that inhibits ALDH activity, there appears to be an association between neuronal damage and ALDH inhibition; proteasomal inhibition by the carbendazim moiety is not sufficient to kill cells under the same conditions. Data are expressed as percent relative to vehicle controls (0.01% DMSO). $*P < 0.05$, $**P < 0.01$, $***P < 0.0001$.

to investigate neurotoxicity (25). To test the specificity of benomyl neurotoxicity in a vertebrate system, a model was developed using transgenic zebrafish (*Danio rerio*) lines that label specific neuronal populations with GFP that can be visualized because embryos are transparent. Zebrafish have a well-developed dopaminergic system. The anterior clusters shown in Fig. 5 *A* and *B* correspond to aminergic neurons in the olfactory bulb and telencephalon of *ETvmat2:GFP* zebrafish (26) embryos; the posterior clusters contain the diencephalon. These clusters are predominantly dopaminergic, although they also include some (nor)adrenergic neurons (27). Exposure to 1 μM benomyl from 5 h until 120 h postfertilization resulted in a 24 ± 9% decrease in $VMAT2^+$ (vesicular monoamine transporter) neuronal counts in anterior clusters ($P = 0.041$, $n = 19$; Fig. 5*G*) and an 18 ± 9% decrease in diencephalic clusters ($P = 0.15$), constituting an overall 22 ± 8% decrease in $VMAT2^+$ neurons ($P = 0.043$). Fluorescence similarly trended lower by 25 ± 13% (anterior, $P = 0.16$; Fig. 5*H*), 38 ± 13% (diencephalon, $P = 0.061$), and 27 ± 12% (overall, $P = 0.089$). *Tg(isl1[ss]:Gal4-VP16,UAS:EGFP)*^{zf154} embryos (28) that were exposed to the same conditions exhibited no significant differences in neuron counts or fluorescence in Rohon-Beard (Fig. 5 *C* and *D*) or trigeminal (Fig. 5 *E* and *F*) sensory neurons. Even the complex axons were unaffected, adding further evidence that benomyl is toxic to dopaminergic neurons in a selective manner (Fig. 5 *G* and *H*). Benomyl exposure under these conditions was not lethal to zebrafish embryos, but swimming behavior was altered. After 2 wk of exposure, benomyl-treated zebrafish exhibited a 45 ± 10% deficit in spontaneous swimming distance versus unexposed zebrafish ($P = 0.006$, $n = 11$–15), suggesting that benomyl's selective toxicity to dopaminergic neurons has functional significance in vivo.

Epidemiologic Association. Potential association between benomyl exposure and PD occurrence was investigated in an epidemiologic study to determine the possible relevance of these findings that benomyl exposure resulted in selective dopaminergic neuronal damage in vitro and in vivo. These analyses included 360 PD patients ("cases") and 754 neurologically normal subjects ("controls") (Table S1). PD risk increased 67% for individuals with estimated ambient benomyl exposure at their workplace equal to or above the median level (OR = 1.67, 95%CI: 1.19–2.34; $P = 0.0027$; Table S2). This risk increased to almost twofold for those with estimated exposures in the highest quartile (OR = 1.97, 95%CI: 1.29–3.02; $P = 0.0017$), revealing a dose–response trend ($P = 0.0019$; Table 1). There was no trend between benomyl exposure and PD based on residential addresses. These analyses had been adjusted for known PD risk factors (e.g., age, sex), and the findings did not change in sensitivity analyses adjusting for race/ethnicity or family history of PD, or when excluding subjects potentially overrepresenting particular residential clusters or missing 1 or more years of occupational data.

Discussion

PD etiology has proven very difficult to determine using various genetic models and epidemiologic studies. It likely includes a combination of genetic and environmental contributions, so investigations involving environmental toxicants may help elucidate the complex mechanisms at play. The recognition of new epidemiologic contributors to PD etiology expands the consideration of possible mechanisms involved. The proposed environmental contributor here is benomyl, recognized in an epidemiologic investigation, and this suggests ALDH inhibition in humans contracting PD. Because direct causality of environmental risk factors cannot be tested in humans, this investigation sought to determine if exposure in experimental models could recapitulate some of the pathologic features of PD. Here we report selective dopaminergic neuronal damage in both an in vitro system (primary cultures) and an in vivo zebrafish model. There was significant loss in zebrafish aminergic neurons measured both by neuron counts and fluorescence, whereas the nonaminergic trigeminal and Rohon-Beard sensory neurons remained intact after benomyl exposure. A selective loss of dopaminergic neurons was similarly observed in mesencephalic cultures exposed to benomyl, reflecting the preferential loss of dopaminergic neurons characteristic of PD.

Benomyl's action as a fungicide is thought to be due to its ability to impair microtubule assembly, interfering with mitosis and other processes (29, 30). Microtubule inhibitors such as nocodazole and rotenone also inhibit the UPS (17). We found that the carbendazim moiety of benomyl, a known microtubule inhibitor, confers benomyl's UPS inhibitory activity. However, it is unlikely that microtubule or UPS dysfunction is responsible for benomyl's toxicity observed in primary cultures or zebrafish, given the low concentrations used relative to its IC_{50} (5.7 μM). [Because concentrations in the range of 1.3–50 μM are necessary for benomyl's use as a fungicide in the environment (31–33), we used a conservative concentration range (0.1–1 μM) in primary cultures and zebrafish to enhance relevance to actual exposures for humans.] Furthermore, carbendazim had no effect on neuronal survival at 1 μM, whereas MBT recapitulated benomyl's

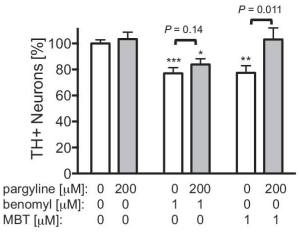

Fig. 4. Monoamine oxidase (MAO) inhibitor protects against neurotoxicity because of DOPAL accumulation. Neuronal loss resulting from 1 μM benomyl or MBT exposure was mitigated by cotreatment with the MAO inhibitor pargyline (200 μM, n = 13–28). Because MAO inhibition reduces the metabolism of dopamine to DOPAL, this suggests that DOPAL is toxic to dopaminergic neurons and that benomyl is toxic via DOPAL accumulation as a result of ALDH inhibition. Data are expressed as percent relative to vehicle controls (0.01% DMSO). $*P = 0.0027$, $**P = 2.4 \times 10^{-4}$, $***P = 6.1 \times 10^{-5}$.

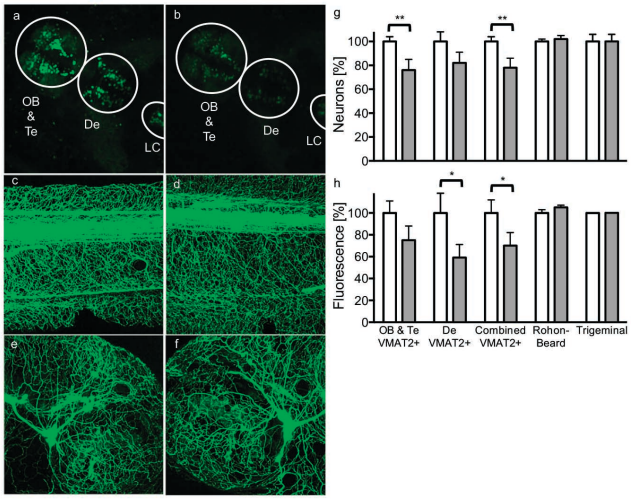

Fig. 5. Aminergic neuronal damage in *Danio rerio* embryos exposed to benomyl. Representative confocal images of zebrafish embryos (*A*, *C*, and *E*) unexposed or (*B*, *D*, and *F*) bathed in 1 μM benomyl from 5 h until 120 h postfertilization are shown. (*G*) Neuronal counts (*A* and *B*) decreased in VMAT2$^+$ anterior and diencephalic clusters of *ETvmat2:GFP* zebrafish exposed to benomyl (solid bars) but were unaffected in (*C* and *D*) Rohon-Beard and (*E* and *F*) trigeminal neurons in *Tg(isl1[ss]:Gal4-VP16,UAS:EGFP)*^{zf154} zebrafish. (*H*) Measurement of total fluorescence yielded similar results. Data are expressed as percent relative to vehicle controls (0.01% DMSO). *$P < 0.1$, **$P < 0.05$. De, diencephalon; LC, locus coeruleus; OB, olfactory bulb; Te, telencephalon.

toxicity. Because benomyl and its metabolite MBT, but not carbendazim, inhibit ALDH activity at the concentrations used, ALDH inhibition likely confers benomyl's neurotoxicity. Additional support for the potential role of toxicant-induced ALDH inhibition in the pathogenesis of PD comes from a report from Wey et al. that describes TH$^+$ neuronal loss, DOPAL accumulation, and motobehavioral deficits in mice lacking cytosolic and mitochondrial ALDH (*Aldh1a1*$^{-/-}$*xAldh2*$^{-/-}$) (34). Their work demonstrated that ALDH inhibition can recapitulate some pathologic aspects of PD in an in vivo model. It is remarkable that the environmental impact of benomyl exposure in the present work yielded similar results in vitro and in vivo as their targeted genetic approach. This is in contrast to another fungicide, ziram, which increases α-synuclein levels and damages dopaminergic cells by inhibiting E1 ligase activity in the UPS (35). Benomyl appears to act via a novel mechanism (ALDH inhibition), damaging dopaminergic cells via alterations in DA homeostasis, independent of α-synuclein.

Our observed alterations in DA metabolites after benomyl exposure add further evidence that ALDH inhibition is the cause of benomyl's neurotoxicity. Goldstein et al. similarly found that striatal [DOPAL]:[DA] was four times higher in postmortem PD brains (36). They also observed decreased VMAT2 activity (37). Burke et al. reported that DOPAL is 400-fold more toxic to dopaminergic neurons in vivo than its precursor (i.e., DA) or its ALDH product (i.e., DOPAC) (21–23), potentially because of

Table 1. Associations between estimated ambient occupational or residential benomyl exposures and PD risk in the UCLA PEG Study

Exposure, *n* (%)*	Cases (*n* = 360)	Controls (*n* = 754)	OR (95%CI)†	*P* value‡
Occupational				
No	217 (60.3)	531 (70.4)	Reference	
First quartile	23 (6.4)	55 (7.3)	0.90 (0.53–1.53)	0.69
Second quartile	26 (7.2)	51 (6.8)	1.07 (0.64–1.79)	0.81
Third quartile	40 (11.1)	62 (8.2)	1.38 (0.88–2.17)	0.16
Fourth quartile	54 (15.0)	55 (7.3)	1.97 (1.29–3.02)	0.0017
Trend *P* value				0.0019
Residential				
No	209 (58.1)	467 (61.9)	Reference	
First quartile	31 (8.6)	71 (9.4)	0.87 (0.54–1.40)	0.56
Second quartile	41 (11.4)	72 (9.5)	1.14 (0.73–1.77)	0.57
Third quartile	31 (8.6)	73 (9.7)	0.79 (0.49–1.27)	0.34
Fourth quartile	48 (13.3)	71 (9.4)	1.20 (0.78–1.86)	0.40
Trend *P* value				0.071

CI, confidence interval; OR, unconditional logistic odds ratio.

*Exposure quartiles defined using distributions of exposed controls, separately for occupational or residential estimates. Two cases and one control with incomplete occupational data and one case with incomplete residential data were assumed to be unexposed.

†Adjusted for age (continuous), sex (male/female), smoking status (current/former/never), county (Fresno/Kern/Tulare, California), and education (<12 y/=12 y/>12 y).

‡For multiple testing considerations, 8 tests were performed so a *P* value of 0.006 was considered statistically significant.

the formation of reactive radicals and quinones (38). VMAT2 inhibition could provide a larger reservoir of cytosolic DA, making neurons more susceptible to DOPAL toxicity. Thus, benomyl's selective toxicity to dopaminergic neurons can be explained by ALDH inhibition leading to toxic DOPAL accumulation. Consistent with this hypothesis, reducing DOPAL synthesis with an MAO inhibitor mitigated benomyl's toxicity.

The present work reveals ALDH inhibition as a toxicant-induced neurotoxic mechanism and adds an epidemiologic association that suggests the relevance of this mechanism in a human population. The University of California Los Angeles (UCLA) Parkinson's Environment and Genes (PEG) Study is unique in its ability to use data from state-mandated commercial agricultural Pesticide Use Reporting forms to overcome subject recall bias and to determine associations with specific toxicants in a heavy pesticide use region of California. Here we show that chronic exposure to ambient benomyl at the workplace was associated with 67% to almost twofold increases in risk of developing PD after adjusting for known PD risk factors. Analyses based on workplace addresses potentially incorporate the best estimates of subjects' ambient benomyl exposures because pesticide applications occur during the workday when subjects would have been at their workplace rather than their residence. Notably, this model only estimates relative ambient exposures and does not take into account other routes of exposures such as occupational handling of pesticides and drinking well water, both associated with increased risk of PD, which could exacerbate the estimated risk even further (39–41). We have used this method to report positive associations between PD onset and exposures to ziram, maneb, and paraquat (42, 43). In a logistic regression model that includes our benomyl variable and a variable for the combination of ziram, maneb, and paraquat, the benomyl association remains robust and the confidence interval excludes the null.

Concluding Remarks

Benomyl was widely used in the United States for three decades until toxicological evidence revealed its potential to elicit liver tumors, brain malformations, reproductive effects, and carcinogenesis. In 2001, the registrants of benomyl voluntarily canceled their commercial use registrations, and the US Environmental Protection Agency has not granted additional registrations (14). The present work adds a PD association to these toxicological investigations and demonstrates the possibility for long-lasting toxicological effects of pesticide use even a decade after chronic exposure. This work suggests that exposure to an environmental toxicant may inhibit ALDH sufficiently to damage dopaminergic neurons and increase the risk of exposed humans developing PD. This finding may be generalizable to all PD patients, so augmenting ALDH activity may be a potential therapeutic target for designing disease-modifying therapies for PD regardless of environmental exposures.

Methods

ALDH Activity Assays. All procedures using animals were approved by the UCLA Animal Research Committee. Mesencephalic neurons (postnatal day 2) were dissected and dissociated as described for primary cultures below. Instead of plating, neurons were resuspended in buffer from the Aldefluor kit (STEMCELL Technologies). Aldefluor was added (1 μL/mL) to the neuronal suspension, and 300-μL aliquots were immediately transferred to culture tubes containing 3 μL of test compound solutions, resulting in final concentrations of 100 nM–20 μM. Culture tubes were incubated at 37 °C for 30 min with periodic gentle shaking. Using FACS (XL-MCL, Beckman), cells were gated by forward- and side-scatter, and intracellular green fluorescence was measured on channel FL1. ALDH inhibition was determined by comparing fluorescence in the presence or absence of test compounds.

Rat hepatic mitochondria were isolated using published protocols (44, 45). These preparations (10 μL) were exposed to test compounds for 5 min in 170 μL of 50 mM pyrophosphate buffer (pH 9.0), 50 mM NAD^+, 0.1 mM pyrazole, 0.5% (wt/vol) sodium deoxycholate, and 2 μM rotenone (added in 2.7 μL methanol). Absorbance at 340 nm was monitored for 10 min at 5-s intervals after 1 mM acetaldehyde (20 μL) was added (SpectraMax $340PC^{384}$ Absorbance Microplate Reader, SoftMax Pro software, Molecular Devices). ALDH activity was determined from the slope as the increase in absorbance over time from 1 to 3 min.

26S UPS Activity Assay. The 26S UPS activity was determined by FACS as previously described (24). Briefly, neuroblastoma SK-*N*-MC cells transfected with an EGFP–degron fusion protein and passaged multiple times were exposed to test compounds for 48 h at 2 mL/well before FACS analysis (Beckman XL-MCL). UPS inhibition was inferred from high fluorescence corresponding to the level of EGFP–degron fusion protein that was not selectively degraded by the proteasome (46).

Primary Neuronal Cultures. Primary neuronal cultures were prepared using a protocol adapted from Rayport et al. and previously described (35, 47). Briefly, mesencephalic cells containing the *substantia nigra pars compacta* (excluding the ventral tegmental area) were dissected from coronal sections of brains from postnatal day 1 or 2 rat pups, dissociated in papain, and plated onto glial cells at densities of 4×10^5 per coverslip. Cultures were grown for 6–8 d and then treated by exchanging 1 mL of the media in each plate with 1 mL of fresh media amended with test compound(s) and vehicle (0.01% DMSO).

Cultures after 48-h treatment were fixed in paraformaldehyde (4% wt/vol) for 30 min, washed with PBS, blocked with normal donkey serum (5% vol/vol) and Triton X-100 (0.5% vol/vol) in PBS for 1–2 h, incubated with antibodies against TH (1:1,500, anti-rabbit, Calbiochem) and NeuN (1:200, anti-mouse, Millipore) overnight at 4 °C, washed with 3× and 1× PBS, incubated with Alexa Fluor 488 (1:200, Invitrogen) and 555 (1:1,500, Invitrogen) secondary antibodies at room temperature for 2 h, and washed with Tween-20 (0.1%) in PBS and then with PBS before coverslipping. All TH-immunoreactive neurons were counted, and NeuN-immunoreactive neuron counts were estimated for each coverslip from neurons quantified in five representative fields of view using a 20× objective. Quantification was determined by blinded raters. Some cultures were incubated with antibodies against TH and α-synuclein (1:500, anti-mouse, BD Biosciences). Relative levels of α-synuclein in TH^+ cells were determined as previously described (35), using the GNU Image Manipulation Program (GIMP 2.6).

To determine cell levels of dopamine and its metabolites, some cultures were extracted with perchloric acid (100 mM) and EDTA (0.1% wt/vol) and stored at −80 °C until HPLC analysis. Samples were separated on a C18 reverse phase column (TSKgel Super ODS 2 μm particle size, 10 × 2.1 mm, maintained at 33 °C, Tosoh Bioscience) using a mobile phase (2.5% methanol, 100 mg/L sodium-1-octane sulfonate, 42 mM citric acid, 38 mM sodium acetate, 50 mg/L EDTA) pumped at 0.2 mL/min (LC-10AD pump, Shimadzu). Monoamines and metabolites were oxidized on a glassy carbon electrode against an Ag/AgCl reference (Antec Leyden) with an applied potential of 0.75V. Data were collected using EzChrom software (Agilent).

In Vivo Studies. Zebrafish embryos were bathed in 1 μM benomyl or vehicle (0.01% DMSO) in E3 medium for zebrafish embryos from 5 h until 120 h postfertilization, anesthetized using tricaine methanesulfonate (0.02%), fixed in paraformaldehyde (4%) overnight, and mounted in agarose (1.2% wt/vol) for confocal imaging at 20× magnification. Zebrafish expressing GFP tagged to vesicular monoamine transporter protein (*ETvmat2:GFP*) were used to identify $VMAT2^+$ (dopaminergic, (nor)adrenergic, serotonergic) neurons in whole embryos (26). Approximately 100 optical sections were gathered for each embryo, spaced 1.34 μM apart, using a Zeiss LSM 5 Pascal inverted microscope. Images were reconstituted, and clusters of anterior (including olfactory bulb and telencephalon) and diencephalic neurons were identified for analyses. Peripheral sensory neurons (trigeminal and Rohon-Beard) were visualized using the *Tg(isl1[ss]:Gal4-VP16,UAS:EGFP)*^{zf154} transgenic line, which has been referred to as *Tg(sensory:GFP)* (28). Approximately 60 optical sections were spaced 3 μM apart, using a Zeiss LSM 510 inverted microscope. Cells were counted blindly in 3D projections, and fluorescence in composite images was measured blindly using ImageJ (National Institutes of Health). Spontaneous zebrafish movement was monitored with ZebraLab (Viewpoint Life Sciences, Inc.). Total distance was measured by tracking individual embryos for 30 min. Embryos were considered immobile at 0–2 mm/s.

Epidemiologic Study. This investigation was conducted as part of the UCLA PEG Study (Table S1). Written informed consent was obtained from all enrolled subjects, and all procedures were approved by the UCLA Human Subjects Committee. Subject recruitment methods and case definition criteria have been described in detail (42). Pesticide exposure assessments were performed using a geographic information system–based computer model

incorporating Pesticide Use Reporting forms that have been mandated by the California Department of Pesticide Regulation since 1974 and provide information on the location, date, and amount of pesticide in each commercial application (43, 48–50). Geocoded lifetime occupational and residential addresses were considered separately. Ambient exposure was assumed to be proportional to the amount of pesticide applied to crop acreage within a 500-m radius surrounding the subject's address averaged over the 26-y period (1974–1999). Exposure was categorized by the median in controls, resulting in a three-level variable (unexposed, exposure below the median, exposure equal to or above the median). For quartile analyses, exposure was categorized by quartiles in exposed controls, resulting in a five-level variable (unexposed, four quartiles).

Statistical Analyses. Demographic characteristics were compared for deviation from expected by χ^2 test (categorical variables) or for difference in mean by *t* test (age). Logistic regression analyses were performed on the epidemiologic data using SAS 9.1 (SAS Institute Inc.). Odds ratios and 95% confidence intervals were estimated after adjusting for age (continuous variable), sex (male/female), county of residence (Fresno/Kern/Tulare, California), education (less than 12 y of schooling/12 y or completion of general education development test/more than 12 y), and smoking status (current/former/never). Sensitivity analyses were performed to assess the effects of adjustments for race (Caucasian/non-Caucasian) and family history of PD (first-degree family history present/absent). Additional sensitivity analyses were performed excluding 23 controls who had lived in the same cluster as another control at the time of recruitment for at least 2 y before 1999, and excluding 44 cases and 95 controls who were missing one or more occupational addresses from 1974 to 1999. For trend tests, quartile categories were assigned scores of 0, 1, 2, 3, or 4 and entered into the logistic regression equation as a linear term. The Wald statistic was used as a test for linear trend of the odds ratio. In biochemical assays, IC_{50} values were determined using sigmoidal curve fits of percent inhibition at varying concentrations (PRISM 5, GraphPad). For all other analyses, statistical significance was determined using a paired *t* test.

ACKNOWLEDGMENTS. We thank Dr. Neil Harris for use of the Zeiss LSM 5 Pascal microscope. This work was funded in part by National Institute of Environmental Health Sciences Grants P01ES016732, R01ES010544, 5R21ES16446-2, and U54ES012078; National Institute of Neurological Disorders and Stroke Grant NS038367; the Veterans Affairs Healthcare System (Southwest Parkinson's Disease Research, Education, and Clinical Center); the Michael J. Fox Foundation; the Levine Foundation; and the Parkinson Alliance. A.G.F. was supported in part by a National Defense Science and Engineering Graduate Fellowship and US Department of Health and Human Services Ruth L. Kirschstein Institutional National Research Service Award T32ES015457 in Molecular Toxicology (to the University of California, Los Angeles).

1. Fearnley JM, Lees AJ (1991) Ageing and Parkinson's disease: Substantia nigra regional selectivity. *Brain* 114(Pt 5):2283–2301.
2. Nalls MA, et al.; International Parkinson Disease Genomics Consortium (2011) Imputation of sequence variants for identification of genetic risks for Parkinson's disease: A meta-analysis of genome-wide association studies. *Lancet* 377(9766):641–649.
3. Priyadarshi A, Khuder SA, Schaub EA, Priyadarshi SS (2001) Environmental risk factors and Parkinson's disease: A metaanalysis. *Environ Res* 86(2):122–127.
4. Ascherio A, et al. (2006) Pesticide exposure and risk for Parkinson's disease. *Ann Neurol* 60(2):197–203.
5. Firestone JA, et al. (2005) Pesticides and risk of Parkinson disease: A population-based case-control study. *Arch Neurol* 62(1):91–95.
6. Moisan F, et al. (2011) The relation between type of farming and prevalence of Parkinson's disease among agricultural workers in five French districts. *Mov Disord* 26(2):271–279.
7. Petrovitch H, et al. (2002) Plantation work and risk of Parkinson disease in a population-based longitudinal study. *Arch Neurol* 59(11):1787–1792.
8. Kamel F, et al. (2007) Pesticide exposure and self-reported Parkinson's disease in the agricultural health study. *Am J Epidemiol* 165(4):364–374.
9. Tanner CM, et al. (2011) Rotenone, paraquat, and Parkinson's disease. *Environ Health Perspect* 119(6):866–872.
10. Dhillon AS, et al. (2008) Pesticide/environmental exposures and Parkinson's disease in East Texas. *J Agromed* 13(1):37–48.
11. Hancock DB, Martin ER, Vance JM, Scott WK (2008) Nitric oxide synthase genes and their interactions with environmental factors in Parkinson's disease. *Neurogenetics* 9(4):249–262.
12. Elbaz A, et al. (2004) CYP2D6 polymorphism, pesticide exposure, and Parkinson's disease. *Ann Neurol* 55(3):430–434.
13. Hatcher JM, Pennell KD, Miller GW (2008) Parkinson's disease and pesticides: a toxicological perspective. *Trends Pharmacol Sci* 29(6):322–329.
14. Environmental Protection Agency (2001) Benomyl's cancellation order. *Fed Regist* 66: 41589–41591.
15. Gupta K, et al. (2004) Antimitotic antifungal compound benomyl inhibits brain microtubule polymerization and dynamics and cancer cell proliferation at mitosis, by binding to a novel site in tubulin. *Biochemistry* 43(21):6645–6655.
16. Ren Y, Liu W, Jiang H, Jiang Q, Feng J (2005) Selective vulnerability of dopaminergic neurons to microtubule depolymerization. *J Biol Chem* 280(40):34105–34112.
17. Chou AP, Li S, Fitzmaurice AG, Bronstein JM (2010) Mechanisms of rotenone-induced proteasome inhibition. *Neurotoxicology* 31(4):367–372.
18. Staub RE, Quistad GB, Casida JE (1998) Mechanism for benomyl action as a mitochondrial aldehyde dehydrogenase inhibitor in mice. *Chem Res Toxicol* 11(5):535–543.
19. Leiphon LJ, Picklo MJ, Sr. (2007) Inhibition of aldehyde detoxification in CNS mitochondria by fungicides. *Neurotoxicology* 28(1):143–149.
20. Marchitti SA, Deitrich RA, Vasiliou V (2007) Neurotoxicity and metabolism of the catecholamine-derived 3,4-dihydroxyphenylacetaldehyde and 3,4-dihydroxyphenylglycolaldehyde: The role of aldehyde dehydrogenase. *Pharmacol Rev* 59(2):125–150.
21. Burke WJ, et al. (2004) Neurotoxicity of MAO metabolites of catecholamine neurotransmitters: Role in neurodegenerative diseases. *Neurotoxicology* 25(1-2):101–115.
22. Burke WJ, Li SW, Williams EA, Nonneman R, Zahm DS (2003) 3,4-Dihydroxyphenylacetaldehyde is the toxic dopamine metabolite *in vivo*: Implications for Parkinson's disease pathogenesis. *Brain Res* 989(2):205–213.
23. Panneton WM, Kumar VB, Gan Q, Burke WJ, Galvin JE (2010) The neurotoxicity of DOPAL: Behavioral and stereological evidence for its role in Parkinson disease pathogenesis. *PLoS ONE* 5(12):e15251.
24. Wang XF, Li S, Chou AP, Bronstein JM (2006) Inhibitory effects of pesticides on proteasome activity: Implication in Parkinson's disease. *Neurobiol Dis* 23(1):198–205.
25. Levin ED, Tanguay RL (2011) Introduction to zebrafish: Current discoveries and emerging technologies for neurobehavioral toxicology and teratology. *Neurotoxicol Teratol* 33(6):607.
26. Wen L, et al. (2008) Visualization of monoaminergic neurons and neurotoxicity of MPTP in live transgenic zebrafish. *Dev Biol* 314(1):84–92.
27. Holzschuh J, Ryu S, Aberger F, Driever W (2001) Dopamine transporter expression distinguishes dopaminergic neurons from other catecholaminergic neurons in the developing zebrafish embryo. *Mech Dev* 101(1-2):237–243.
28. Sagasti A, Guido MR, Raible DW, Schier AF (2005) Repulsive interactions shape the morphologies and functional arrangement of zebrafish peripheral sensory arbors. *Curr Biol* 15(9):804–814.
29. Morpurgo G, Bellincampi D, Gualandi G, Baldinelli L, Crescenzi OS (1979) Analysis of mitotic nondisjunction with *Aspergillus nidulans*. *Environ Health Perspect* 31(1):81–95.
30. Oakley BR, Morris NR (1980) Nuclear movement is beta—tubulin-dependent in *Aspergillus nidulans*. *Cell* 19(1):255–262.
31. Boubaker H, Saadi B, Boudyach EH, Benaoumar AA (2008) Resistance of *Verticillium theobromae* to benzimidazole fungicides in Morocco. *J Appl Sci* 8(21):3903–3909.
32. Potocnik I, et al. (2009) *In vitro* toxicity of selected fungicides from the groups of benzimidazoles and demethylation inhibitors to *Cladobotryum dendroides* and *Agaricus bisporus*. *J Environ Sci Health B* 44(4):365–370.
33. Kataria HR, Grover RK (1976) Effect of benomyl and thiophanate-methyl on metabolic activities of *Rhizoctonia solani* Kühn. *Ann Microbiol (Paris)* 127A(2):297–306.
34. Wey MC, et al. (2012) Neurodegeneration and motor dysfunction in mice lacking cytosolic and mitochondrial aldehyde dehydrogenases: implications for Parkinson's disease. *PLoS ONE* 7(2):e31522.
35. Chou AP, et al. (2008) Ziram causes dopaminergic cell damage by inhibiting E1 ligase of the proteasome. *J Biol Chem* 283(50):34696–34703.
36. Goldstein DS, et al. (2011) Catechols in post-mortem brain of patients with Parkinson disease. *Eur J Neurol* 18(5):703–710.
37. Goldstein DS, Holmes C, Kopin IJ, Sharabi Y (2011) Intra-neuronal vesicular uptake of catecholamines is decreased in patients with Lewy body diseases. *J Clin Invest* 121(8): 3320–3330.
38. Anderson DG, Mariappan SV, Buettner GR, Doorn JA (2011) Oxidation of 3,4-dihydroxyphenylacetaldehyde, a toxic dopaminergic metabolite, to a semiquinone radical and an ortho-quinone. *J Biol Chem* 286(30):26978–26986.
39. Gatto NM, Cockburn M, Bronstein J, Manthripragada AD, Ritz B (2009) Well-water consumption and Parkinson's disease in rural California. *Environ Health Perspect* 117(12):1912–1918.
40. Goldman SM, et al. (2012) Solvent exposures and Parkinson disease risk in twins. *Ann Neurol* 71(6):776–784.
41. Tanaka K, et al. (2011) Occupational risk factors for Parkinson's disease: A case-control study in Japan. *BMC Neurol* 11(83):1–6.
42. Costello S, Cockburn M, Bronstein J, Zhang X, Ritz B (2009) Parkinson's disease and residential exposure to maneb and paraquat from agricultural applications in the central valley of California. *Am J Epidemiol* 169(8):919–926.
43. Wang A, et al. (2011) Parkinson's disease risk from ambient exposure to pesticides. *Eur J Epidemiol* 26(7):547–555.
44. Quistad GB, Sparks SE, Casida JE (1994) Aldehyde dehydrogenase of mice inhibited by thiocarbamate herbicides. *Life Sci* 55(20):1537–1544.
45. Tottmar SO, Pettersson H, Kiessling KH (1973) The subcellular distribution and properties of aldehyde dehydrogenases in rat liver. *Biochem J* 135(4):577–586.
46. Bence NF, Sampat RM, Kopito RR (2001) Impairment of the ubiquitin-proteasome system by protein aggregation. *Science* 292(5521):1552–1555.
47. Rayport S, et al. (1992) Identified postnatal mesolimbic dopamine neurons in culture: Morphology and electrophysiology. *J Neurosci* 12(11):4264–4280.
48. Ritz BR, et al. (2009) Dopamine transporter genetic variants and pesticides in Parkinson's disease. *Environ Health Perspect* 117(6):964–969.
49. Goldberg DW, Wilson JP, Knoblock CA, Ritz B, Cockburn MG (2008) An effective and efficient approach for manually improving geocoded data. *Int J Health Geogr* 7(60):1–20.
50. Rull RP, Ritz B (2003) Historical pesticide exposure in California using pesticide use reports and land-use surveys: An assessment of misclassification error and bias. *Environ Health Perspect* 111(13):1582–1589.

Appendix B

© 2014. Published by The Company of Biologists Ltd | Disease Models & Mechanisms (2014) 7, 571-582 doi:10.1242/dmm.013185

RESEARCH ARTICLE

Axon degeneration and PGC-1α-mediated protection in a zebrafish model of α-synuclein toxicity

Kelley C. O'Donnell[1], Aaron Lulla[2], Mark C. Stahl[2], Nickolas D. Wheat[1], Jeff M. Bronstein[2,3] and Alvaro Sagasti[1,*]

ABSTRACT

α-synuclein (aSyn) expression is implicated in neurodegenerative processes, including Parkinson's disease (PD) and dementia with Lewy bodies (DLB). In animal models of these diseases, axon pathology often precedes cell death, raising the question of whether aSyn has compartment-specific toxic effects that could require early and/or independent therapeutic intervention. The relevance of axonal pathology to degeneration can only be addressed through longitudinal, *in vivo* monitoring of different neuronal compartments. With current imaging methods, dopaminergic neurons do not readily lend themselves to such a task in any vertebrate system. We therefore expressed human wild-type aSyn in zebrafish peripheral sensory neurons, which project elaborate superficial axons that can be continuously imaged *in vivo*. Axonal outgrowth was normal in these neurons but, by 2 days post-fertilization (dpf), many aSyn-expressing axons became dystrophic, with focal varicosities or diffuse beading. Approximately 20% of aSyn-expressing cells died by 3 dpf. Time-lapse imaging revealed that focal axonal swelling, but not overt fragmentation, usually preceded cell death. Co-expressing aSyn with a mitochondrial reporter revealed deficits in mitochondrial transport and morphology even when axons appeared overtly normal. The axon-protective protein Wallerian degeneration slow (WldS) delayed axon degeneration but not cell death caused by aSyn. By contrast, the transcriptional coactivator PGC-1α, which has roles in the regulation of mitochondrial biogenesis and reactive-oxygen-species detoxification, abrogated aSyn toxicity in both the axon and the cell body. The rapid onset of axonal pathology in this system, and the relatively moderate degree of cell death, provide a new model for the study of aSyn toxicity and protection. Moreover, the accessibility of peripheral sensory axons will allow effects of aSyn to be studied in different neuronal compartments and might have utility in screening for novel disease-modifying compounds.

KEY WORDS: PGC1α, Alpha synuclein, Axon, Mitochondria, Neurodegeneration, Zebrafish

INTRODUCTION

Parkinson's disease (PD) is a movement disorder characterized pathologically by the loss of dopaminergic cells in the midbrain, and by the appearance of Lewy bodies (Braak et al., 1999; Braak et al., 2003), which are intracellular protein aggregates composed primarily of ubiquitin and α-synuclein (aSyn) (Spillantini et al., 1997; Spillantini et al., 1998). *SNCA*, the gene that encodes aSyn, was the first gene to be associated with PD: duplications, triplications and mutations in this gene are associated with rare hereditary forms of the disease (Polymeropoulos et al., 1997; Krüger et al., 1998; Singleton et al., 2003; Fuchs et al., 2007), and variants are also associated with the more common sporadic form of PD (Satake et al., 2009; Simón-Sánchez et al., 2009; Wu-Chou et al., 2013). aSyn is a synaptic protein (Maroteaux et al., 1988; Boassa et al., 2013). Aggregate formation in the synapse and axon precedes Lewy body formation and cell death in multiple cell types (Galvin et al., 1999; Orimo et al., 2008; Schulz-Schaeffer, 2010; Nakata et al., 2012). These recent findings have led to the hypothesis that PD degeneration is initiated in the axon (O'Malley, 2010; Burke and O'Malley, 2012). Whether axon degeneration leads to cell death or proceeds independently, however, is unknown.

A number of lines of evidence support the hypothesis that mitochondrial dysfunction contributes to PD pathogenesis. Mitochondrial dysfunction has been observed in postmortem samples from individuals with PD (Schapira et al., 1990; Penn et al., 1995; Navarro et al., 2009), and a number of genes associated with mitochondrial function are associated with hereditary forms of the disease (Martin, 2006; Dodson and Guo, 2007; Sai et al., 2012). Although aSyn itself is not a mitochondrial protein, it is capable of binding mitochondria directly (Nakamura et al., 2011) and can accumulate on the inner and outer mitochondrial membranes (Li et al., 2007; Zhu et al., 2012). Its overexpression or mutation alters mitochondrial morphology in a number of systems and cell types (Martin et al., 2006; Li et al., 2007; Kamp et al., 2010; Nakamura et al., 2011; Xie and Chung, 2012; Zhu et al., 2012), and is associated with respiratory chain defects, oxidative stress and mitochondrial fragmentation (Parihar et al., 2008; Chinta et al., 2010; Zhu et al., 2012). A better understanding of the effect of aSyn on mitochondrial transport and function *in vivo* could provide insight into PD pathophysiology and potential therapeutic targets.

Each of the models used to study aSyn-induced degeneration has advantages and limitations. *In vitro* studies can shed light on the cell biology of aSyn oligomerization and aggregation, but their relevance to pathophysiology in living animals is unknown. By contrast, studies in mammalian systems recapitulate some disease phenotypes, but *in vivo* cell biological studies are difficult (Martin et al., 2006; Chesselet, 2008). A better understanding of aSyn toxicity requires a model system in which neurons can be visualized and manipulated *in vivo*. Larval zebrafish are increasingly recognized as being a genetically and pharmacologically tractable model system useful in high-throughput screens for PD-associated phenotypes (Bretaud et al., 2004; Flinn et al., 2008). Moreover, their optical transparency permits the visualization of cellular processes

[1]Department of Molecular, Cell and Developmental Biology, University of California, Los Angeles, CA 90095, USA. [2]Department of Neurology, David Geffen School of Medicine at UCLA, Los Angeles, CA 90095, USA. [3]Parkinson's Disease Research, Education, and Clinical Center, Greater Los Angeles Veterans Affairs Medical Center, Los Angeles, CA 90073, USA.

*Author for correspondence (sagasti@mcdb.ucla.edu)

Received 4 June 2013; Accepted 26 February 2014

Disease Models & Mechanisms (2014) doi:10.1242/dmm.013185

TRANSLATIONAL IMPACT

Clinical issue

Accumulation of the neuronal protein α-synuclein (aSyn) is associated with multiple neurodegenerative disease processes, including Parkinson's disease. The sequence of subcellular events that underlie neurodegeneration in these diseases is not well understood. However, recent studies suggest that axon pathology might arise early in pathogenesis and might lead to the functional deficits that precede and eventually lead to cell loss. Attempts to preserve neuronal circuitry and prevent neurodegeneration therefore require a better understanding of the mechanisms by which axons degenerate, which can only be achieved through longitudinal, *in vivo* monitoring of different neuronal compartments.

Results

In this study, the authors establish an *in vivo* model for longitudinally studying the effects of aSyn accumulation on axonal integrity by expressing human wild-type aSyn in zebrafish peripheral sensory neurons, which are accessible to imaging in living animals. They report that the expression of aSyn induces cell death in peripheral sensory neurons but that axon pathology occurs earlier and more frequently than cell death. Time-lapse imaging reveals that axonal fragmentation does not consistently proceed in a retrograde direction from the axon terminal to the cell body. The authors then use *in vivo* imaging of axonal mitochondria to reveal early defects in mitochondrial morphology and transport, and eventual accumulation of the organelles in axonal varicosities. Notably, the axon-protective protein Wallerian degeneration slow (WldS) delays the onset of axonopathy in the zebrafish model but does not affect cell death or axonal fragmentation, whereas overexpression of PGC-1α, which has roles in mitochondrial biogenesis and reactive-oxygen-species scavenging, provides robust protection against both axon pathology and cell death.

Implications and future directions

These results suggest that axonopathy is an early consequence of aSyn accumulation, which only sometimes leads to cell death. They also suggest that mitochondrial impairment might be relevant to the pathophysiology of neurodegenerative diseases that involve aSyn accumulation, and that PGC-1α-mediated protection could be a promising therapeutic target. More generally, because the axonal compartment is especially sensitive to disruptions in mitochondrial function and transport, a better understanding of the relationship between mitochondrial function and axonal integrity could identify new therapeutic targets that act on pathways either upstream of or parallel to cell death. Further use of the model system established here might therefore yield new insights into the vulnerability of the axonal compartment to aSyn toxicity, and into the relationship between axon degeneration and cell death in neurodegenerative diseases.

in living animals, including mitochondrial transport (Plucińska et al., 2012). The zebrafish model could therefore prove to be a useful tool for studying the relationship between aSyn expression and neurodegeneration at the cellular level.

We expressed human aSyn in zebrafish Rohon-Beard neurons, peripheral sensory neurons in the developing spinal cord that project sensory axons to the skin. Both the cell bodies and the elaborate peripheral arbors of these cells can be monitored *in vivo*, permitting visualization of axonal transport and degeneration (Plucińska et al., 2012). Co-expressing aSyn and GFP resulted in moderate cell death, and many axons exhibited diffuse or focal swellings associated with degeneration of this compartment. Expression of the axon-protective protein Wallerian degeneration slow (WldS) (Lunn et al., 1989; Coleman et al., 1998) delayed axon degeneration, but did not affect cell death. Early defects in mitochondrial morphology and transport suggested that mitochondrial toxicity might be relevant to this observed pathogenesis. Consistent with this hypothesis, expression of PGC-1α, a transcriptional coactivator with roles in mitochondrial biogenesis and reactive oxygen species (ROS) detoxification, prevented both axonopathy and cell death caused by aSyn.

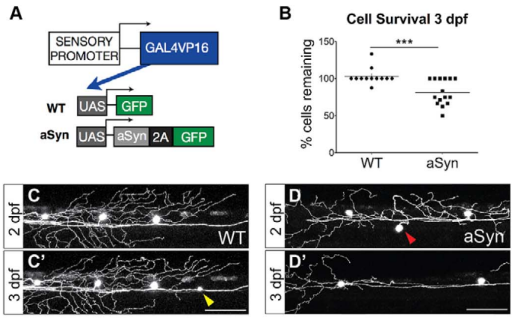

Fig. 1. Alpha-synuclein is moderately toxic to zebrafish sensory neurons between 2 and 3 dpf. (A) Transgenes to express GFP (WT) or aSyn-2A-GFP (aSyn) were injected into wild-type embryos at the one-cell stage. The *CREST3* enhancer drove expression in peripheral sensory neurons. The Gal4-UAS system was used to amplify gene expression, and a viral 2A sequence was cloned between aSyn and GFP to generate two proteins from a single transcript. (B-D) Approximately 20% of aSyn-expressing neurons died between 2 and 3 days post-fertilization (dpf) (WT 3-dpf survival: 102.9±3.2%; aSyn: 81.7±4.4%; $n \geq 12$ embryos, ***P=0.0010). Some cells newly expressed GFP during the imaging period (yellow arrowhead in C). Red arrowhead in D points to a cell that died between 2 and 3 dpf. Scale bars: 100 µm.

RESULTS

Zebrafish Rohon-Beard neurons in the spinal cord arborize in the skin, making them readily accessible to *in vivo* imaging of dynamic intracellular processes. We generated transgenes to overexpress aSyn in these cells, using a sensory-neuron promoter and the Gal4-UAS binary transcription system to drive robust gene expression (Fig. 1). To co-express aSyn and GFP, we used the viral 2A system (Donnelly et al., 2001), which provides bright reporter expression earlier than the aSyn-2A-DsRed transgene previously reported (Prabhudesai et al., 2012). The viral 2A system permits visualization of cells expressing the transgene, but circumvents the possibility of increased aggregation that could potentially be observed with a fusion protein. Consistent with a previous report (Prabhudesai et al., 2012), immunostaining for human aSyn revealed protein expression and aggregate formation by 2 days post-fertilization (dpf) in aSyn-injected cells, but not in control cells expressing GFP alone (supplementary material Fig. S1).

When the HuC promoter is used to drive aSyn expression in larval zebrafish neurons, embryos exhibit massive cell death and gross morphological abnormalities, and die within 2-3 dpf (Prabhudesai et al., 2012). When we drove expression using a sensory-neuron promoter, only a small number of embryos exhibited such defects; most were morphologically normal. Only the latter were retained for subsequent studies, and in these embryos lethality was not observed at levels higher than in wild type.

Alpha-synuclein causes moderate cell death in larval zebrafish sensory neurons

To determine whether aSyn caused early toxicity in sensory neurons, we injected the aSyn-2A-GFP construct into transgenic embryos from a stable line expressing DsRed in sensory neurons,

and screened for reporter expression at 1 dpf. Cells were imaged hourly between 32 and 44 hours post-fertilization (hpf) (supplementary material Fig. S2A,B). Because transient aSyn-2A-GFP expression was sparse, some neurons expressed only DsRed; these served as an internal control for development and cell death. Over the course of the imaging period, peripheral sensory axons extended normally in aSyn-expressing neurons (supplementary material Fig. S2B), and cell survival between the first and last time point was not different between the two groups (supplementary material Fig. S2C). These observations indicate that aSyn is not toxic at early stages.

Having determined that aSyn expression does not impair development of peripheral sensory neurons by 44 hpf, we investigated whether it affected cell survival at later time points (Fig. 1B-D). Cohorts of embryos expressing GFP (WT) or aSyn-2A-GFP were monitored between 2 and 3 dpf, and Rohon-Beard neurons were counted at each time point (Fig. 1B-D). Approximately 20% of cells in aSyn-expressing embryos died between 2 and 3 dpf (Fig. 1B; WT 3-dpf survival: 102.9±3.2%; aSyn: 81.7±4.4%; n≥12 embryos, P=0.0010).

Alpha-synuclein expression causes axonopathy

Axon pathology is often characterized by swelling or beading in the axon that might precede fragmentation (Beirowski et al., 2010; Nikić et al., 2011). To quantify axonal dystrophy in cells expressing DsRed and either GFP or aSyn-2A-GFP at 2 and 3 dpf (Fig. 2A), we developed a 5-point staging system (supplementary material Fig. S3). At 2 dpf, before cell death had been observed, the majority (14/19, 73.7%) of aSyn-expressing axons exhibited a beaded morphology, quantified as degeneration stage 2-3 (Fig. 2; WT degeneration stage: 1.08±0.08; aSyn: 2.05±0.14; n≥12 axons, P<0.0001). When the same axons were imaged the following day, degeneration was further advanced (Fig. 2B; WT degeneration stage: 1.42±0.33; aSyn: 3.05±0.35; n≥12 axons, P=0.0033). One control axon died between 2 and 3 dpf (degeneration stage 5), and one exhibited mild beading (stage 2). The remaining ten control axons were smooth and continuous (stage 1). Among aSyn-expressing axons, by contrast, 17/19 axons (89.5%) received a degeneration score of 2 or higher, with six degenerating entirely (stage 5).

Axonopathy, but not axonal fragmentation, precedes cell death in aSyn-expressing cells

It has recently been proposed that the axon degeneration observed in PD represents an early, and potentially independent, process in pathophysiology (O'Malley, 2010; Burke and O'Malley, 2012; Jellinger, 2012). In zebrafish neurons expressing aSyn, the percentage of cells with dystrophic axons between 2 and 3 dpf was higher than the percentage of cells that died during that period. To determine whether severe axonopathy always preceded cell death, we conducted time-lapse imaging at 20-minute intervals between 56 and 68 hpf (Fig. 3A,B). In cells that died during the imaging period, the onset of axonal dystrophy (beading or fragmentation) was compared with morphological changes in the soma that herald cell death. In all cases (n=9), focal or diffuse swellings (axonopathy stage 2-3) were seen in axons several hours before cell death (Fig. 3A,B). Axonal fragmentation, however, did not precede apoptotic changes in the cell body (Fig. 3A,B, arrows). Overt axonal breakdown therefore does not proceed directly to the death of the cell body in this model. However, because axonal dystrophy preceded cell death, it is likely that the axonal compartment is more vulnerable to aSyn toxicity.

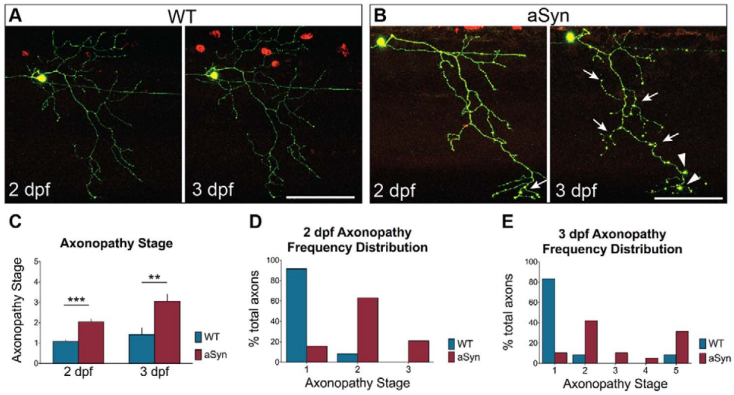

Fig. 2. Early axonopathy in aSyn-expressing peripheral sensory neurons. Axon pathology was scored at 2 and 3 days post-fertilization (dpf) in WT and aSyn-expressing axons, using the 5-point staging system described in supplementary material Fig. S3. (A) At 2 dpf (48-58 hpf) and 3 dpf (72-82 hpf), WT axons were smooth and continuous (score of 1). (B) At 2 dpf, axonal beading (arrows) was observed in many aSyn-expressing cells. By 3 dpf, axonal dystrophy in aSyn-expressing cells was more severe, with more diffuse beading (arrows) and larger varicosities (arrowheads). (C) Quantification of average axonopathy stage in wild-type and aSyn-expressing embryos. aSyn-expressing axons were more dystrophic at both 2 dpf (WT degeneration stage: 1.03±0.08, n=12 axons in 5 animals; aSyn: 2.05±0.14; n=19 axons in 8 animals; ***P<0.0001) and 3 dpf (WT: 1.42±0.34; aSyn: 3.05±0.35; n≥12 axons in ≥5 animals as above; **P=0.0033). (D,E) Histograms representing frequency distribution of axonopathy stage. At 2 dpf (D), 11/12 wild-type axons (91.7%) were smooth and continuous (stage 1); one exhibited mild beading (stage 2). By contrast, only 3/19 (15.8%) aSyn-expressing axons were at stage 1; 12/19 (63.2%) exhibited mild beading (stage 2), and 4/19 (21.1%) exhibited more severe axonopathy (stage 3). (E) Frequency histogram of axonopathy distribution in the same cells at 3 dpf. One wild-type axon (8.3%) exhibited mild beading (stage 2), and one wild-type cell had undergone developmental cell death (stage 5). All remaining wild-type axons (10/12, 83.3%) were smooth and continuous (stage 1). By contrast, only 2/19 (10.5%) aSyn-expressing axons remained at stage 1 by 3 dpf. 6/19 (31.6%) had fully degenerated (stage 5), and the remaining 11/19 (57.9%) were in intermediate stages of degeneration (8/19 in stage 2; 2/19 in stage 3; 1/19 in stage 4). Scale bars: 100 µm.

Disease Models & Mechanisms (2014) doi:10.1242/dmm.013185

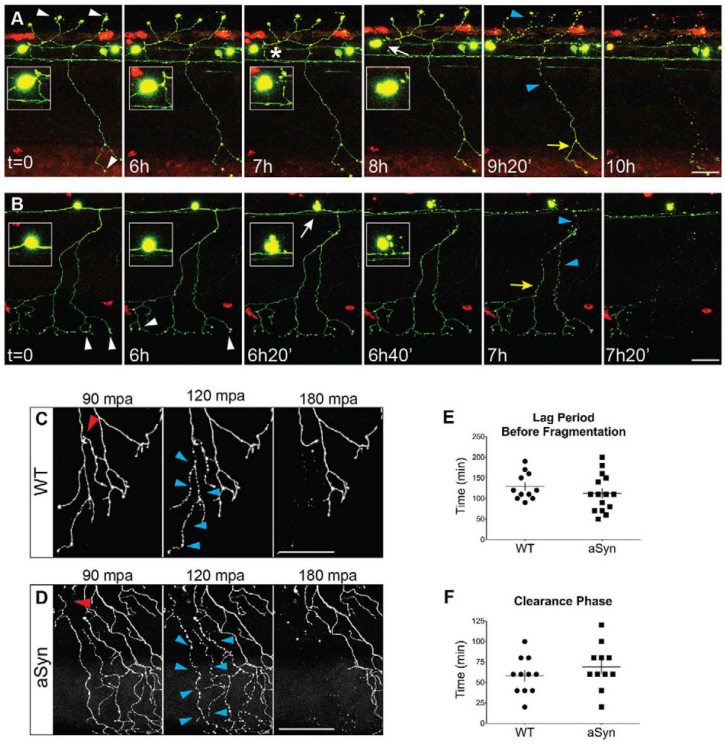

Fig. 3. Axonopathy is not followed by 'dying back' or Wallerian-like degeneration in aSyn-expressing neurons. (A,B) Time-lapse imaging of neurodegeneration. Cells were imaged every 20 minutes beginning 54 hours post-fertilization (hpf). Axons from at least 11 embryos from each group were transected; representative images from aSyn-expressing animals are shown. Time stamps in images are relative to the start of the imaging period. Axonal varicosities were observed (white arrowheads) several hours before cell death. White arrows point to morphological changes indicative of cell death. Inset represents cell body magnified 2×. Asterisk in A indicates separation of the axon from the cell body. Axonal fragmentation (blue arrowheads) usually did not occur before cell death, and was not stereotyped: it did not occur synchronously along the length of the axon, nor in a retrograde direction (yellow arrows point to distal portions of the axon that are still intact). (C,D) Representative images of wild-type (C) and aSyn-expressing (D) axons undergoing WD after transection with a two-photon laser. Axons were transected with a two-photon laser at 2 dpf, and embryos were imaged every 30 minutes for up to 12 hours. Red arrowhead points to site of transection. After injury, in both wild-type and aSyn-expressing axons, fragmentation was synchronous along the length of the transected axon (blue arrowheads). mpa, minutes post-axotomy. (E) There was no difference in the duration of the lag period between transection and fragmentation (WT: 129.1±10.0 minutes, n=11 axons from 11 animals; aSyn: 112.7±11.7 minutes; n=15 axons from 15 animals, P=0.3173). (F) The time between fragmentation and clearance of all axonal debris was not significantly different between the two groups (WT: 58.2±6.9 minutes; aSyn: 69.1±8.3 minutes; P=0.3213). Scale bars: 50 µm.

Axonal injury increases cell death in aSyn-expressing neurons

To further investigate the sensitivity of the axon and cell body to aSyn toxicity, we examined the effect of aSyn expression on the rate of Wallerian degeneration (WD) after injury. WD is the process by which severed axons degenerate after separation from the cell body. In most neuronal populations, including zebrafish peripheral sensory neurons (Martin et al., 2010), WD after axonal transection is compartment-specific: the distal fragment degenerates, whereas the proximal axon and cell body survive. To determine whether aSyn expression alters these characteristics, we transected axons at 2 dpf and conducted time-lapse confocal imaging to visualize WD *in vivo* (Fig. 3C,D). aSyn expression did not change the duration of the lag phase before fragmentation (Fig. 3E), or the clearance of axonal debris (Fig. 3F). WD in aSyn-expressing axons therefore proceeds with the same rapid and stereotyped kinetics as in wild-type axons. In aSyn axons, as in wild type, fragmentation of the distal axon was synchronous (Fig. 3C,D), unlike the axon degeneration observed in uninjured aSyn-expressing cells (Fig. 3A,B).

Consistent with the compartment specificity of WD, in both wild-type and aSyn-expressing axons the cell body and proximal axon remained intact, whereas the distal fragment underwent degeneration (data not shown). However, when we imaged transected cells at 3 dpf, 24 hours after injury, 50% of aSyn-expressing cells (5/10) had died, whereas all axotomized WT cells (n=11) were still intact. Because 20% of uninjured aSyn-expressing cells died between 2 and 3 dpf (Fig. 1B), this higher percentage suggests that direct axonal injury exacerbates aSyn toxicity.

WldS delays axon degeneration caused by aSyn toxicity

To further characterize aSyn-induced degeneration, we sought to determine whether it could be prevented by the axon-protective

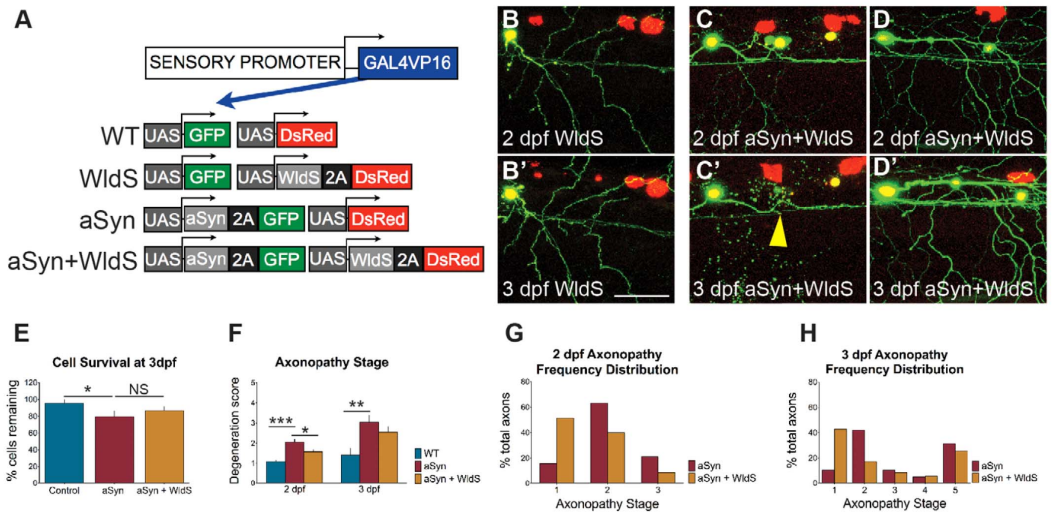

Fig. 4. WldS delays axonopathy but does not prevent cell death caused by aSyn toxicity. (A) Transgenes used to visualize the effect of aSyn and WldS expression on peripheral sensory neurons. (B) Representative images of WldS-expressing control cells at 2 (B) and 3 (B′) days post-fertilization (dpf). Axons were smooth and continuous. (C,D) Representative images of cells expressing both aSyn and WldS. At 2 dpf, aSyn+WldS-expressing axons were on average more continuous (compare with aSyn in Fig. 2). WldS did not prevent degeneration of axons in cells that died between 2 and 3 dpf (C,C′; yellow arrowhead points to degenerated soma). Axons that remained connected to cell bodies were relatively preserved (D,D′). (E) WldS did not affect survival of aSyn-expressing cells between 2 and 3 dpf (WT: 95.65±4.35%; aSyn: 79.36±6.62%; WldS+aSyn: 86.86±4.43%; n=22 animals per group; *P=0.3515). (F) Average axonopathy stage at 2 and 3 dpf. WldS-expressing aSyn axons were significantly protected at 2 dpf (aSyn: 2.05±0.14, n=19 axons from 8 animals; WldS+aSyn: 1.57±0.11; n=35 axons from 11 animals, *P=0.0114). By 3 dpf, this difference was no longer significant (aSyn: 3.05±0.35; WldS+aSyn: 2.54±0.28; P=0.2766). ***P<0.0001; **P=0.0033. (G,H) Frequency distribution of axonopathy scores at 2 (G) and 3 (H) dpf. At 3 dpf, axons that underwent cell death (aSyn: 6/19, 31.6%; aSyn+WldS: 9/35, 25.7%) had fully degenerated (axonopathy stage 5), regardless of whether or not WldS was expressed. Wild-type and aSyn axonopathy data were replotted from Fig. 2. Scale bar: 50 µm.

protein WldS (Fig. 4). This protein was first discovered to delay WD of transected axons (Coleman et al., 1998; Mack et al., 2001) and subsequently found to be protective of axons in many animal models of neurodegenerative disease (Sajadi et al., 2004; Hasbani and O'Malley, 2006; Press and Milbrandt, 2008; Cheng and Burke, 2010). aSyn and WldS were co-expressed in peripheral sensory neurons (Fig. 4A,C,D), and cell survival and axon pathology were quantified between 2 and 3 dpf (Fig. 4C-H). WldS did not significantly protect against cell death induced by aSyn (Fig. 4E). Axon degeneration, however, was delayed in WldS-expressing cells (Fig. 4F-H). Degeneration scores were lower at 2 dpf in WldS-expressing cells but, by 3 dpf, this difference was no longer significant (Fig. 4F). In cells that died between 2 and 3 dpf, WldS had no axon-protective effect (stage 5; Fig. 4C,H). However, a higher percentage of cells expressing WldS had healthy (stage 1) axons at both 2 dpf (Fig. 4G) and 3 dpf (Fig. 4H) than cells expressing aSyn alone. WldS therefore provided moderate protection against aSyn toxicity in the axonal compartment, reducing the incidence of focal swellings in axons connected to intact cell bodies. However, WldS could delay neither aSyn-induced cell death nor the axon degeneration associated with it.

Mitochondrial pathology in axons of aSyn-expressing neurons

Multiple *in vitro* and histological studies suggest that both wild-type and mutant aSyn interact with mitochondria (Martin et al., 2006; Parihar et al., 2008; Banerjee et al., 2010; Chinta et al., 2010; Devi and Anandatheerthavarada, 2010; Nakamura et al., 2011; Calì et al., 2012; Reeve et al., 2012; Zhu et al., 2012). To determine whether axonal mitochondria were affected by aSyn expression in our model, DsRed fused to the cox8 mitochondrial matrix targeting signal was co-expressed in sensory neurons with either GFP or aSyn-2A-GFP (Fig. 5A-C). Mitochondrial density was significantly higher in aSyn-expressing cells, even in the absence of overt axonopathy (Fig. 5C,D). Mitochondria in aSyn-expressing axons were less elongated than in wild-type cells (Fig. 5C,E; WT length/width: 2.01±0.11; aSyn: 1.48±0.05; n≥54 mitochondria from ≥5 embryos; P<0.0001), with a higher percentage of spherical mitochondria (ratio of 1), a phenotype associated with respiratory chain dysfunction (Benard and Rossignol, 2008). In dystrophic aSyn-expressing axons (Fig. 5F), many mitochondria exhibited pathological swelling characteristic of the mitochondrial permeability transition (Haworth and Hunter, 1979; Kowaltowski et al., 1996; Brustovetsky et al., 2002).

Because mitochondrial transport arrest is associated with axon degeneration (Baloh et al., 2007; Kim-Han et al., 2011; Sterky et al., 2011; Avery et al., 2012), we investigated whether aSyn expression induced mitochondrial transport impairments at 2 dpf, prior to axonal fragmentation and cell death. Mitochondrial transport was evaluated along 50-µm axonal segments for 6 minutes in wild-type or aSyn-expressing sensory neurons. Kymographs were generated to quantify overall motility, defined as the percentage of mitochondria that moved within a 6-minute time-lapse movie. Mitochondrial motility was significantly reduced in aSyn-expressing axons (Fig. 5G). A higher percentage of the total distance traveled by the remaining motile mitochondria was in the retrograde

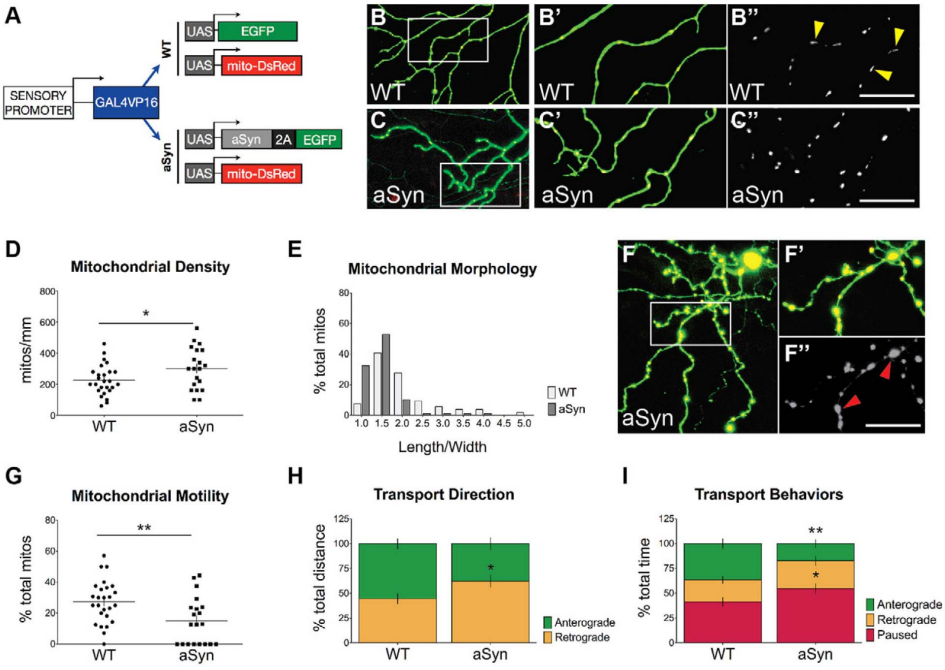

Fig. 5. Early mitochondrial pathology and transport impairments in aSyn-expressing axons. (A) Transgenes used to visualize mitochondria in GFP- (WT) or aSyn-2A-GFP-expressing peripheral sensory neurons. Transgenes were co-injected into wild-type embryos at the one-cell stage. WT (B-B″) and aSyn-expressing (C-C″) cells were imaged at 2 dpf. Yellow arrowheads point to elongated mitochondria in wild-type axons. (D) Mitochondrial density was higher in aSyn-expressing cells (WT: 226.2±19.1 mitochondria/μm, *n*=26 axons in 12 animals; aSyn: 302.0±29.8 mitochondria/μm; *n*=20 axons in 10 animals, **P*=0.031). (E) Mitochondrial morphology was quantified as the ratio of length to width in individual mitochondria. Values were binned and the frequency distribution was plotted on a histogram. Mitochondria in aSyn-expressing axons were more spherical than in wild-type axons, with fewer mitochondria exhibiting a high length:width ratio. (F) Large, swollen mitochondria occupied the spheroids in dystrophic aSyn-expressing axons. Boxed region in F is represented in F′-F″. Red arrowheads point to enlarged mitochondria. [Note that the scale bar in F″ is the same as in B″ and C″ (100 μm).] (G) Mitochondrial transport was evaluated along 50-μm axonal segments every second. Overall mitochondrial transport was significantly reduced in aSyn-expressing axons (WT % motile: 27.4±2.7%; aSyn: 15.05±3.4%; *n*≥20 axons in ≥10 animals per group, as above; ***P*=0.0061). (H) A higher percentage of distance traveled by motile mitochondria was in the retrograde direction (WT % retrograde distance: 44.61±5.07%; aSyn: 62.17±6.06%; *n*≥52 mitochondria; **P*=0.0300). (I) Motile mitochondria spent less time moving in the anterograde direction (WT: 36.44±4.80%; aSyn: 17.39±4.05%; *n*≥52 mitochondria; ***P*=0.0063), and a greater percentage of time paused than in wild-type axons (WT: 41.25±4.43%; aSyn: 54.82±4.85%; *n*≥52 mitochondria; **P*=0.0478).

direction (Fig. 5H). Motile mitochondria spent less time moving in the anterograde direction, and a greater percentage of time paused than mitochondria in wild-type axons (Fig. 5I). The speed of uninterrupted runs in either the anterograde or retrograde direction, however, was not significantly different between wild-type and aSyn-expressing cells (WT anterograde speed: 0.56±0.04 μm/s; aSyn: 0.53±0.06 μm/s; *n*≥27 mitochondria, *P*=0.7137; WT retrograde speed: 0.57±0.04 μm/s; aSyn: 0.64±0.07 μm/s; *n*≥38 mitochondria from ≥10 embryos). Early mitochondrial pathology in aSyn-expressing axons might therefore contribute to degeneration in this model.

PGC-1α expression mitigates toxicity in aSyn-expressing sensory neurons

Because mitochondrial defects appeared early in aSyn-expressing axons, we hypothesized that mitochondrial dysfunction was directly involved in degeneration. To investigate whether improved mitochondrial function could prevent degeneration in aSyn-expressing sensory neurons, the transcriptional coactivator PGC-1α was expressed in these cells. PGC-1α plays a number of regulatory roles in mitochondrial biogenesis and ROS detoxification (Wu et al., 1999; St-Pierre et al., 2006), and PGC-1α overexpression is protective in multiple models of neurodegeneration (St-Pierre et al., 2006; Keeney et al., 2009; Shin et al., 2011; Mudò et al., 2012). We have documented that PGC-1α expression in zebrafish peripheral sensory neurons increases mitochondrial volume and density, and prevents injury-induced changes in mitochondrial redox homeostasis (O'Donnell et al., 2013). Co-expressing PGC-1α and aSyn in peripheral sensory neurons (Fig. 6A) robustly protected against aSyn toxicity between 2 and 3 dpf (Fig. 6B-E). Unlike WldS, PGC-1α reversed both cell death (Fig. 6D) and axonopathy (Fig. 6E) in aSyn-expressing cells. These results are consistent with mitochondrial dysfunction playing a key role in aSyn-induced toxicity.

DISCUSSION

aSyn accumulation is associated with neurodegeneration, but the cellular mechanisms that underlie its toxicity are not well understood. We have expressed human wild-type aSyn in zebrafish

Disease Models & Mechanisms (2014) doi:10.1242/dmm.013185

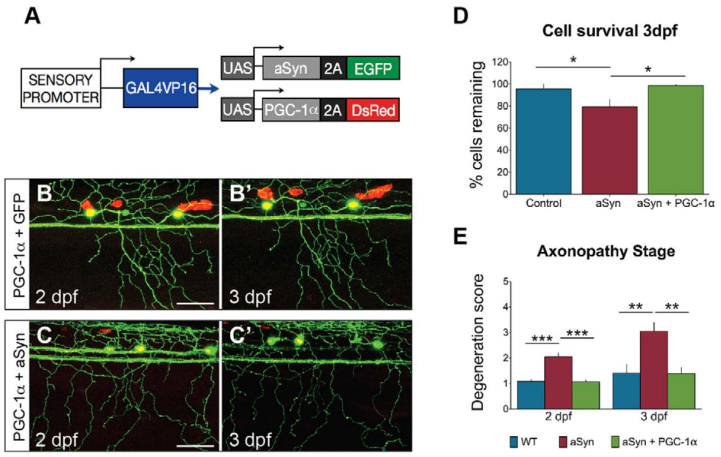

Fig. 6. PGC-1α mitigates aSyn toxicity. (A) Transgenes co-injected to express PGC-1α and aSyn in sensory neurons. (B,C) Cells were imaged between 2 and 3 dpf. (D) PGC-1α prevented cell death in aSyn-expressing cells at 3 dpf (aSyn: 79.36±6.62%; aSyn+PGC-1α: 98.61±0.95%; $n \geq 18$; $^{*}P=0.0129$). (E) PGC-1α prevented axonopathy at 2 dpf (aSyn degeneration score: 2.05±0.14; aSyn+PGC-1α: 1.07±0.07; $n \geq 15$; $^{***}P<0.0001$). At 3 dpf, PGC-1α-expressing axons were still protected at a level equivalent to controls (WT degeneration score: 1.42±0.34, $n=12$ axons in 6 animals; aSyn: 3.05±0.35, $n=19$ axons in 8 animals; aSyn+PGC-1α: 1.40±0.22; $n=10$ axons in 5 animals; one-way ANOVA with Newman-Keuls post-test, $^{**}P=0.0052$). Scale bars: 50 µm. Wild-type and aSyn data were replotted from Fig. 2.

peripheral sensory neurons, and observed aggregate formation and moderate cell death. Cell death was often preceded by axonal dystrophy, which coincided with aberrations in mitochondrial morphology and transport. The transcriptional coactivator PGC-1α but not WldS prevented both cell death and axonopathy in aSyn-expressing neurons, suggesting that regulation of mitochondrial biogenesis and ROS production might be therapeutically relevant *in vivo*.

Wild-type human aSyn has been expressed in mice (Masliah et al., 2000; van der Putten et al., 2000; Fleming et al., 2004), flies (Feany and Bender, 2000; Auluck et al., 2002) and worms (Lakso et al., 2003) in an effort to understand the relevance of this protein to PD. None of these model systems recapitulates all aspects of disease, but all have strengths that can be exploited to interrogate various aspects of aSyn toxicity (Fernagut and Chesselet, 2004; Chesselet, 2008; Lim and Ng, 2009). The limitations of the model we describe include its rapid onset, high levels of synuclein expression and confinement to peripheral sensory neurons, none of which characterize human pathophysiology in PD. However, these very limitations are also strengths of the system. Embryonic and larval zebrafish are increasingly recognized as a promising model organism for neurodegeneration research because early and robust phenotypes permit high-throughput analysis of potential therapeutic targets in a living vertebrate system (Tomasiewicz et al., 2002; Bandmann and Burton, 2010). Moreover, the optical transparency of zebrafish and the superficial location of peripheral sensory neurons present a novel method for identification and interrogation of compartment-specific degeneration pathways in aSyn toxicity.

aSyn causes axonopathy in peripheral sensory neurons

In postmortem neurons from individuals with PD, aSyn aggregates are often observed in the axon prior to the cell body (Braak et al., 1999; Galvin et al., 1999), a feature that has also been observed in some disease models (Marui et al., 2002; Orimo et al., 2008; Schulz-Schaeffer, 2010; Volpicelli-Daley et al., 2011; Boassa et al., 2013). Early aggregation might result in early dysfunction at the presynaptic terminal, causing defects in neurotransmission long before cell death. In multiple models of PD, both toxin-induced (Herkenham et al., 1991; Orimo et al., 2008; Li et al., 2009a; Cartelli et al., 2010; Arnold et al., 2011; Kim-Han et al., 2011; Mijatovic et al., 2011) and genetic (Li et al., 2009b; Decressac et al., 2012) axon degeneration is observed prior to cell death, and in a higher percentage of cells. This has raised the question of whether PD represents a 'dying back' of dopaminergic neurons (Hornykiewicz, 1998), with synapse loss initiating a retrograde degenerative process that leads to cell death. We observed early axon pathology in aSyn-expressing cells, with focal swellings or widespread beading in the axon, before cell death. A higher percentage of cells exhibited axonopathy than cell death, suggesting that axon degeneration might lead to death. However, time-lapse imaging revealed that, although axonal varicosities were observed early, axonal fragmentation was not stereotyped, and did not always occur prior to death of the cell body. By contrast, after transection, WD of the distal axon proceeded with stereotyped kinetics in aSyn-expressing axons, like in wild-type cells. The early axonopathy observed in uninjured axons therefore does not cause a 'functional' axotomy, and the fragmentation that later occurs is not prevented by WldS. Together, these results suggest that aSyn-induced axon degeneration is not Wallerian-like. They also indicate that degeneration is not a 'dying back' process in which axon degeneration is required for cell death. Nevertheless, the early axonopathy could be associated with significant functional impairment, and likely represents an important therapeutic target.

Our characterization of the relationship between axonal fragmentation and cell death in this model does not rule out the possibility that independent, compartment-specific degeneration pathways are activated by aSyn. Indeed, dopaminergic neurons in JNK2/3 double-knockout mice do not die after MPTP administration, but their axons degenerate, suggesting that separate mechanisms underlie degeneration in the two compartments in a PD model (Ries et al., 2008). Likewise, WldS is protective against axon degeneration but not cell death after systemic MPTP treatment (Hasbani and O'Malley, 2006; Antenor-Dorsey and O'Malley, 2012) or application of 6-hydroxydopamine (Sajadi et al., 2004). Retrograde axonal degeneration is therefore not required for cell death in these acute models, but might benefit from independent protection. In zebrafish peripheral sensory neurons, WldS delayed the early axonopathy caused by aSyn, and had no effect on cell death, consistent with the aforementioned toxin studies. However, in WldS-expressing cells that died, axons were not preserved. Because WldS protection is dose-dependent (Mack et al., 2001), it is possible that aSyn toxicity was initiated before levels were

sufficient to provide lasting protection. Future studies with inducible aSyn expression could address this question.

Mitochondrial dysfunction and axon degeneration

Mitochondrial dysfunction might be upstream of axon degeneration in aSyn-expressing cells. At 2 dpf, we observed changes in mitochondrial density and morphology that were consistent with mitochondrial fragmentation, even in the absence of axonal dystrophy. This phenotype is consistent with recent *in vitro* studies indicating that aSyn associates directly with mitochondria, causing mitochondrial fragmentation that is associated with respiratory chain dysfunction and impaired calcium homeostasis (Chinta et al., 2010; Kamp et al., 2010; Nakamura et al., 2011; Butler et al., 2012). In mouse dopaminergic neurons, mitochondrial fragmentation causes selective degeneration of the axonal compartment, leading to motor deficits that occur before (Pham et al., 2012) or in the absence of (Lee et al., 2012) nigral cell death. It is possible, then, that aSyn increases mitochondrial fragmentation *in vivo*, impairing redox homeostasis and ATP synthesis, and thus sensitizing the axonal compartment to further insults such as mechanical injury, oxidant stress or aSyn aggregation (Gu et al., 2010).

The early mitochondrial transport deficits we observed in aSyn-expressing axons might also be pathologically relevant. Mitochondrial motility was reduced, and motile mitochondria in aSyn-expressing cells favored retrograde transport towards the cell body. Deficits in anterograde transport of mitochondria are associated with synaptic dysfunction and degeneration (Stowers et al., 2002; Weihofen et al., 2009; Misko et al., 2010; Misko et al., 2012). Mitochondrial transport deficits have been reported in the MPTP model (Cartelli et al., 2010; Kim-Han et al., 2011), and in cells expressing the PD-associated A53T mutant form of aSyn (Xie and Chung, 2012). The transport impairment we observed could therefore underlie later dysfunction. Alternatively, reduced motility could be a protective response to mitochondrial dysfunction. PINK1 and parkin orchestrate the transport arrest of depolarized mitochondria (Wang et al., 2011; Cai et al., 2012; Liu et al., 2012), which is thought to limit network impairment. The increased retrograde transport in aSyn-expressing axons could thus represent trafficking of damaged mitochondria to lysosomes in the cell body, where mitophagy is thought to occur.

A better understanding of mitochondrial dysfunction in this model could provide insight into PD pathogenesis. Many genes associated with hereditary PD converge on mitochondrial function and quality control (Cardoso, 2011; Sai et al., 2012), and both genetic and pharmacological models of PD implicate mitochondrial dysfunction in pathogenesis (Cassarino et al., 1997; Przedborski and Jackson-Lewis, 1998; Exner et al., 2012; Van Laar and Berman, 2013). In our model, focal varicosities in severely beaded axons were occupied by swollen, rounded mitochondria, similar to mice expressing a disease-associated form of human aSyn (A53T) (Martin et al., 2006; Chinta et al., 2010). Mitochondrial swelling is consistent with opening of the mitochondrial permeability transition pore (mPTP), which is sufficient to induce axon degeneration in some cell types (Barrientos et al., 2011). Opening of the mPTP is induced by calcium overload in the mitochondria (Haworth and Hunter, 1979; Gunter et al., 1994), and facilitated by ROS accumulation (Costantini et al., 1996; Kowaltowski et al., 1996; Vercesi et al., 1997). Normal pacemaking through L-type calcium channels in dopaminergic neurons causes oxidant stress and might lower the threshold for mPTP formation (Guzman et al., 2010; Surmeier et al., 2011; Goldberg et al., 2012), which could underlie the selective vulnerability of dopaminergic neurons to cell death in PD. Indeed, mitochondria isolated from the rat striatum are more sensitive to calcium influx than cortical mitochondria (Brustovetsky et al., 2003).

PGC-1α protects against aSyn toxicity

The transcriptional coactivator PGC-1α plays crucial roles in regulating mitochondrial biogenesis and ROS scavenging, and could be a therapeutically relevant target in the treatment of neurodegenerative disease (Anderson and Prolla, 2009; Handschin, 2009; Zheng et al., 2010). Defects in PGC-1α activity were recently reported in fibroblasts from individuals with early-onset, parkin-deficient PD (Pacelli et al., 2011), and genome-wide association studies identified reduced expression of many PGC-1α-regulated genes in tissues from individuals with PD (Zheng et al., 2010). We found that overexpression of mouse PGC-1α protects against aSyn toxicity in both the axon and the cell body. Others have reported that it protects mouse dopaminergic neurons from MPTP toxicity (St-Pierre et al., 2006; Mudò et al., 2012). This effect seems to be mediated by upregulation of ROS detoxification programs, including increased expression of mitochondrial superoxide dismutase (SOD2) (St-Pierre et al., 2006). Siddiqui and colleagues recently reported that aSyn associates with PGC-1α during oxidative stress, inhibiting these protective effects; however, overexpression of PGC-1α reestablished protection (Siddiqui et al., 2012). PGC-1α and its downstream target genes might therefore be relevant therapeutic targets in the treatment of synucleinopathies (Tsunemi and La Spada, 2012).

MATERIALS AND METHODS

Fish

Fish were raised on a 14 hour/10 hour light/dark cycle at 28.5°C. Embryos were kept in a 28.5°C incubator. Experiments were approved by the Chancellor's Animal Research Care Committee at the University of California, Los Angeles.

Transgenes

A plasmid encoding aSyn and the viral T2A cDNA sequence cloned into pDsRed-Monomer N1 vector (Clontech) has been described elsewhere (Prabhudesai et al., 2012), and was cloned into the p3E entry vector of the Tol2/Gateway zebrafish kit (Kwan et al., 2007). The T2A sequence causes ribosomal 'skipping' (Donnelly et al., 2001), generating two proteins from a single open reading frame and resulting in stoichiometric expression of the gene of interest and the fluorescent reporter (Tang et al., 2009). The T2A-DsRed cDNA was cloned into the p3E entry vector of the Gateway system (Invitrogen), downstream of a multiple cloning site (MCS) (Kwan et al., 2007). Because GFP expression is brighter than monomeric DsRed and is therefore preferable for axon imaging, the T2A sequence was also cloned into the p3E entry vector between an MCS and GFP. aSyn was then cloned into the MCS to generate p3E-aSyn-2A-GFP. WldS or mouse PGC-1α (Hanai et al., 2007) (gift from Dr Shintaro Imamura) was inserted into the p3E-MCS-T2A-DsRed plasmid. In all constructs, the *CREST3* enhancer (gift of H. Okamoto) (Uemura et al., 2005) in the p5E entry vector drove expression of Gal4 and 14×UAS (Köster and Fraser, 2001) in pME, and these were recombined with one of the p3E donor vectors to generate the following transgenes:

A: *CREST3*:Gal4:UAS:GFP
B: *CREST3*:Gal4:UAS:aSyn-2A-GFP
C: *CREST3*:Gal4:UAS:DsRed
D: *CREST3*:Gal4:UAS:WldS-2A-DsRed
E: *CREST3*:Gal4:UAS:PGC-1α-2A-DsRed.

To visualize mitochondria, a cox8 mitochondrial targeting sequence was added to DsRed and cloned into the Gateway system to generate UAS-mitoDsRed-polyA (mitoDsRed; gift of Carla Kohler laboratory, University of California, Los Angeles, CA). This was co-injected with Plasmid A or B above so that the *CREST3* enhancer drove expression of GFP (+/− aSyn) and

mitoDsRed in the same neurons. Approximately 15 pg of each transgene were injected into embryos at the one-cell stage for transient, mosaic transgene expression in sensory neurons, and embryos were screened at 1 and 2 dpf for reporter expression. Because DsRed maturation proceeds more slowly than GFP, robust expression of DsRed reporter transgenes was not observed until 2 dpf, so this was the earliest time point for all experiments.

Immunohistochemistry

At 48 hpf, embryos were dechorionated and fixed with 4% paraformaldehyde in PBS, pH 7.4, at 4°C overnight. Fixed embryos were cryoprotected with 30% sucrose and embedded into OCT Compound (Electron Microscopy Sciences) for frozen sectioning. 10-µm sections were produced using a cryostat (Leica CM3050) and bonded to glass slides. Sections were washed with PBS, blocked with 10% normal goat serum, and incubated with anti-aSyn mouse IgG primary antibody (BD Biosciences) at 1:500 dilution at 4°C in a humidified chamber overnight. Slides were again washed in PBS and incubated with Alexa-Fluor-594-conjugated goat anti-mouse IgG (Invitrogen) secondary antibody at 1:500 dilution for 2 hours at room temperature and with 4′,6′-diamidino-2-phenylindole (DAPI) for nuclear staining. Single-channel images were obtained with a fluorescence microscope (Eclipse e400, Nikon) and merged using Adobe Photoshop software.

Imaging

Embryos were dechorionated, anesthetized in 0.01% tricaine, mounted in 1.2% low-melt agarose (Promega) in sealed chambers (O'Brien et al., 2009) and imaged on a heated stage with a 20× air objective on a confocal microscope (Zeiss LSM 510), using a 488 nm laser line for GFP and 543 nm for DsRed. Cell death was initially quantified in cells expressing only GFP or aSyn-2A-GFP. The counts were also performed in embryos co-injected with a DsRed reporter transgene, to allow later comparison with WldS- and PGC-1α-expressing cells.

For time-lapse analysis of axon degeneration and cell death, embryos were imaged every 20-60 minutes for up to 12 hours. Images were compiled into projections and movies with QuickTime software.

To determine the effect of aSyn expression on mitochondrial density and morphology, mitoDsRed-expressing embryos were imaged at 2 dpf using a 40× oil objective and 3× digital zoom. Mitochondrial transport was visualized by time-lapse imaging of a single optical section using only the 543 nm laser, at a frequency of ~1 Hz, for 6 minutes.

Axon transection

GFP- and aSyn-2A-GFP-expressing axons were cut using a Zeiss 710 microscope equipped with a multiphoton laser (O'Brien et al., 2009). Embryos were imaged with a 25× water objective and 488/543 nm laser scanning to identify the axonal region of interest, then 1-5 scans of the two-photon laser (tuned to 910 nm) were used to transect an axonal region of interest at 100× digital zoom.

Quantification of mitochondrial morphology and transport

All axons within an image were traced using ImageJ software. Line length was calibrated to convert pixels to distance, and the Measure plugin was used to quantify total axon length. Density was calculated as mitochondria/axon length. Mitochondrial morphology was calculated as the ratio of length to width; all mitochondria within an image were quantified. Mitochondrial motility was defined as the percent of total mitochondria that moved in a 50-µm axon segment during a 6-minute movie, and was quantified using the Kymograph macro for ImageJ. A mitochondrion was considered to be moving only if it traveled at least 2 µm at a speed of at least 0.1 µm/s (Misgeld et al., 2007). Speed was calculated as the slope of distance (x) over time (y, in pixels) on the kymograph, and direction was determined by the sign of the slope. Mitochondrial transport behaviors were characterized by quantifying the percentage of time that motile mitochondria spent paused or moving in the anterograde or retrograde direction.

Data analysis

Data were analyzed with GraphPad Prism software. Unpaired *t*-tests were used to evaluate changes in mitochondrial morphology and transport between WT and aSyn-expressing cells, and to quantify cell death in GFP- and aSyn-2A-GFP-expressing cells. Minimal significance was set at $P<0.05$. One-way ANOVA and planned, unpaired Student's *t*-tests were used to evaluate the effect of aSyn on cell death and axon degeneration, and the ability of PGC-1α or WldS to prevent those effects. One-way ANOVA was followed by the appropriate post-test to correct for multiple comparisons.

Acknowledgements

We thank Meghan E. Johnson and Carla Koehler for the mitoDsRed construct, and Dr Shintaro Imamura for mouse PGC-1α.

Competing interests

The authors declare no competing financial interests.

Author contributions

K.C.O., J.M.B. and A.S. conceived and designed the experiments. K.C.O., N.D.W., A.L. and M.C.S. performed the experiments. K.C.O., A.L. and M.C.S. analyzed the data. J.M.B. contributed reagents. K.C.O. and A.S. wrote the paper.

Funding

N.D.W. was supported by the California Alliance for Minority Participation and the NIH Initiative for Maximizing Student Diversity. This work was supported by grants to A.S. from the National Institutes of Dental and Craniofacial Research (RO1 DE018496) and the American Parkinson Disease Association Pilot Fund (20082501). K.C.O. was supported by a training grant from the UCLA Training Program in Neural Repair (NINDS T32 NS07449:13).

Supplementary material

Supplementary material available online at
http://dmm.biologists.org/lookup/suppl/doi:10.1242/dmm.013185/-/DC1

References

Anderson, R. and Prolla, T. (2009). PGC-1alpha in aging and anti-aging interventions. *Biochim. Biophys. Acta* **1790**, 1059-1066.

Antenor-Dorsey, J. A. and O'Malley, K. L. (2012). WldS but not Nmnat1 protects dopaminergic neurites from MPP+ neurotoxicity. *Mol. Neurodegener.* **7**, 5.

Arnold, B., Cassady, S. J., VanLaar, V. S. and Berman, S. B. (2011). Integrating multiple aspects of mitochondrial dynamics in neurons: age-related differences and dynamic changes in a chronic rotenone model. *Neurobiol. Dis.* **41**, 189-200.

Auluck, P. K., Chan, H. Y., Trojanowski, J. Q., Lee, V. M. and Bonini, N. M. (2002). Chaperone suppression of alpha-synuclein toxicity in a Drosophila model for Parkinson's disease. *Science* **295**, 865-868.

Avery, M. A., Rooney, T. M., Pandya, J. D., Wishart, T. M., Gillingwater, T. H., Geddes, J. W., Sullivan, P. G. and Freeman, M. R. (2012). WldS prevents axon degeneration through increased mitochondrial flux and enhanced mitochondrial Ca2+ buffering. *Curr. Biol.* **22**, 596-600.

Baloh, R. H., Schmidt, R. E., Pestronk, A. and Milbrandt, J. (2007). Altered axonal mitochondrial transport in the pathogenesis of Charcot-Marie-Tooth disease from mitofusin 2 mutations. *J. Neurosci.* **27**, 422-430.

Bandmann, O. and Burton, E. A. (2010). Genetic zebrafish models of neurodegenerative diseases. *Neurobiol. Dis.* **40**, 58-65.

Banerjee, K., Sinha, M., Pham, C. L., Jana, S., Chanda, D., Cappai, R. and Chakrabarti, S. (2010). Alpha-synuclein induced membrane depolarization and loss of phosphorylation capacity of isolated rat brain mitochondria: implications in Parkinson's disease. *FEBS Lett.* **584**, 1571-1576.

Barrientos, S. A., Martinez, N. W., Yoo, S., Jara, J. S., Zamorano, S., Hetz, C., Twiss, J. L., Alvarez, J. and Court, F. A. (2011). Axonal degeneration is mediated by the mitochondrial permeability transition pore. *J. Neurosci.* **31**, 966-978.

Beirowski, B., Nógrádi, A., Babetto, E., Garcia-Alias, G. and Coleman, M. P. (2010). Mechanisms of axonal spheroid formation in central nervous system Wallerian degeneration. *J. Neuropathol. Exp. Neurol.* **69**, 455-472.

Benard, G. and Rossignol, R. (2008). Ultrastructure of the mitochondrion and its bearing on function and bioenergetics. *Antioxid. Redox Signal.* **10**, 1313-1342.

Boassa, D., Berlanga, M. L., Yang, M. A., Terada, M., Hu, J., Bushong, E. A., Hwang, M., Masliah, E., George, J. M. and Ellisman, M. H. (2013). Mapping the subcellular distribution of α-synuclein in neurons using genetically encoded probes for correlated light and electron microscopy: implications for Parkinson's disease pathogenesis. *J. Neurosci.* **33**, 2605-2615.

Braak, H., Sandmann-Keil, D., Gai, W. and Braak, E. (1999). Extensive axonal Lewy neurites in Parkinson's disease: a novel pathological feature revealed by alpha-synuclein immunocytochemistry. *Neurosci. Lett.* **265**, 67-69.

Braak, H., Del Tredici, K., Rüb, U., de Vos, R. A., Jansen Steur, E. N. and Braak, E. (2003). Staging of brain pathology related to sporadic Parkinson's disease. *Neurobiol. Aging* **24**, 197-211.

Bretaud, S., Lee, S. and Guo, S. (2004). Sensitivity of zebrafish to environmental toxins implicated in Parkinson's disease. *Neurotoxicol. Teratol.* **26**, 857-864.

Brustovetsky, N., Brustovetsky, T., Jemmerson, R. and Dubinsky, J. M. (2002). Calcium-induced cytochrome c release from CNS mitochondria is associated with the permeability transition and rupture of the outer membrane. *J. Neurochem.* **80**, 207-218.

Brustovetsky, N., Brustovetsky, T., Purl, K. J., Capano, M., Crompton, M. and Dubinsky, J. M. (2003). Increased susceptibility of striatal mitochondria to calcium-induced permeability transition. *J. Neurosci.* **23**, 4858-4867.
Burke, R. E. and O'Malley, K. (2013). Axon degeneration in Parkinson's disease. *Exp. Neurol.* 246, 72-83. PubMed
Butler, E. K., Voigt, A., Lutz, A. K., Toegel, J. P., Gerhardt, E., Karsten, P., Falkenburger, B., Reinartz, A., Winklhofer, K. F. and Schulz, J. B. (2012). The mitochondrial chaperone protein TRAP1 mitigates α-Synuclein toxicity. *PLoS Genet.* **8**, e1002488.
Cai, Q., Zakaria, H. M., Simone, A. and Sheng, Z. H. (2012). Spatial parkin translocation and degradation of damaged mitochondria via mitophagy in live cortical neurons. *Curr. Biol.* **22**, 545-552.
Calì, T., Ottolini, D., Negro, A. and Brini, M. (2012). α-Synuclein controls mitochondrial calcium homeostasis by enhancing endoplasmic reticulum-mitochondria interactions. *J. Biol. Chem.* **287**, 17914-17929.
Cardoso, S. M. (2011). The mitochondrial cascade hypothesis for Parkinson's disease. *Curr. Pharm. Des.* **17**, 3390-3397.
Cartelli, D., Ronchi, C., Maggioni, M. G., Rodighiero, S., Giavini, E. and Cappelletti, G. (2010). Microtubule dysfunction precedes transport impairment and mitochondria damage in MPP+ -induced neurodegeneration. *J. Neurochem.* **115**, 247-258.
Cassarino, D. S., Fall, C. P., Swerdlow, R. H., Smith, T. S., Halvorsen, E. M., Miller, S. W., Parks, J. P., Parker, W. D., Jr and Bennett, J. P., Jr (1997). Elevated reactive oxygen species and antioxidant enzyme activities in animal and cellular models of Parkinson's disease. *Biochim. Biophys. Acta* **1362**, 77-86.
Cheng, H. C. and Burke, R. E. (2010). The Wld(S) mutation delays anterograde, but not retrograde, axonal degeneration of the dopaminergic nigro-striatal pathway in vivo. *J. Neurochem.* **113**, 683-691.
Chesselet, M. F. (2008). In vivo alpha-synuclein overexpression in rodents: a useful model of Parkinson's disease? *Exp. Neurol.* **209**, 22-27.
Chinta, S. J., Mallajosyula, J. K., Rane, A. and Andersen, J. K. (2010). Mitochondrial α-synuclein accumulation impairs complex I function in dopaminergic neurons and results in increased mitophagy in vivo. *Neurosci. Lett.* **486**, 235-239.
Coleman, M. P., Conforti, L., Buckmaster, E. A., Tarlton, A., Ewing, R. M., Brown, M. C., Lyon, M. F. and Perry, V. H. (1998). An 85-kb tandem triplication in the slow Wallerian degeneration (Wlds) mouse. *Proc. Natl. Acad. Sci. USA* **95**, 9985-9990.
Costantini, P., Chernyak, B. V., Petronilli, V. and Bernardi, P. (1996). Modulation of the mitochondrial permeability transition pore by pyridine nucleotides and dithiol oxidation at two separate sites. *J. Biol. Chem.* **271**, 6746-6751.
Decressac, M., Mattsson, B., Lundblad, M., Weikop, P. and Björklund, A. (2012). Progressive neurodegenerative and behavioural changes induced by AAV-mediated overexpression of α-synuclein in midbrain dopamine neurons. *Neurobiol. Dis.* **45**, 939-953.
Devi, L. and Anandatheerthavarada, H. K. (2010). Mitochondrial trafficking of APP and alpha synuclein: Relevance to mitochondrial dysfunction in Alzheimer's and Parkinson's diseases. *Biochim. Biophys. Acta* **1802**, 11-19.
Dodson, M. W. and Guo, M. (2007). Pink1, Parkin, DJ-1 and mitochondrial dysfunction in Parkinson's disease. *Curr. Opin. Neurobiol.* **17**, 331-337.
Donnelly, M. L., Luke, G., Mehrotra, A., Li, X., Hughes, L. E., Gani, D. and Ryan, M. D. (2001). Analysis of the aphthovirus 2A/2B polyprotein 'cleavage' mechanism indicates not a proteolytic reaction, but a novel translational effect: a putative ribosomal 'skip'. *J. Gen. Virol.* **82**, 1013-1025.
Exner, N., Lutz, A. K., Haass, C. and Winklhofer, K. F. (2012). Mitochondrial dysfunction in Parkinson's disease: molecular mechanisms and pathophysiological consequences. *EMBO J.* **31**, 3038-3062.
Feany, M. B. and Bender, W. W. (2000). A Drosophila model of Parkinson's disease. *Nature* **404**, 394-398.
Fernagut, P. O. and Chesselet, M. F. (2004). Alpha-synuclein and transgenic mouse models. *Neurobiol. Dis.* **17**, 123-130.
Fleming, S. M., Salcedo, J., Fernagut, P. O., Rockenstein, E., Masliah, E., Levine, M. S. and Chesselet, M. F. (2004). Early and progressive sensorimotor anomalies in mice overexpressing wild-type human alpha-synuclein. *J. Neurosci.* **24**, 9434-9440.
Flinn, L., Bretaud, S., Lo, C., Ingham, P. W. and Bandmann, O. (2008). Zebrafish as a new animal model for movement disorders. *J. Neurochem.* **106**, 1991-1997.
Fuchs, J., Nilsson, C., Kachergus, J., Munz, M., Larsson, E. M., Schüle, B., Langston, J. W., Middleton, F. A., Ross, O. A., Hulihan, M. et al. (2007). Phenotypic variation in a large Swedish pedigree due to SNCA duplication and triplication. *Neurology* **68**, 916-922.
Galvin, J. E., Uryu, K., Lee, V. M. and Trojanowski, J. Q. (1999). Axon pathology in Parkinson's disease and Lewy body dementia hippocampus contains alpha-, beta-, and gamma-synuclein. *Proc. Natl. Acad. Sci. USA* **96**, 13450-13455.
Goldberg, J. A., Guzman, J. N., Estep, C. M., Ilijic, E., Kondapalli, J., Sanchez-Padilla, J. and Surmeier, D. J. (2012). Calcium entry induces mitochondrial oxidant stress in vagal neurons at risk in Parkinson's disease. *Nat. Neurosci.* **15**, 1414-1421.
Gu, Z., Nakamura, T. and Lipton, S. A. (2010). Redox reactions induced by nitrosative stress mediate protein misfolding and mitochondrial dysfunction in neurodegenerative diseases. *Mol. Neurobiol.* **41**, 55-72.
Gunter, T. E., Gunter, K. K., Sheu, S. S. and Gavin, C. E. (1994). Mitochondrial calcium transport: physiological and pathological relevance. *Am. J. Physiol.* **267**, C313-C339.
Guzman, J. N., Sanchez-Padilla, J., Wokosin, D., Kondapalli, J., Ilijic, E., Schumacker, P. T. and Surmeier, D. J. (2010). Oxidant stress evoked by pacemaking in dopaminergic neurons is attenuated by DJ-1. *Nature* **468**, 696-700.
Hanai, J., Cao, P., Tanksale, P., Imamura, S., Koshimizu, E., Zhao, J., Kishi, S., Yamashita, M., Phillips, P. S., Sukhatme, V. P. et al. (2007). The muscle-specific ubiquitin ligase atrogin-1/MAFbx mediates statin-induced muscle toxicity. *J. Clin. Invest.* **117**, 3940-3951.
Handschin, C. (2009). The biology of PGC-1α and its therapeutic potential. *Trends Pharmacol. Sci.* **30**, 322-329.
Hasbani, D. M. and O'Malley, K. L. (2006). Wld(S) mice are protected against the Parkinsonian mimetic MPTP. *Exp. Neurol.* **202**, 93-99.
Haworth, R. A. and Hunter, D. R. (1979). The Ca2+-induced membrane transition in mitochondria. II. Nature of the Ca2+ trigger site. *Arch. Biochem. Biophys.* **195**, 460-467.
Herkenham, M., Little, M. D., Bankiewicz, K., Yang, S. C., Markey, S. P. and Johannessen, J. N. (1991). Selective retention of MPP+ within the monoaminergic systems of the primate brain following MPTP administration: an in vivo autoradiographic study. *Neuroscience* **40**, 133-158.
Hornykiewicz, O. (1998). Biochemical aspects of Parkinson's disease. *Neurology* **51 Suppl. 2**, S2-S9.
Jellinger, K. A. (2012). Neuropathology of sporadic Parkinson's disease: evaluation and changes of concepts. *Mov. Disord.* **27**, 8-30.
Kamp, F., Exner, N., Lutz, A. K., Wender, N., Hegermann, J., Brunner, B., Nuscher, B., Bartels, T., Giese, A., Beyer, K. et al. (2010). Inhibition of mitochondrial fusion by α-synuclein is rescued by PINK1, Parkin and DJ-1. *EMBO J.* **29**, 3571-3589.
Keeney, P. M., Quigley, C. K., Dunham, L. D., Papageorge, C. M., Iyer, S., Thomas, R. R., Schwarz, K. M., Trimmer, P. A., Khan, S. M., Portell, F. R. et al. (2009). Mitochondrial gene therapy augments mitochondrial physiology in a Parkinson's disease cell model. *Hum. Gene Ther.* **20**, 897-907.
Kim-Han, J. S., Antenor-Dorsey, J. A. and O'Malley, K. L. (2011). The parkinsonian mimetic, MPP+, specifically impairs mitochondrial transport in dopamine axons. *J. Neurosci.* **31**, 7212-7221.
Köster, R. W. and Fraser, S. E. (2001). Tracing transgene expression in living zebrafish embryos. *Dev. Biol.* **233**, 329-346.
Kowaltowski, A. J., Castilho, R. F. and Vercesi, A. E. (1996). Opening of the mitochondrial permeability transition pore by uncoupling or inorganic phosphate in the presence of Ca2+ is dependent on mitochondrial-generated reactive oxygen species. *FEBS Lett.* **378**, 150-152.
Krüger, R., Kuhn, W., Müller, T., Woitalla, D., Graeber, M., Kösel, S., Przuntek, H., Epplen, J. T., Schöls, L. and Riess, O. (1998). Ala30Pro mutation in the gene encoding alpha-synuclein in Parkinson's disease. *Nat. Genet.* **18**, 106-108.
Kwan, K. M., Fujimoto, E., Grabher, C., Mangum, B. D., Hardy, M. E., Campbell, D. S., Parant, J. M., Yost, H. J., Kanki, J. P. and Chien, C. B. (2007). The Tol2kit: a multisite gateway-based construction kit for Tol2 transposon transgenesis constructs. *Dev. Dyn.* **236**, 3088-3099.
Lakso, M., Vartiainen, S., Moilanen, A. M., Sirviö, J., Thomas, J. H., Nass, R., Blakely, R. D. and Wong, G. (2003). Dopaminergic neuronal loss and motor deficits in Caenorhabditis elegans overexpressing human alpha-synuclein. *J. Neurochem.* **86**, 165-172.
Lee, S., Sterky, F. H., Mourier, A., Terzioglu, M., Cullheim, S., Olson, L. and Larsson, N. G. (2012). Mitofusin 2 is necessary for striatal axonal projections of midbrain dopamine neurons. *Hum. Mol. Genet.* **21**, 4827-4835.
Li, W. W., Yang, R., Guo, J. C., Ren, H. M., Zha, X. L., Cheng, J. S. and Cai, D. F. (2007). Localization of alpha-synuclein to mitochondria within midbrain of mice. *Neuroreport* **18**, 1543-1546.
Li, L. H., Qin, H. Z., Wang, J. L., Wang, J., Wang, X. L. and Gao, G. D. (2009a). Axonal degeneration of nigra-striatum dopaminergic neurons induced by 1-methyl-4-phenyl-1,2,3,6-tetrahydropyridine in mice. *J. Int. Med. Res.* **37**, 455-463.
Li, Y., Liu, W., Oo, T. F., Wang, L., Tang, Y., Jackson-Lewis, V., Zhou, C., Geghman, K., Bogdanov, M., Przedborski, S. et al. (2009b). Mutant LRRK2(R1441G) BAC transgenic mice recapitulate cardinal features of Parkinson's disease. *Nat. Neurosci.* **12**, 826-828.
Lim, K. L. and Ng, C. H. (2009). Genetic models of Parkinson disease. *Biochim. Biophys. Acta* **1792**, 604-615.
Liu, S., Sawada, T., Lee, S., Yu, W., Silverio, G., Alapatt, P., Millan, I., Shen, A., Saxton, W., Kanao, T. et al. (2012). Parkinson's disease-associated kinase PINK1 regulates Miro protein level and axonal transport of mitochondria. *PLoS Genet.* **8**, e1002537.
Lunn, E. R., Perry, V. H., Brown, M. C., Rosen, H. and Gordon, S. (1989). Absence of Wallerian Degeneration does not Hinder Regeneration in Peripheral Nerve. *Eur. J. Neurosci.* **1**, 27-33.
Mack, T. G., Reiner, M., Beirowski, B., Mi, W., Emanuelli, M., Wagner, D., Thomson, D., Gillingwater, T., Court, F., Conforti, L. et al. (2001). Wallerian degeneration of injured axons and synapses is delayed by a Ube4b/Nmnat chimeric gene. *Nat. Neurosci.* **4**, 1199-1206.
Maroteaux, L., Campanelli, J. T. and Scheller, R. H. (1988). Synuclein: a neuron-specific protein localized to the nucleus and presynaptic nerve terminal. *J. Neurosci.* **8**, 2804-2815.
Martin, L. J. (2006). Mitochondriopathy in Parkinson disease and amyotrophic lateral sclerosis. *J. Neuropathol. Exp. Neurol.* **65**, 1103-1110.
Martin, L. J., Pan, Y., Price, A. C., Sterling, W., Copeland, N. G., Jenkins, N. A., Price, D. L. and Lee, M. K. (2006). Parkinson's disease alpha-synuclein transgenic mice develop neuronal mitochondrial degeneration and cell death. *J. Neurosci.* **26**, 41-50.
Martin, S. M., O'Brien, G. S., Portera-Cailliau, C. and Sagasti, A. (2010). Wallerian degeneration of zebrafish trigeminal axons in the skin is required for regeneration and developmental pruning. *Development* **137**, 3985-3994.
Marui, W., Iseki, E., Nakai, T., Miura, S., Kato, M., Uéda, K. and Kosaka, K. (2002). Progression and staging of Lewy pathology in brains from patients with dementia with Lewy bodies. *J. Neurol. Sci.* **195**, 153-159.

Masliah, E., Rockenstein, E., Veinbergs, I., Mallory, M., Hashimoto, M., Takeda, A., Sagara, Y., Sisk, A. and Mucke, L. (2000). Dopaminergic loss and inclusion body formation in alpha-synuclein mice: implications for neurodegenerative disorders. *Science* **287**, 1265-1269.
Mijatovic, J., Piltonen, M., Alberton, P., Männistö, P. T., Saarma, M. and Piepponen, T. P. (2011). Constitutive Ret signaling is protective for dopaminergic cell bodies but not for axonal terminals. *Neurobiol. Aging* **32**, 1486-1494.
Misgeld, T., Kerschensteiner, M., Bareyre, F. M., Burgess, R. W. and Lichtman, J. W. (2007). Imaging axonal transport of mitochondria in vivo. *Nat. Methods* **4**, 559-561.
Misko, A., Jiang, S., Wegorzewska, I., Milbrandt, J. and Baloh, R. H. (2010). Mitofusin 2 is necessary for transport of axonal mitochondria and interacts with the Miro/Milton complex. *J. Neurosci.* **30**, 4232-4240.
Misko, A. L., Sasaki, Y., Tuck, E., Milbrandt, J. and Baloh, R. H. (2012). Mitofusin2 mutations disrupt axonal mitochondrial positioning and promote axon degeneration. *J. Neurosci.* **32**, 4145-4155.
Mudò, G., Mäkelä, J., Di Liberto, V., Tselykh, T. V., Olivieri, M., Piepponen, P., Eriksson, O., Mälkiä, A., Bonomo, A., Kairisalo, M. et al. (2012). Transgenic expression and activation of PGC-1α protect dopaminergic neurons in the MPTP mouse model of Parkinson's disease. *Cell. Mol. Life Sci.* **69**, 1153-1165.
Nakamura, K., Nemani, V. M., Azarbal, F., Skibinski, G., Levy, J. M., Egami, K., Munishkina, L., Zhang, J., Gardner, B., Wakabayashi, J. et al. (2011). Direct membrane association drives mitochondrial fission by the Parkinson disease-associated protein alpha-synuclein. *J. Biol. Chem.* **286**, 20710-20726.
Nakata, Y., Yasuda, T., Fukaya, M., Yamamori, S., Itakura, M., Nihira, T., Hayakawa, H., Kawanami, A., Kataoka, M., Nagai, M. et al. (2012). Accumulation of α-synuclein triggered by presynaptic dysfunction. *J. Neurosci.* **32**, 17186-17196.
Navarro, A., Boveris, A., Bández, M. J., Sánchez-Pino, M. J., Gómez, C., Muntané, G. and Ferrer, I. (2009). Human brain cortex: mitochondrial oxidative damage and adaptive response in Parkinson disease and in dementia with Lewy bodies. *Free Radic. Biol. Med.* **46**, 1574-1580.
Nikić, I., Merkler, D., Sorbara, C., Brinkoetter, M., Kreutzfeldt, M., Bareyre, F. M., Brück, W., Bishop, D., Misgeld, T. and Kerschensteiner, M. (2011). A reversible form of axon damage in experimental autoimmune encephalomyelitis and multiple sclerosis. *Nat. Med.* **17**, 495-499.
O'Brien, G., Rieger, S., Martin, S., Cavanaugh, A., Portera-Cailliau, C. and Sagasti, A. (2009). Two-photon axotomy and time-lapse confocal imaging in live zebrafish embryos. *J. Vis. Exp.* **24**, pii: 1129. doi: 10.3791/1129.
O'Donnell, K. C., Vargas, M. E. and Sagasti, A. (2013). WldS and PGC-1α regulate mitochondrial transport and oxidation state after axonal injury. *J. Neurosci.* **33**, 14778-14790.
O'Malley, K. L. (2010). The role of axonopathy in Parkinson's disease. *Exp Neurobiol* **19**, 115-119.
Orimo, S., Uchihara, T., Nakamura, A., Mori, F., Kakita, A., Wakabayashi, K. and Takahashi, H. (2008). Axonal alpha-synuclein aggregates herald centripetal degeneration of cardiac sympathetic nerve in Parkinson's disease. *Brain* **131**, 642-650.
Pacelli, C., De Rasmo, D., Signorile, A., Grattagliano, I., di Tullio, G., D'Orazio, A., Nico, B., Comi, G. P., Ronchi, D., Ferranini, E. et al. (2011). Mitochondrial defect and PGC-1α dysfunction in parkin-associated familial Parkinson's disease. *Biochim. Biophys. Acta* **1812**, 1041-1053.
Palanca, A. M., Lee, S. L., Yee, L. E., Joe-Wong, C., Trinh, L. A., Hiroyasu, E., Husain, M., Fraser, S. E., Pellegrini, M. and Sagasti, A. (2013). New transgenic reporters identify somatosensory neuron subtypes in larval zebrafish. *Dev. Neurobiol.* **73**, 152-167. PubMed
Parihar, M. S., Parihar, A., Fujita, M., Hashimoto, M. and Ghafourifar, P. (2008). Mitochondrial association of alpha-synuclein causes oxidative stress. *Cell. Mol. Life Sci.* **65**, 1272-1284.
Penn, A. M., Roberts, T., Hodder, J., Allen, P. S., Zhu, G. and Martin, W. R. (1995). Generalized mitochondrial dysfunction in Parkinson's disease detected by magnetic resonance spectroscopy of muscle. *Neurology* **45**, 2097-2099.
Pham, A. H., Meng, S., Chu, Q. N. and Chan, D. C. (2012). Loss of Mfn2 results in progressive, retrograde degeneration of dopaminergic neurons in the nigrostriatal circuit. *Hum. Mol. Genet.* **21**, 4817-4826.
Plucińska, G., Paquet, D., Hruscha, A., Godinho, L., Haass, C., Schmid, B. and Misgeld, T. (2012). In vivo imaging of disease-related mitochondrial dynamics in a vertebrate model system. *J. Neurosci.* **32**, 16203-16212.
Polymeropoulos, M. H., Lavedan, C., Leroy, E., Ide, S. E., Dehejia, A., Dutra, A., Pike, B., Root, H., Rubenstein, J., Boyer, R. et al. (1997). Mutation in the alpha-synuclein gene identified in families with Parkinson's disease. *Science* **276**, 2045-2047.
Prabhudesai, S., Sinha, S., Attar, A., Kotagiri, A., Fitzmaurice, A. G., Lakshmanan, R., Ivanova, M. I., Loo, J. A., Klärner, F. G., Schrader, T. et al. (2012). A novel "molecular tweezer" inhibitor of α-synuclein neurotoxicity in vitro and in vivo. *Neurotherapeutics* **9**, 464-476.
Press, C. and Milbrandt, J. (2008). Nmnat delays axonal degeneration caused by mitochondrial and oxidative stress. *J. Neurosci.* **28**, 4861-4871.
Przedborski, S. and Jackson-Lewis, V. (1998). Mechanisms of MPTP toxicity. *Mov. Disord.* **13 Suppl. 1**, 35-38.
Reeve, A. K., Park, T. K., Jaros, E., Campbell, G. R., Lax, N. Z., Hepplewhite, P. D., Krishnan, K. J., Elson, J. L., Morris, C. M., McKeith, I. G. et al. (2012). Relationship between mitochondria and α-synuclein: a study of single substantia nigra neurons. *Arch. Neurol.* **69**, 385-393.
Ries, V., Silva, R. M., Oo, T. F., Cheng, H. C., Rzhetskaya, M., Kholodilov, N., Flavell, R. A., Kuan, C. Y., Rakic, P. and Burke, R. E. (2008). JNK2 and JNK3 combined are essential for apoptosis in dopamine neurons of the substantia nigra, but are not required for axon degeneration. *J. Neurochem.* **107**, 1578-1588.
Sai, Y., Zou, Z., Peng, K. and Dong, Z. (2012). The Parkinson's disease-related genes act in mitochondrial homeostasis. *Neurosci. Biobehav. Rev.* **36**, 2034-2043.
Sajadi, A., Schneider, B. L. and Aebischer, P. (2004). Wlds-mediated protection of dopaminergic fibers in an animal model of Parkinson disease. *Curr. Biol.* **14**, 326-330.
Satake, W., Nakabayashi, Y., Mizuta, I., Hirota, Y., Ito, C., Kubo, M., Kawaguchi, T., Tsunoda, T., Watanabe, M., Takeda, A. et al. (2009). Genome-wide association study identifies common variants at four loci as genetic risk factors for Parkinson's disease. *Nat. Genet.* **41**, 1303-1307.
Schapira, A. H., Cooper, J. M., Dexter, D., Clark, J. B., Jenner, P. and Marsden, C. D. (1990). Mitochondrial complex I deficiency in Parkinson's disease. *J. Neurochem.* **54**, 823-827.
Schulz-Schaeffer, W. J. (2010). The synaptic pathology of alpha-synuclein aggregation in dementia with Lewy bodies, Parkinson's disease and Parkinson's disease dementia. *Acta Neuropathol.* **120**, 131-143.
Shin, J. H., Ko, H. S., Kang, H., Lee, Y., Lee, Y. I., Pletinkova, O., Troconso, J. C., Dawson, V. L. and Dawson, T. M. (2011). PARIS (ZNF746) repression of PGC-1α contributes to neurodegeneration in Parkinson's disease. *Cell* **144**, 689-702.
Siddiqui, A., Chinta, S. J., Mallajosyula, J. K., Rajagopolan, S., Hanson, I., Rane, A., Melov, S. and Andersen, J. K. (2012). Selective binding of nuclear alpha-synuclein to the PGC1alpha promoter under conditions of oxidative stress may contribute to losses in mitochondrial function: implications for Parkinson's disease. *Free Radic. Biol. Med.* **53**, 993-1003.
Simón-Sánchez, J., Schulte, C., Bras, J. M., Sharma, M., Gibbs, J. R., Berg, D., Paisan-Ruiz, C., Lichtner, P., Scholz, S. W., Hernandez, D. G. et al. (2009). Genome-wide association study reveals genetic risk underlying Parkinson's disease. *Nat. Genet.* **41**, 1308-1312.
Singleton, A. B., Farrer, M., Johnson, J., Singleton, A., Hague, S., Kachergus, J., Hulihan, M., Peuralinna, T., Dutra, A., Nussbaum, R. et al. (2003). alpha-Synuclein locus triplication causes Parkinson's disease. *Science* **302**, 841.
Spillantini, M. G., Schmidt, M. L., Lee, V. M., Trojanowski, J. Q., Jakes, R. and Goedert, M. (1997). Alpha-synuclein in Lewy bodies. *Nature* **388**, 839-840.
Spillantini, M. G., Crowther, R. A., Jakes, R., Hasegawa, M. and Goedert, M. (1998). alpha-Synuclein in filamentous inclusions of Lewy bodies from Parkinson's disease and dementia with lewy bodies. *Proc. Natl. Acad. Sci. USA* **95**, 6469-6473.
St-Pierre, J., Drori, S., Uldry, M., Silvaggi, J. M., Rhee, J., Jäger, S., Handschin, C., Zheng, K., Lin, J., Yang, W. et al. (2006). Suppression of reactive oxygen species and neurodegeneration by the PGC-1 transcriptional coactivators. *Cell* **127**, 397-408.
Sterky, F. H., Lee, S., Wibom, R., Olson, L. and Larsson, N. G. (2011). Impaired mitochondrial transport and Parkin-independent degeneration of respiratory chain-deficient dopamine neurons in vivo. *Proc. Natl. Acad. Sci. USA* **108**, 12937-12942.
Stowers, R. S., Megeath, L. J., Górska-Andrzejak, J., Meinertzhagen, I. A. and Schwarz, T. L. (2002). Axonal transport of mitochondria to synapses depends on milton, a novel Drosophila protein. *Neuron* **36**, 1063-1077.
Surmeier, D. J., Guzman, J. N., Sanchez-Padilla, J. and Schumacker, P. T. (2011). The role of calcium and mitochondrial oxidant stress in the loss of substantia nigra pars compacta dopaminergic neurons in Parkinson's disease. *Neuroscience* **198**, 221-231.
Tang, W., Ehrlich, I., Wolff, S. B., Michalski, A. M., Wölfl, S., Hasan, M. T., Lüthi, A. and Sprengel, R. (2009). Faithful expression of multiple proteins via 2A-peptide self-processing: a versatile and reliable method for manipulating brain circuits. *J. Neurosci.* **29**, 8621-8629.
Tomasiewicz, H. G., Flaherty, D. B., Soria, J. P. and Wood, J. G. (2002). Transgenic zebrafish model of neurodegeneration. *J. Neurosci. Res.* **70**, 734-745.
Tsunemi, T. and La Spada, A. R. (2012). PGC-1α at the intersection of bioenergetics regulation and neuron function: from Huntington's disease to Parkinson's disease and beyond. *Prog. Neurobiol.* **97**, 142-151.
Uemura, O., Okada, Y., Ando, H., Guedj, M., Higashijima, S., Shimazaki, T., Chino, N., Okano, H. and Okamoto, H. (2005). Comparative functional genomics revealed conservation and diversification of three enhancers of the isl1 gene for motor and sensory neuron-specific expression. *Dev. Biol.* **278**, 587-606.
van der Putten, H., Wiederhold, K. H., Probst, A., Barbieri, S., Mistl, C., Danner, S., Kauffmann, S., Hofele, K., Spooren, W. P., Ruegg, M. A. et al. (2000). Neuropathology in mice expressing human alpha-synuclein. *J. Neurosci.* **20**, 6021-6029.
Van Laar, V. S. and Berman, S. B. (2013). The interplay of neuronal mitochondrial dynamics and bioenergetics: Implications for Parkinson's disease. *Neurobiol. Dis.* **51**, 43-55. PubMed
Vercesi, A. E., Kowaltowski, A. J., Grijalba, M. T., Meinicke, A. R. and Castilho, R. F. (1997). The role of reactive oxygen species in mitochondrial permeability transition. *Biosci. Rep.* **17**, 43-52.
Volpicelli-Daley, L. A., Luk, K. C., Patel, T. P., Tanik, S. A., Riddle, D. M., Stieber, A., Meaney, D. F., Trojanowski, J. Q. and Lee, V. M. (2011). Exogenous α-synuclein fibrils induce Lewy body pathology leading to synaptic dysfunction and neuron death. *Neuron* **72**, 57-71.
Wang, X., Winter, D., Ashrafi, G., Schlehe, J., Wong, Y. L., Selkoe, D., Rice, S., Steen, J., LaVoie, M. J. and Schwarz, T. L. (2011). PINK1 and Parkin target Miro for phosphorylation and degradation to arrest mitochondrial motility. *Cell* **147**, 893-906.
Weihofen, A., Thomas, K. J., Ostaszewski, B. L., Cookson, M. R. and Selkoe, D. J. (2009). Pink1 forms a multiprotein complex with Miro and Milton, linking Pink1 function to mitochondrial trafficking. *Biochemistry* **48**, 2045-2052.

Wu, Z., Puigserver, P., Andersson, U., Zhang, C., Adelmant, G., Mootha, V., Troy, A., Cinti, S., Lowell, B., Scarpulla, R. C. et al. (1999). Mechanisms controlling mitochondrial biogenesis and respiration through the thermogenic coactivator PGC-1. *Cell* **98**, 115-124.

Wu-Chou, Y. H., Chen, Y. T., Yeh, T. H., Chang, H. C., Weng, Y. H., Lai, S. C., Huang, C. L., Chen, R. S., Huang, Y. Z., Chen, C. C. et al. (2013). Genetic variants of SNCA and LRRK2 genes are associated with sporadic PD susceptibility: A replication study in a Taiwanese cohort. *Parkinsonism Relat. Disord.* **19**, 251-255.

Xie, W. and Chung, K. K. (2012). Alpha-synuclein impairs normal dynamics of mitochondria in cell and animal models of Parkinson's disease. *J. Neurochem.* **122**, 404-414.

Zheng, B., Liao, Z., Locascio, J. J., Lesniak, K. A., Roderick, S. S., Watt, M. L., Eklund, A. C., Zhang-James, Y., Kim, P. D., Hauser, M. A. et al.; Global PD Gene Expression (GPEX) Consortium (2010). PGC-1α, a potential therapeutic target for early intervention in Parkinson's disease. *Sci. Transl. Med.* **2**, 52ra73.

Zhu, M., Li, W. and Lu, C. (2012). Role of alpha-synuclein protein levels in mitochondrial morphology and cell survival in cell lines. *PLoS ONE* **7**, e36377.

Reference Section

Abbas N, Lucking CB, Ricard S, Durr A, Bonifati V, De Michele G, et al. 1999. A wide variety of mutations in the parkin gene are responsible for autosomal recessive parkinsonism in europe. French parkinson's disease genetics study group and the european consortium on genetic susceptibility in parkinson's disease. Human molecular genetics 8:567-574.

Abeliovich A, Schmitz Y, Farinas I, Choi-Lundberg D, Ho WH, Castillo PE, et al. 2000. Mice lacking alpha-synuclein display functional deficits in the nigrostriatal dopamine system. Neuron 25:239-252.

Abeliovich H, Dunn WA, Jr., Kim J, Klionsky DJ. 2000. Dissection of autophagosome biogenesis into distinct nucleation and expansion steps. The Journal of cell biology 151:1025-1034.

Acharya S, Safaie BM, Wongkongkathep P, Ivanova MI, Attar A, Klarner FG, et al. 2014. Molecular basis for preventing alpha-synuclein aggregation by a molecular tweezer. The Journal of biological chemistry 289:10727-10737.

Agency USEP. 2004. Registration eligibility decision for ziram. (Registration Eligibility Decision).EPA.

Agency USEP. 2015. Label amendment- remove use on blackberry on the label per epa request, product name: Ziram 76df fungicide. 70506-173. http://www3.epa.gov/pesticides/chem_search/ppls/070506-00173-20151002.pdf:Environmental Protection Agency.

Anglade P, Vyas S, Javoy-Agid F, Herrero MT, Michel PP, Marquez J, et al. 1997. Apoptosis and autophagy in nigral neurons of patients with parkinson's disease. Histology and histopathology 12:25-31.

Arighi CN, Hartnell LM, Aguilar RC, Haft CR, Bonifacino JS. 2004. Role of the mammalian retromer in sorting of the cation-independent mannose 6-phosphate receptor. The Journal of cell biology 165:123-133.

Ascherio A, Chen H, Weisskopf MG, O'Reilly E, McCullough ML, Calle EE, et al. 2006. Pesticide exposure and risk for parkinson's disease. Annals of neurology 60:197-203.

Attar A, Ripoli C, Riccardi E, Maiti P, Li Puma DD, Liu T, et al. 2012. Protection of primary neurons and mouse brain from alzheimer's pathology by molecular tweezers. Brain : a journal of neurology 135:3735-3748.

Attar A, Bitan G. 2014. Disrupting self-assembly and toxicity of amyloidogenic protein oligomers by "molecular tweezers" - from the test tube to animal models. Current pharmaceutical design 20:2469-2483.

Attar N, Cullen PJ. 2010. The retromer complex. Advances in enzyme regulation 50:216-236.

Barbour R, Kling K, Anderson JP, Banducci K, Cole T, Diep L, et al. 2008. Red blood cells are the major source of alpha-synuclein in blood. Neuro-degenerative diseases 5:55-59.

Barcelos RC, Benvegnu DM, Boufleur N, Pase C, Teixeira AM, Reckziegel P, et al. 2011. Short term dietary fish oil supplementation improves motor deficiencies related to reserpine-induced parkinsonism in rats. Lipids 46:143-149.

Bartels T, Choi JG, Selkoe DJ. 2011. Alpha-synuclein occurs physiologically as a helically folded tetramer that resists aggregation. Nature 477:107-110.

Bence NF, Bennett EJ, Kopito RR. 2005. Application and analysis of the gfpu family of ubiquitin-proteasome system reporters. Methods in enzymology 399:481-490.

Berardelli A, Rothwell JC, Thompson PD, Hallett M. 2001. Pathophysiology of bradykinesia in parkinson's disease. Brain : a journal of neurology 124:2131-2146.

Betarbet R, Sherer TB, MacKenzie G, Garcia-Osuna M, Panov AV, Greenamyre JT. 2000. Chronic systemic pesticide exposure reproduces features of parkinson's disease. Nature neuroscience 3:1301-1306.

Biancalana M, Koide S. 2010. Molecular mechanism of thioflavin-t binding to amyloid fibrils. Biochimica et biophysica acta 1804:1405-1412.

Bieschke J, Russ J, Friedrich RP, Ehrnhoefer DE, Wobst H, Neugebauer K, et al. 2010. Egcg remodels mature alpha-synuclein and amyloid-beta fibrils and reduces cellular toxicity. Proceedings of the National Academy of Sciences of the United States of America 107:7710-7715.

Bill BR, Petzold AM, Clark KJ, Schimmenti LA, Ekker SC. 2009. A primer for morpholino use in zebrafish. Zebrafish 6:69-77.

Bodhicharla R, Nagarajan A, Winter J, Adenle A, Nazir A, Brady D, et al. 2012. Effects of alpha-synuclein overexpression in transgenic caenorhabditis elegans strains. CNS & neurological disorders drug targets 11:965-975.

Bonifati V, Rizzu P, van Baren MJ, Schaap O, Breedveld GJ, Krieger E, et al. 2003. Mutations in the dj-1 gene associated with autosomal recessive early-onset parkinsonism. Science 299:256-259.

Bonifati V. 2006. Parkinson's disease: The lrrk2-g2019s mutation: Opening a novel era in parkinson's disease genetics. European journal of human genetics : EJHG 14:1061-1062.

Boya P, Gonzalez-Polo RA, Casares N, Perfettini JL, Dessen P, Larochette N, et al. 2005. Inhibition of macroautophagy triggers apoptosis. Molecular and cellular biology 25:1025-1040.

Braak H, Braak E. 2000. Pathoanatomy of parkinson's disease. Journal of neurology 247 Suppl 2:II3-10.

Braak H, Rub U, Gai WP, Del Tredici K. 2003. Idiopathic parkinson's disease: Possible routes by which vulnerable neuronal types may be subject to neuroinvasion by an unknown pathogen. Journal of neural transmission 110:517-536.

Braak H, de Vos RA, Bohl J, Del Tredici K. 2006. Gastric alpha-synuclein immunoreactive inclusions in meissner's and auerbach's plexuses in cases staged for parkinson's disease-related brain pathology. Neuroscience letters 396:67-72.

Bretaud S, Li Q, Lockwood BL, Kobayashi K, Lin E, Guo S. 2007. A choice behavior for morphine reveals experience-dependent drug preference and underlying neural substrates in developing larval zebrafish. Neuroscience 146:1109-1116.

Brighina L, Frigerio R, Schneider NK, Lesnick TG, de Andrade M, Cunningham JM, et al. 2008. Alpha-synuclein, pesticides, and parkinson disease: A case-control study. Neurology 70:1461-1469.

Briquet M, Sabadie-Pialoux N, Goffeau A. 1976. Ziram, a sulfhydryl reagent and specific inhibitor of yeast mitochondrial dehydrogenases. Archives of biochemistry and biophysics 174:684-694.

Brown TP, Rumsby PC, Capleton AC, Rushton L, Levy LS. 2006. Pesticides and parkinson's disease--is there a link? Environmental health perspectives 114:156-164.

Burgess HA, Granato M. 2007. Modulation of locomotor activity in larval zebrafish during light adaptation. The Journal of experimental biology 210:2526-2539.

Burke WJ, Kumar VB, Pandey N, Panneton WM, Gan Q, Franko MW, et al. 2008. Aggregation of alpha-synuclein by dopal, the monoamine oxidase metabolite of dopamine. Acta neuropathologica 115:193-203.

Campbell BC, Li QX, Culvenor JG, Jakala P, Cappai R, Beyreuther K, et al. 2000. Accumulation of insoluble alpha-synuclein in dementia with lewy bodies. Neurobiology of disease 7:192-200.

Casida JE, Ford B, Jinsmaa Y, Sullivan P, Cooney A, Goldstein DS. 2014. Benomyl, aldehyde dehydrogenase, dopal, and the catecholaldehyde hypothesis for the pathogenesis of parkinson's disease. Chemical research in toxicology.

Chan P, DeLanney LE, Irwin I, Langston JW, Di Monte D. 1991. Rapid atp loss caused by 1-methyl-4-phenyl-1,2,3,6-tetrahydropyridine in mouse brain. Journal of neurochemistry 57:348-351.

Chandra S, Fornai F, Kwon HB, Yazdani U, Atasoy D, Liu X, et al. 2004. Double-knockout mice for alpha- and beta-synucleins: Effect on synaptic functions. Proceedings of the National Academy of Sciences of the United States of America 101:14966-14971.

Chartier-Harlin MC, Kachergus J, Roumier C, Mouroux V, Douay X, Lincoln S, et al. 2004. Alpha-synuclein locus duplication as a cause of familial parkinson's disease. Lancet 364:1167-1169.

Chen YC, Cheng CH, Chen GD, Hung CC, Yang CH, Hwang SP, et al. 2009. Recapitulation of zebrafish sncga expression pattern and labeling the habenular complex in transgenic zebrafish using green fluorescent protein reporter gene. Developmental dynamics : an official publication of the American Association of Anatomists 238:746-754.

Chesselet MF, Richter F, Zhu C, Magen I, Watson MB, Subramaniam SR. 2012. A progressive mouse model of parkinson's disease: The thy1-asyn ("line 61") mice. Neurotherapeutics : the journal of the American Society for Experimental NeuroTherapeutics 9:297-314.

Choi JM, Woo MS, Ma HI, Kang SY, Sung YH, Yong SW, et al. 2008. Analysis of park genes in a korean cohort of early-onset parkinson disease. Neurogenetics 9:263-269.

Chou AP, Maidment N, Klintenberg R, Casida JE, Li S, Fitzmaurice AG, et al. 2008. Ziram causes dopaminergic cell damage by inhibiting e1 ligase of the proteasome. The Journal of biological chemistry 283:34696-34703.

Chou AP, Li S, Fitzmaurice AG, Bronstein JM. 2010. Mechanisms of rotenone-induced proteasome inhibition. Neurotoxicology 31:367-372.

Ciechanover A, Iwai K. 2004. The ubiquitin system: From basic mechanisms to the patient bed. IUBMB life 56:193-201.

Ciliax BJ, Heilman C, Demchyshyn LL, Pristupa ZB, Ince E, Hersch SM, et al. 1995. The dopamine transporter: Immunochemical characterization and localization in brain. The Journal of neuroscience : the official journal of the Society for Neuroscience 15:1714-1723.

Clark IE, Dodson MW, Jiang C, Cao JH, Huh JR, Seol JH, et al. 2006. Drosophila pink1 is required for mitochondrial function and interacts genetically with parkin. Nature 441:1162-1166.

Conway KA, Rochet JC, Bieganski RM, Lansbury PT, Jr. 2001. Kinetic stabilization of the alpha-synuclein protofibril by a dopamine-alpha-synuclein adduct. Science 294:1346-1349.

Cuervo AM, Dice JF. 1996. A receptor for the selective uptake and degradation of proteins by lysosomes. Science 273:501-503.

Cuervo AM, Dice JF. 2000. When lysosomes get old. Experimental gerontology 35:119-131.

Cuervo AM, Stefanis L, Fredenburg R, Lansbury PT, Sulzer D. 2004. Impaired degradation of mutant alpha-synuclein by chaperone-mediated autophagy. Science 305:1292-1295.

Danzer KM, Haasen D, Karow AR, Moussaud S, Habeck M, Giese A, et al. 2007. Different species of alpha-synuclein oligomers induce calcium influx and seeding. The Journal of neuroscience : the official journal of the Society for Neuroscience 27:9220-9232.

Dauer W, Przedborski S. 2003. Parkinson's disease: Mechanisms and models. Neuron 39:889-909.

Deniau JM, Mailly P, Maurice N, Charpier S. 2007. The pars reticulata of the substantia nigra: A window to basal ganglia output. Progress in brain research 160:151-172.

Dettmer U, Newman AJ, Soldner F, Luth ES, Kim NC, von Saucken VE, et al. 2015. Parkinson-causing alpha-synuclein missense mutations shift native tetramers to monomers as a mechanism for disease initiation. Nature communications 6:7314.

Dorsey ER, Constantinescu R, Thompson JP, Biglan KM, Holloway RG, Kieburtz K, et al. 2007. Projected number of people with parkinson disease in the most populous nations, 2005 through 2030. Neurology 68:384-386.

Doty RL, Deems DA, Stellar S. 1988. Olfactory dysfunction in parkinsonism: A general deficit unrelated to neurologic signs, disease stage, or disease duration. Neurology 38:1237-1244.

Driever W, Solnica-Krezel L, Schier AF, Neuhauss SC, Malicki J, Stemple DL, et al. 1996. A genetic screen for mutations affecting embryogenesis in zebrafish. Development 123:37-46.

Du TT, Wang L, Duan CL, Lu LL, Zhang JL, Gao G, et al. 2015. Gba deficiency promotes snca/alpha-synuclein accumulation through autophagic inhibition by inactivated ppp2a. Autophagy 11:1803-1820.

Eisen JS, Smith JC. 2008. Controlling morpholino experiments: Don't stop making antisense. Development 135:1735-1743.

Eliezer D, Kutluay E, Bussell R, Jr., Browne G. 2001. Conformational properties of alpha-synuclein in its free and lipid-associated states. Journal of molecular biology 307:1061-1073.

Facheris M, Strain KJ, Lesnick TG, de Andrade M, Bower JH, Ahlskog JE, et al. 2005. Uchl1 is associated with parkinson's disease: A case-unaffected sibling and case-unrelated control study. Neuroscience letters 381:131-134.

Farrell TC, Cario CL, Milanese C, Vogt A, Jeong JH, Burton EA. 2011. Evaluation of spontaneous propulsive movement as a screening tool to detect rescue of parkinsonism phenotypes in zebrafish models. Neurobiology of disease 44:9-18.

Farrer M, Chan P, Chen R, Tan L, Lincoln S, Hernandez D, et al. 2001. Lewy bodies and parkinsonism in families with parkin mutations. Annals of neurology 50:293-300.

Farrer M, Kachergus J, Forno L, Lincoln S, Wang DS, Hulihan M, et al. 2004. Comparison of kindreds with parkinsonism and alpha-synuclein genomic multiplications. Annals of neurology 55:174-179.

Fauvet B, Mbefo MK, Fares MB, Desobry C, Michael S, Ardah MT, et al. 2012. Alpha-synuclein in central nervous system and from erythrocytes, mammalian cells, and escherichia coli exists predominantly as disordered monomer. The Journal of biological chemistry 287:15345-15364.

Feany MB, Bender WW. 2000. A drosophila model of parkinson's disease. Nature 404:394-398.

Feng CW, Wen ZH, Huang SY, Hung HC, Chen CH, Yang SN, et al. 2014. Effects of 6-hydroxydopamine exposure on motor activity and biochemical expression in zebrafish (danio rerio) larvae. Zebrafish 11:227-239.

Fitzmaurice AG, Rhodes SL, Lulla A, Murphy NP, Lam HA, O'Donnell KC, et al. 2013. Aldehyde dehydrogenase inhibition as a pathogenic mechanism in parkinson disease. Proceedings of the National Academy of Sciences of the United States of America 110:636-641.

Fitzmaurice AG, Rhodes SL, Cockburn M, Ritz B, Bronstein JM. 2014. Aldehyde dehydrogenase variation enhances effect of pesticides associated with parkinson disease. Neurology 82:419-426.

Fleming A, Diekmann H, Goldsmith P. 2013. Functional characterisation of the maturation of the blood-brain barrier in larval zebrafish. PloS one 8:e77548.

Fleming L, Mann JB, Bean J, Briggle T, Sanchez-Ramos JR. 1994. Parkinson's disease and brain levels of organochlorine pesticides. Annals of neurology 36:100-103.

Fokkens M, Schrader T, Klarner FG. 2005. A molecular tweezer for lysine and arginine. Journal of the American Chemical Society 127:14415-14421.

Follett J, Norwood SJ, Hamilton NA, Mohan M, Kovtun O, Tay S, et al. 2014. The vps35 d620n mutation linked to parkinson's disease disrupts the cargo sorting function of retromer. Traffic 15:230-244.

Freed CR, Greene PE, Breeze RE, Tsai WY, DuMouchel W, Kao R, et al. 2001. Transplantation of embryonic dopamine neurons for severe parkinson's disease. The New England journal of medicine 344:710-719.

Freundt EC, Maynard N, Clancy EK, Roy S, Bousset L, Sourigues Y, et al. 2012. Neuron-to-neuron transmission of alpha-synuclein fibrils through axonal transport. Annals of neurology 72:517-524.

Fumagalli F, Gainetdinov RR, Wang YM, Valenzano KJ, Miller GW, Caron MG. 1999. Increased methamphetamine neurotoxicity in heterozygous vesicular monoamine transporter 2 knock-out mice. The Journal of neuroscience : the official journal of the Society for Neuroscience 19:2424-2431.

Gaig C, Marti MJ, Ezquerra M, Rey MJ, Cardozo A, Tolosa E. 2007. G2019s lrrk2 mutation causing parkinson's disease without lewy bodies. Journal of neurology, neurosurgery, and psychiatry 78:626-628.

Gatto NM, Cockburn M, Bronstein J, Manthripragada AD, Ritz B. 2009. Well-water consumption and parkinson's disease in rural california. Environmental health perspectives 117:1912-1918.

Gatto NM, Rhodes SL, Manthripragada AD, Bronstein J, Cockburn M, Farrer M, et al. 2010. Alpha-synuclein gene may interact with environmental factors in increasing risk of parkinson's disease. Neuroepidemiology 35:191-195.

George JM, Jin H, Woods WS, Clayton DF. 1995. Characterization of a novel protein regulated during the critical period for song learning in the zebra finch. Neuron 15:361-372.

Gibb WR, Lees AJ. 1988. The relevance of the lewy body to the pathogenesis of idiopathic parkinson's disease. Journal of neurology, neurosurgery, and psychiatry 51:745-752.

Gilks WP, Abou-Sleiman PM, Gandhi S, Jain S, Singleton A, Lees AJ, et al. 2005. A common lrrk2 mutation in idiopathic parkinson's disease. Lancet 365:415-416.

Gitler AD, Bevis BJ, Shorter J, Strathearn KE, Hamamichi S, Su LJ, et al. 2008. The parkinson's disease protein alpha-synuclein disrupts cellular rab homeostasis. Proceedings of the National Academy of Sciences of the United States of America 105:145-150.

Glick D, Barth S, Macleod KF. 2010. Autophagy: Cellular and molecular mechanisms. The Journal of pathology 221:3-12.

Goker-Alpan O, Schiffmann R, LaMarca ME, Nussbaum RL, McInerney-Leo A, Sidransky E. 2004. Parkinsonism among gaucher disease carriers. Journal of medical genetics 41:937-940.

Goldman SM. 2014. Environmental toxins and parkinson's disease. Annual review of pharmacology and toxicology 54:141-164.

Goldstein DS, Sullivan P, Holmes C, Miller GW, Alter S, Strong R, et al. 2013. Determinants of buildup of the toxic dopamine metabolite dopal in parkinson's disease. Journal of neurochemistry 126:591-603.

Greene JC, Whitworth AJ, Kuo I, Andrews LA, Feany MB, Pallanck LJ. 2003. Mitochondrial pathology and apoptotic muscle degeneration in drosophila parkin mutants. Proceedings of the National Academy of Sciences of the United States of America 100:4078-4083.

Gunnarsson L, Jauhiainen A, Kristiansson E, Nerman O, Larsson DG. 2008. Evolutionary conservation of human drug targets in organisms used for environmental risk assessments. Environmental science & technology 42:5807-5813.

Hadjigeorgiou GM, Xiromerisiou G, Gourbali V, Aggelakis K, Scarmeas N, Papadimitriou A, et al. 2006. Association of alpha-synuclein rep1 polymorphism and parkinson's disease: Influence of rep1 on age at onset. Movement disorders : official journal of the Movement Disorder Society 21:534-539.

Haendel MA, Tilton F, Bailey GS, Tanguay RL. 2004. Developmental toxicity of the dithiocarbamate pesticide sodium metam in zebrafish. Toxicological sciences : an official journal of the Society of Toxicology 81:390-400.

Haffter P, Granato M, Brand M, Mullins MC, Hammerschmidt M, Kane DA, et al. 1996. The identification of genes with unique and essential functions in the development of the zebrafish, danio rerio. Development 123:1-36.

Hansen C, Angot E, Bergstrom AL, Steiner JA, Pieri L, Paul G, et al. 2011. Alpha-synuclein propagates from mouse brain to grafted dopaminergic neurons and seeds aggregation in cultured human cells. The Journal of clinical investigation 121:715-725.

Hashimoto M, Hsu LJ, Xia Y, Takeda A, Sisk A, Sundsmo M, et al. 1999. Oxidative stress induces amyloid-like aggregate formation of nacp/alpha-synuclein in vitro. Neuroreport 10:717-721.

He C, Bartholomew CR, Zhou W, Klionsky DJ. 2009. Assaying autophagic activity in transgenic gfp-lc3 and gfp-gabarap zebrafish embryos. Autophagy 5:520-526.

Henry JP, Scherman D. 1989. Radioligands of the vesicular monoamine transporter and their use as markers of monoamine storage vesicles. Biochemical pharmacology 38:2395-2404.

Hershko A, Heller H, Elias S, Ciechanover A. 1983. Components of ubiquitin-protein ligase system. Resolution, affinity purification, and role in protein breakdown. The Journal of biological chemistry 258:8206-8214.

Hershko A, Ciechanover A. 1998. The ubiquitin system. Annual review of biochemistry 67:425-479.

Hertzman C, Wiens M, Bowering D, Snow B, Calne D. 1990. Parkinson's disease: A case-control study of occupational and environmental risk factors. American journal of industrial medicine 17:349-355.

Hodge GK, Butcher LL. 1980. Pars compacta of the substantia nigra modulates motor activity but is not involved importantly in regulating food and water intake. Naunyn-Schmiedeberg's archives of pharmacology 313:51-67.

Hodge HC, Maynard EA, Downs WL, Coye RD, Jr., Steadman LT. 1956. Chronic oral toxicity of ferric dimethyldithiocarbamate (ferbam) and zinc dimethyldithiocarbamate (ziram). The Journal of pharmacology and experimental therapeutics 118:174-181.

Holzschuh J, Ryu S, Aberger F, Driever W. 2001. Dopamine transporter expression distinguishes dopaminergic neurons from other catecholaminergic neurons in the developing zebrafish embryo. Mechanisms of development 101:237-243.

Houlden H, Singleton AB. 2012. The genetics and neuropathology of parkinson's disease. Acta neuropathologica 124:325-338.

Howe K, Clark MD, Torroja CF, Torrance J, Berthelot C, Muffato M, et al. 2013. The zebrafish reference genome sequence and its relationship to the human genome. Nature 496:498-503.

Huang Y, Chegini F, Chua G, Murphy K, Gai W, Halliday GM. 2012. Macroautophagy in sporadic and the genetic form of parkinson's disease with the a53t alpha-synuclein mutation. Translational neurodegeneration 1:2.

Hughes AJ, Daniel SE, Blankson S, Lees AJ. 1993. A clinicopathologic study of 100 cases of parkinson's disease. Archives of neurology 50:140-148.

Hwang WY, Fu Y, Reyon D, Maeder ML, Tsai SQ, Sander JD, et al. 2013. Efficient genome editing in zebrafish using a crispr-cas system. Nature biotechnology 31:227-229.

Ibanez P, Bonnet AM, Debarges B, Lohmann E, Tison F, Pollak P, et al. 2004. Causal relation between alpha-synuclein gene duplication and familial parkinson's disease. Lancet 364:1169-1171.

International Parkinson Disease Genomics C, Nalls MA, Plagnol V, Hernandez DG, Sharma M, Sheerin UM, et al. 2011. Imputation of sequence variants for identification of genetic risks for parkinson's disease: A meta-analysis of genome-wide association studies. Lancet 377:641-649.

Iwata A, Christianson JC, Bucci M, Ellerby LM, Nukina N, Forno LS, et al. 2005a. Increased susceptibility of cytoplasmic over nuclear polyglutamine aggregates to autophagic degradation. Proceedings of the National Academy of Sciences of the United States of America 102:13135-13140.

Iwata A, Riley BE, Johnston JA, Kopito RR. 2005b. Hdac6 and microtubules are required for autophagic degradation of aggregated huntingtin. The Journal of biological chemistry 280:40282-40292.

Jankovic J. 2008. Parkinson's disease: Clinical features and diagnosis. Journal of neurology, neurosurgery, and psychiatry 79:368-376.

Jenner P. 2003. The contribution of the mptp-treated primate model to the development of new treatment strategies for parkinson's disease. Parkinsonism & related disorders 9:131-137.

Kabeya Y, Mizushima N, Ueno T, Yamamoto A, Kirisako T, Noda T, et al. 2000. Lc3, a mammalian homologue of yeast apg8p, is localized in autophagosome membranes after processing. The EMBO journal 19:5720-5728.

Kamrin MA. 1997. Pesticide profiles: Toxicity, environmental impact, and fate. New York:Lewis Publishers.

Kim RH, Smith PD, Aleyasin H, Hayley S, Mount MP, Pownall S, et al. 2005. Hypersensitivity of dj-1-deficient mice to 1-methyl-4-phenyl-1,2,3,6-tetrahydropyrindine (mptp) and oxidative stress. Proceedings of the National Academy of Sciences of the United States of America 102:5215-5220.

Kitada T, Asakawa S, Hattori N, Matsumine H, Yamamura Y, Minoshima S, et al. 1998. Mutations in the parkin gene cause autosomal recessive juvenile parkinsonism. Nature 392:605-608.

Klionsky DJ, Abdalla FC, Abeliovich H, Abraham RT, Acevedo-Arozena A, Adeli K, et al. 2012. Guidelines for the use and interpretation of assays for monitoring autophagy. Autophagy 8:445-544.

Kong B, Yang T, Gu JW, Kuang YQ, Cheng L, Yang WT, et al. 2013. The association between lysosomal protein glucocerebrosidase and parkinson's disease. European review for medical and pharmacological sciences 17:143-151.

Kopin IJ, Markey SP. 1988. Mptp toxicity: Implications for research in parkinson's disease. Annual review of neuroscience 11:81-96.

Kordower JH, Chu Y, Hauser RA, Freeman TB, Olanow CW. 2008. Lewy body-like pathology in long-term embryonic nigral transplants in parkinson's disease. Nature medicine 14:504-506.

Kramer ML, Schulz-Schaeffer WJ. 2007. Presynaptic alpha-synuclein aggregates, not lewy bodies, cause neurodegeneration in dementia with lewy bodies. The Journal of neuroscience : the official journal of the Society for Neuroscience 27:1405-1410.

Kruger R, Kuhn W, Muller T, Woitalla D, Graeber M, Kosel S, et al. 1998. Ala30pro mutation in the gene encoding alpha-synuclein in parkinson's disease. Nature genetics 18:106-108.

Lam HA, Wu N, Cely I, Kelly RL, Hean S, Richter F, et al. 2011. Elevated tonic extracellular dopamine concentration and altered dopamine modulation of synaptic activity precede dopamine loss in the striatum of mice overexpressing human alpha-synuclein. Journal of neuroscience research 89:1091-1102.

Lang AE, Lozano AM. 1998. Parkinson's disease. First of two parts. The New England journal of medicine 339:1044-1053.

Lashuel HA, Hartley D, Petre BM, Walz T, Lansbury PT, Jr. 2002. Neurodegenerative disease: Amyloid pores from pathogenic mutations. Nature 418:291.

Lebouvier T, Chaumette T, Damier P, Coron E, Touchefeu Y, Vrignaud S, et al. 2008. Pathological lesions in colonic biopsies during parkinson's disease. Gut 57:1741-1743.

Lesage S, Durr A, Tazir M, Lohmann E, Leutenegger AL, Janin S, et al. 2006. Lrrk2 g2019s as a cause of parkinson's disease in north african arabs. The New England journal of medicine 354:422-423.

Li JY, Englund E, Holton JL, Soulet D, Hagell P, Lees AJ, et al. 2008. Lewy bodies in grafted neurons in subjects with parkinson's disease suggest host-to-graft disease propagation. Nature medicine 14:501-503.

Lieschke GJ, Currie PD. 2007. Animal models of human disease: Zebrafish swim into view. Nature reviews Genetics 8:353-367.

Lim KL, Tan JM. 2007. Role of the ubiquitin proteasome system in parkinson's disease. BMC biochemistry 8 Suppl 1:S13.

Lindersson E, Beedholm R, Hojrup P, Moos T, Gai W, Hendil KB, et al. 2004. Proteasomal inhibition by alpha-synuclein filaments and oligomers. The Journal of biological chemistry 279:12924-12934.

Lucking CB, Durr A, Bonifati V, Vaughan J, De Michele G, Gasser T, et al. 2000. Association between early-onset parkinson's disease and mutations in the parkin gene. The New England journal of medicine 342:1560-1567.

Luk KC, Kehm V, Carroll J, Zhang B, O'Brien P, Trojanowski JQ, et al. 2012. Pathological alpha-synuclein transmission initiates parkinson-like neurodegeneration in nontransgenic mice. Science 338:949-953.

Ma Y, Dhawan V, Mentis M, Chaly T, Spetsieris PG, Eidelberg D. 2002. Parametric mapping of [18f]fpcit binding in early stage parkinson's disease: A pet study. Synapse 45:125-133.

Manzoni C, Lewis PA. 2013. Dysfunction of the autophagy/lysosomal degradation pathway is a shared feature of the genetic synucleinopathies. FASEB journal : official publication of the Federation of American Societies for Experimental Biology 27:3424-3429.

Maraganore DM, Lesnick TG, Elbaz A, Chartier-Harlin MC, Gasser T, Kruger R, et al. 2004. Uchl1 is a parkinson's disease susceptibility gene. Annals of neurology 55:512-521.

Maraganore DM, de Andrade M, Elbaz A, Farrer MJ, Ioannidis JP, Kruger R, et al. 2006. Collaborative analysis of alpha-synuclein gene promoter variability and parkinson disease. JAMA : the journal of the American Medical Association 296:661-670.

Maroteaux L, Campanelli JT, Scheller RH. 1988. Synuclein: A neuron-specific protein localized to the nucleus and presynaptic nerve terminal. The Journal of neuroscience : the official journal of the Society for Neuroscience 8:2804-2815.

Marsden CD. 1990. Parkinson's disease. Lancet 335:948-952.

Martin LJ, Pan Y, Price AC, Sterling W, Copeland NG, Jenkins NA, et al. 2006. Parkinson's disease alpha-synuclein transgenic mice develop neuronal mitochondrial degeneration and cell death. The Journal of neuroscience : the official journal of the Society for Neuroscience 26:41-50.

Martinat C, Shendelman S, Jonason A, Leete T, Beal MF, Yang L, et al. 2004. Sensitivity to oxidative stress in dj-1-deficient dopamine neurons: An es- derived cell model of primary parkinsonism. PLoS biology 2:e327.

Martinez-Vicente M, Talloczy Z, Kaushik S, Massey AC, Mazzulli J, Mosharov EV, et al. 2008. Dopamine-modified alpha-synuclein blocks chaperone-mediated autophagy. The Journal of clinical investigation 118:777-788.

Masliah E, Rockenstein E, Veinbergs I, Mallory M, Hashimoto M, Takeda A, et al. 2000. Dopaminergic loss and inclusion body formation in alpha-synuclein mice: Implications for neurodegenerative disorders. Science 287:1265-1269.

Mazzulli JR, Xu YH, Sun Y, Knight AL, McLean PJ, Caldwell GA, et al. 2011. Gaucher disease glucocerebrosidase and alpha-synuclein form a bidirectional pathogenic loop in synucleinopathies. Cell 146:37-52.

McCormack AL, Thiruchelvam M, Manning-Bog AB, Thiffault C, Langston JW, Cory-Slechta DA, et al. 2002. Environmental risk factors and parkinson's disease: Selective degeneration of nigral dopaminergic neurons caused by the herbicide paraquat. Neurobiology of disease 10:119-127.

McNaught KS, Jenner P. 2001. Proteasomal function is impaired in substantia nigra in parkinson's disease. Neuroscience letters 297:191-194.

McNaught KS, Belizaire R, Isacson O, Jenner P, Olanow CW. 2003. Altered proteasomal function in sporadic parkinson's disease. Experimental neurology 179:38-46.

McNaught KS, Perl DP, Brownell AL, Olanow CW. 2004. Systemic exposure to proteasome inhibitors causes a progressive model of parkinson's disease. Annals of neurology 56:149-162.

Meulener MC, Graves CL, Sampathu DM, Armstrong-Gold CE, Bonini NM, Giasson BI. 2005. Dj-1 is present in a large molecular complex in human brain tissue and interacts with alpha-synuclein. Journal of neurochemistry 93:1524-1532.

Meulener MC, Xu K, Thomson L, Ischiropoulos H, Bonini NM. 2006. Mutational analysis of dj-1 in drosophila implicates functional inactivation by oxidative damage and aging. Proceedings of the National Academy of Sciences of the United States of America 103:12517-12522.

Milanese C, Sager JJ, Bai Q, Farrell TC, Cannon JR, Greenamyre JT, et al. 2012. Hypokinesia and reduced dopamine levels in zebrafish lacking beta- and gamma1-synucleins. The Journal of biological chemistry 287:2971-2983.

Miura E, Hasegawa T, Konno M, Suzuki M, Sugeno N, Fujikake N, et al. 2014. Vps35 dysfunction impairs lysosomal degradation of alpha-synuclein and exacerbates neurotoxicity in a drosophila model of parkinson's disease. Neurobiology of disease 71:1-13.

Mizushima N, Yamamoto A, Matsui M, Yoshimori T, Ohsumi Y. 2004. In vivo analysis of autophagy in response to nutrient starvation using transgenic mice expressing a fluorescent autophagosome marker. Molecular biology of the cell 15:1101-1111.

Moore DJ, Zhang L, Troncoso J, Lee MK, Hattori N, Mizuno Y, et al. 2005. Association of dj-1 and parkin mediated by pathogenic dj-1 mutations and oxidative stress. Human molecular genetics 14:71-84.

Mougenot AL, Nicot S, Bencsik A, Morignat E, Verchere J, Lakhdar L, et al. 2012. Prion-like acceleration of a synucleinopathy in a transgenic mouse model. Neurobiology of aging 33:2225-2228.

Myhre R, Toft M, Kachergus J, Hulihan MM, Aasly JO, Klungland H, et al. 2008. Multiple alpha-synuclein gene polymorphisms are associated with parkinson's disease in a norwegian population. Acta neurologica Scandinavica 118:320-327.

Nakatogawa H, Ichimura Y, Ohsumi Y. 2007. Atg8, a ubiquitin-like protein required for autophagosome formation, mediates membrane tethering and hemifusion. Cell 130:165-178.

Nicklas WJ, Vyas I, Heikkila RE. 1985. Inhibition of nadh-linked oxidation in brain mitochondria by 1-methyl-4-phenyl-pyridine, a metabolite of the neurotoxin, 1-methyl-4-phenyl-1,2,5,6-tetrahydropyridine. Life sciences 36:2503-2508.

Norris EH, Uryu K, Leight S, Giasson BI, Trojanowski JQ, Lee VM. 2007. Pesticide exposure exacerbates alpha-synucleinopathy in an a53t transgenic mouse model. The American journal of pathology 170:658-666.

Ogawa S, Ng KW, Ramadasan PN, Nathan FM, Parhar IS. 2012. Habenular kiss1 neurons modulate the serotonergic system in the brain of zebrafish. Endocrinology 153:2398-2407.

Olanow CW, Goetz CG, Kordower JH, Stoessl AJ, Sossi V, Brin MF, et al. 2003. A double-blind controlled trial of bilateral fetal nigral transplantation in parkinson's disease. Annals of neurology 54:403-414.

Olanow CW, Perl DP, DeMartino GN, McNaught KS. 2004. Lewy-body formation is an aggresome-related process: A hypothesis. Lancet neurology 3:496-503.

Oliveras-Salva M, Macchi F, Coessens V, Deleersnijder A, Gerard M, Van der Perren A, et al. 2014. Alpha-synuclein-induced neurodegeneration is exacerbated in pink1 knockout mice. Neurobiology of aging 35:2625-2636.

Outeiro TF, Putcha P, Tetzlaff JE, Spoelgen R, Koker M, Carvalho F, et al. 2008. Formation of toxic oligomeric alpha-synuclein species in living cells. PloS one 3:e1867.

Ozelius LJ, Senthil G, Saunders-Pullman R, Ohmann E, Deligtisch A, Tagliati M, et al. 2006. Lrrk2 g2019s as a cause of parkinson's disease in ashkenazi jews. The New England journal of medicine 354:424-425.

Palanca AM, Lee SL, Yee LE, Joe-Wong C, Trinh le A, Hiroyasu E, et al. 2013. New transgenic reporters identify somatosensory neuron subtypes in larval zebrafish. Developmental neurobiology 73:152-167.

Pan-Montojo F, Anichtchik O, Dening Y, Knels L, Pursche S, Jung R, et al. 2010. Progression of parkinson's disease pathology is reproduced by intragastric administration of rotenone in mice. PloS one 5:e8762.

Pan-Montojo F, Schwarz M, Winkler C, Arnhold M, O'Sullivan GA, Pal A, et al. 2012. Environmental toxins trigger pd-like progression via increased alpha-synuclein release from enteric neurons in mice. Scientific reports 2:898.

Panneton WM, Kumar VB, Gan Q, Burke WJ, Galvin JE. 2010. The neurotoxicity of dopal: Behavioral and stereological evidence for its role in parkinson disease pathogenesis. PloS one 5:e15251.

Paquet D, Bhat R, Sydow A, Mandelkow EM, Berg S, Hellberg S, et al. 2009. A zebrafish model of tauopathy allows in vivo imaging of neuronal cell death and drug evaluation. The Journal of clinical investigation 119:1382-1395.

Park J, Lee SB, Lee S, Kim Y, Song S, Kim S, et al. 2006. Mitochondrial dysfunction in drosophila pink1 mutants is complemented by parkin. Nature 441:1157-1161.

Parkinson J. 2002. An essay on the shaking palsy. 1817. The Journal of neuropsychiatry and clinical neurosciences 14:223-236; discussion 222.

Parng C, Roy NM, Ton C, Lin Y, McGrath P. 2007. Neurotoxicity assessment using zebrafish. Journal of pharmacological and toxicological methods 55:103-112.

Patten SA, Sihra RK, Dhami KS, Coutts CA, Ali DW. 2007. Differential expression of pkc isoforms in developing zebrafish. International journal of developmental neuroscience : the official journal of the International Society for Developmental Neuroscience 25:155-164.

Peng J, Mao XO, Stevenson FF, Hsu M, Andersen JK. 2004. The herbicide paraquat induces dopaminergic nigral apoptosis through sustained activation of the jnk pathway. The Journal of biological chemistry 279:32626-32632.

Petroi D, Popova B, Taheri-Talesh N, Irniger S, Shahpasandzadeh H, Zweckstetter M, et al. 2012. Aggregate clearance of alpha-synuclein in saccharomyces cerevisiae depends more on autophagosome and vacuole function than on the proteasome. The Journal of biological chemistry 287:27567-27579.

Pfeiffer RF. 2003. Gastrointestinal dysfunction in parkinson's disease. Lancet neurology 2:107-116.

Piltonen M, Savolainen M, Patrikainen S, Baekelandt V, Myohanen TT, Mannisto PT. 2013. Comparison of motor performance, brain biochemistry and histology of two a30p alpha-synuclein transgenic mouse strains. Neuroscience 231:157-168.

Pioli EY, Meissner W, Sohr R, Gross CE, Bezard E, Bioulac BH. 2008. Differential behavioral effects of partial bilateral lesions of ventral tegmental area or substantia nigra pars compacta in rats. Neuroscience 153:1213-1224.

Plaas M, Karis A, Innos J, Rebane E, Baekelandt V, Vaarmann A, et al. 2008. Alpha-synuclein a30p point-mutation generates age-dependent nigrostriatal deficiency in mice. Journal of physiology and pharmacology : an official journal of the Polish Physiological Society 59:205-216.

Polymeropoulos MH, Lavedan C, Leroy E, Ide SE, Dehejia A, Dutra A, et al. 1997. Mutation in the alpha-synuclein gene identified in families with parkinson's disease. Science 276:2045-2047.

Pountney DL, Lowe R, Quilty M, Vickers JC, Voelcker NH, Gai WP. 2004. Annular alpha-synuclein species from purified multiple system atrophy inclusions. Journal of neurochemistry 90:502-512.

Prabhudesai S, Sinha S, Attar A, Kotagiri A, Fitzmaurice AG, Lakshmanan R, et al. 2012. A novel "molecular tweezer" inhibitor of alpha-synuclein neurotoxicity in vitro and in vivo. Neurotherapeutics : the journal of the American Society for Experimental NeuroTherapeutics 9:464-476.

Pramstaller PP, Schlossmacher MG, Jacques TS, Scaravilli F, Eskelson C, Pepivani I, et al. 2005. Lewy body parkinson's disease in a large pedigree with 77 parkin mutation carriers. Annals of neurology 58:411-422.

Przedborski S, Jackson-Lewis V. 1998. Mechanisms of mptp toxicity. Movement disorders : official journal of the Movement Disorder Society 13 Suppl 1:35-38.

Purisai MG, McCormack AL, Cumine S, Li J, Isla MZ, Di Monte DA. 2007. Microglial activation as a priming event leading to paraquat-induced dopaminergic cell degeneration. Neurobiology of disease 25:392-400.

Puschmann A, Ross OA, Vilarino-Guell C, Lincoln SJ, Kachergus JM, Cobb SA, et al. 2009. A swedish family with de novo alpha-synuclein a53t mutation: Evidence for early cortical dysfunction. Parkinsonism & related disorders 15:627-632.

R. Jeroen Pasterkamp MPS, J. Peter H. Burbach. 2009. Development and engineering of dopamine neurons. Austin, Texas:Landes Bioscience.

Rajput A, Dickson DW, Robinson CA, Ross OA, Dachsel JC, Lincoln SJ, et al. 2006. Parkinsonism, lrrk2 g2019s, and tau neuropathology. Neurology 67:1506-1508.

Rajput A, Vilarino-Guell C, Rajput ML, Ross OA, Soto-Ortolaza AI, Lincoln SJ, et al. 2009. Alpha-synuclein polymorphisms are associated with parkinson's disease in a saskatchewan population. Movement disorders : official journal of the Movement Disorder Society 24:2411-2414.

Ramesh T, Lyon AN, Pineda RH, Wang C, Janssen PM, Canan BD, et al. 2010. A genetic model of amyotrophic lateral sclerosis in zebrafish displays phenotypic hallmarks of motoneuron disease. Disease models & mechanisms 3:652-662.

Ravid T, Hochstrasser M. 2008. Diversity of degradation signals in the ubiquitin-proteasome system. Nature reviews Molecular cell biology 9:679-690.

Ravikumar B, Duden R, Rubinsztein DC. 2002. Aggregate-prone proteins with polyglutamine and polyalanine expansions are degraded by autophagy. Human molecular genetics 11:1107-1117.

Residues FPoEoPRiFatEatWEGoP. 1996. Pesticide residues in food-1996.115.

Reznichenko L, Cheng Q, Nizar K, Gratiy SL, Saisan PA, Rockenstein EM, et al. 2012. In vivo alterations in calcium buffering capacity in transgenic mouse model of synucleinopathy. The Journal of neuroscience : the official journal of the Society for Neuroscience 32:9992-9998.

Ribeiro MJ, Vidailhet M, Loc'h C, Dupel C, Nguyen JP, Ponchant M, et al. 2002. Dopaminergic function and dopamine transporter binding assessed with positron emission tomography in parkinson disease. Archives of neurology 59:580-586.

Rink E, Wullimann MF. 2002. Development of the catecholaminergic system in the early zebrafish brain: An immunohistochemical study. Brain research Developmental brain research 137:89-100.

Ritz B, Yu F. 2000. Parkinson's disease mortality and pesticide exposure in california 1984-1994. International journal of epidemiology 29:323-329.

Rockenstein E, Mallory M, Hashimoto M, Song D, Shults CW, Lang I, et al. 2002. Differential neuropathological alterations in transgenic mice expressing alpha-synuclein from the platelet-derived growth factor and thy-1 promoters. Journal of neuroscience research 68:568-578.

Rockenstein E, Nuber S, Overk CR, Ubhi K, Mante M, Patrick C, et al. 2014. Accumulation of oligomer-prone alpha-synuclein exacerbates synaptic and neuronal degeneration in vivo. Brain : a journal of neurology 137:1496-1513.

Ross GW, Petrovitch H, Abbott RD, Nelson J, Markesbery W, Davis D, et al. 2004. Parkinsonian signs and substantia nigra neuron density in decendents elders without pd. Annals of neurology 56:532-539.

Ryan SD, Dolatabadi N, Chan SF, Zhang X, Akhtar MW, Parker J, et al. 2013. Isogenic human ipsc parkinson's model shows nitrosative stress-induced dysfunction in mef2-pgc1alpha transcription. Cell 155:1351-1364.

Sagasti A, Guido MR, Raible DW, Schier AF. 2005. Repulsive interactions shape the morphologies and functional arrangement of zebrafish peripheral sensory arbors. Current biology : CB 15:804-814.

Schneider SA, Klein C. 1993. Pink1 type of young-onset parkinson disease. In: Genereviews(r), (Pagon RA, Adam MP, Ardinger HH, Wallace SE, Amemiya A, Bean LJH, et al., eds). Seattle (WA).

Schulman BA, Harper JW. 2009. Ubiquitin-like protein activation by e1 enzymes: The apex for downstream signalling pathways. Nature reviews Molecular cell biology 10:319-331.

Schweitzer J, Lohr H, Filippi A, Driever W. 2012. Dopaminergic and noradrenergic circuit development in zebrafish. Developmental neurobiology 72:256-268.

Seaman MN. 2004. Cargo-selective endosomal sorting for retrieval to the golgi requires retromer. The Journal of cell biology 165:111-122.

Shahed J, Jankovic J. 2007. Exploring the relationship between essential tremor and parkinson's disease. Parkinsonism & related disorders 13:67-76.

Shannon KM, Keshavarzian A, Mutlu E, Dodiya HB, Daian D, Jaglin JA, et al. 2012. Alpha-synuclein in colonic submucosa in early untreated parkinson's disease. Movement disorders : official journal of the Movement Disorder Society 27:709-715.

Shendelman S, Jonason A, Martinat C, Leete T, Abeliovich A. 2004. Dj-1 is a redox-dependent molecular chaperone that inhibits alpha-synuclein aggregate formation. PLoS biology 2:e362.

Sheng D, Qu D, Kwok KH, Ng SS, Lim AY, Aw SS, et al. 2010. Deletion of the wd40 domain of lrrk2 in zebrafish causes parkinsonism-like loss of neurons and locomotive defect. PLoS genetics 6:e1000914.

Sherer TB, Kim JH, Betarbet R, Greenamyre JT. 2003. Subcutaneous rotenone exposure causes highly selective dopaminergic degeneration and alpha-synuclein aggregation. Experimental neurology 179:9-16.

Shpilka T, Weidberg H, Pietrokovski S, Elazar Z. 2011. Atg8: An autophagy-related ubiquitin-like protein family. Genome biology 12:226.

Sinha S, Lopes DH, Du Z, Pang ES, Shanmugam A, Lomakin A, et al. 2011. Lysine-specific molecular tweezers are broad-spectrum inhibitors of assembly and toxicity of amyloid proteins. Journal of the American Chemical Society 133:16958-16969.

Sinha S, Du Z, Maiti P, Klarner FG, Schrader T, Wang C, et al. 2012. Comparison of three amyloid assembly inhibitors: The sugar scyllo-inositol, the polyphenol epigallocatechin gallate, and the molecular tweezer clr01. ACS chemical neuroscience 3:451-458.

Small SA, Kent K, Pierce A, Leung C, Kang MS, Okada H, et al. 2005. Model-guided microarray implicates the retromer complex in alzheimer's disease. Annals of neurology 58:909-919.

Small SA, Petsko GA. 2015. Retromer in alzheimer disease, parkinson disease and other neurological disorders. Nature reviews Neuroscience 16:126-132.

Smeyne RJ, Jackson-Lewis V. 2005. The mptp model of parkinson's disease. Brain research Molecular brain research 134:57-66.

Snyder H, Mensah K, Theisler C, Lee J, Matouschek A, Wolozin B. 2003. Aggregated and monomeric alpha-synuclein bind to the s6' proteasomal protein and inhibit proteasomal function. The Journal of biological chemistry 278:11753-11759.

Song J. 2013. Why do proteins aggregate? "Intrinsically insoluble proteins" and "dark mediators" revealed by studies on "insoluble proteins" solubilized in pure water. F1000Research 2:94.

Spillantini MG, Schmidt ML, Lee VM, Trojanowski JQ, Jakes R, Goedert M. 1997. Alpha-synuclein in lewy bodies. Nature 388:839-840.

Spillantini MG, Crowther RA, Jakes R, Hasegawa M, Goedert M. 1998. Alpha-synuclein in filamentous inclusions of lewy bodies from parkinson's disease and dementia with lewy bodies. Proceedings of the National Academy of Sciences of the United States of America 95:6469-6473.

Spira PJ, Sharpe DM, Halliday G, Cavanagh J, Nicholson GA. 2001. Clinical and pathological features of a parkinsonian syndrome in a family with an ala53thr alpha-synuclein mutation. Annals of neurology 49:313-319.

Stefanis L, Larsen KE, Rideout HJ, Sulzer D, Greene LA. 2001. Expression of a53t mutant but not wild-type alpha-synuclein in pc12 cells induces alterations of the ubiquitin-dependent degradation system, loss of dopamine release, and autophagic cell death. The Journal of neuroscience : the official journal of the Society for Neuroscience 21:9549-9560.

Stefanis L. 2012. Alpha-synuclein in parkinson's disease. Cold Spring Harbor perspectives in medicine 2:a009399.

Stichel CC, Zhu XR, Bader V, Linnartz B, Schmidt S, Lubbert H. 2007. Mono- and double-mutant mouse models of parkinson's disease display severe mitochondrial damage. Human molecular genetics 16:2377-2393.

Sun Z, Gitler AD. 2008. Discovery and characterization of three novel synuclein genes in zebrafish. Developmental dynamics : an official publication of the American Association of Anatomists 237:2490-2495.

Suraweera A, Munch C, Hanssum A, Bertolotti A. 2012. Failure of amino acid homeostasis causes cell death following proteasome inhibition. Molecular cell 48:242-253.

Svensson E, Horvath-Puho E, Thomsen RW, Djurhuus JC, Pedersen L, Borghammer P, et al. 2015. Vagotomy and subsequent risk of parkinson's disease. Annals of neurology 78:522-529.

Tai Y, Chen L, Huang E, Liu C, Yang X, Qiu P, et al. 2014. Protective effect of alpha-synuclein knockdown on methamphetamine-induced neurotoxicity in dopaminergic neurons. Neural regeneration research 9:951-958.

Talbiersky P, Bastkowski F, Klarner FG, Schrader T. 2008. Molecular clip and tweezer introduce new mechanisms of enzyme inhibition. Journal of the American Chemical Society 130:9824-9828.

Tanaka M, Kim YM, Lee G, Junn E, Iwatsubo T, Mouradian MM. 2004. Aggresomes formed by alpha-synuclein and synphilin-1 are cytoprotective. The Journal of biological chemistry 279:4625-4631.

Tanaka Y, Engelender S, Igarashi S, Rao RK, Wanner T, Tanzi RE, et al. 2001. Inducible expression of mutant alpha-synuclein decreases proteasome activity and increases sensitivity to mitochondria-dependent apoptosis. Human molecular genetics 10:919-926.

Tang W, Ehrlich I, Wolff SB, Michalski AM, Wolfl S, Hasan MT, et al. 2009. Faithful expression of multiple proteins via 2a-peptide self-processing: A versatile and reliable method for manipulating brain circuits. The Journal of neuroscience : the official journal of the Society for Neuroscience 29:8621-8629.

Tanik SA, Schultheiss CE, Volpicelli-Daley LA, Brunden KR, Lee VM. 2013. Lewy body-like alpha-synuclein aggregates resist degradation and impair macroautophagy. The Journal of biological chemistry 288:15194-15210.

Tanner CM, Ross GW, Jewell SA, Hauser RA, Jankovic J, Factor SA, et al. 2009. Occupation and risk of parkinsonism: A multicenter case-control study. Archives of neurology 66:1106-1113.

Tanner CM, Kamel F, Ross GW, Hoppin JA, Goldman SM, Korell M, et al. 2011. Rotenone, paraquat, and parkinson's disease. Environmental health perspectives 119:866-872.

Teraoka H, Urakawa S, Nanba S, Nagai Y, Dong W, Imagawa T, et al. 2006. Muscular contractions in the zebrafish embryo are necessary to reveal thiuram-induced notochord distortions. Toxicology and applied pharmacology 212:24-34.

Thiruchelvam M, Richfield EK, Baggs RB, Tank AW, Cory-Slechta DA. 2000. The nigrostriatal dopaminergic system as a preferential target of repeated exposures to combined paraquat and maneb: Implications for parkinson's disease. The Journal of neuroscience : the official journal of the Society for Neuroscience 20:9207-9214.

Tilton F, La Du JK, Vue M, Alzarban N, Tanguay RL. 2006. Dithiocarbamates have a common toxic effect on zebrafish body axis formation. Toxicology and applied pharmacology 216:55-68.

Tomasiewicz HG, Flaherty DB, Soria JP, Wood JG. 2002. Transgenic zebrafish model of neurodegeneration. Journal of neuroscience research 70:734-745.

Tompkins MM, Hill WD. 1997. Contribution of somal lewy bodies to neuronal death. Brain research 775:24-29.

Trinh J, Farrer M. 2013. Advances in the genetics of parkinson disease. Nature reviews Neurology 9:445-454.

Ueda K, Fukushima H, Masliah E, Xia Y, Iwai A, Yoshimoto M, et al. 1993. Molecular cloning of cdna encoding an unrecognized component of amyloid in alzheimer disease. Proceedings of the National Academy of Sciences of the United States of America 90:11282-11286.

Uversky VN, Li J, Fink AL. 2001. Metal-triggered structural transformations, aggregation, and fibrillation of human alpha-synuclein. A possible molecular nk between parkinson's disease and heavy metal exposure. The Journal of biological chemistry 276:44284-44296.

Uversky VN, Li J, Souillac P, Millett IS, Doniach S, Jakes R, et al. 2002. Biophysical properties of the synucleins and their propensities to fibrillate: Inhibition of alpha-synuclein assembly by beta- and gamma-synucleins. The Journal of biological chemistry 277:11970-11978.

Van Den Eeden SK, Tanner CM, Bernstein AL, Fross RD, Leimpeter A, Bloch DA, et al. 2003. Incidence of parkinson's disease: Variation by age, gender, and race/ethnicity. American journal of epidemiology 157:1015-1022.

Vogiatzi T, Xilouri M, Vekrellis K, Stefanis L. 2008. Wild type alpha-synuclein is degraded by chaperone-mediated autophagy and macroautophagy in neuronal cells. The Journal of biological chemistry 283:23542-23556.

Volles MJ, Lee SJ, Rochet JC, Shtilerman MD, Ding TT, Kessler JC, et al. 2001. Vesicle permeabilization by protofibrillar alpha-synuclein: Implications for the pathogenesis and treatment of parkinson's disease. Biochemistry 40:7812-7819.

Volles MJ, Lansbury PT, Jr. 2002. Vesicle permeabilization by protofibrillar alpha-synuclein is sensitive to parkinson's disease-linked mutations and occurs by a pore-like mechanism. Biochemistry 41:4595-4602.

Volpicelli-Daley LA, Gamble KL, Schultheiss CE, Riddle DM, West AB, Lee VM. 2014. Formation of alpha-synuclein lewy neurite-like aggregates in axons impedes the transport of distinct endosomes. Molecular biology of the cell 25:4010-4023.

von Coelln R, Thomas B, Andrabi SA, Lim KL, Savitt JM, Saffary R, et al. 2006. Inclusion body formation and neurodegeneration are parkin independent in a mouse model of alpha-synucleinopathy. The Journal of neuroscience : the official journal of the Society for Neuroscience 26:3685-3696.

Wakabayashi K, Tanji K, Mori F, Takahashi H. 2007. The lewy body in parkinson's disease: Molecules implicated in the formation and degradation of alpha-synuclein aggregates. Neuropathology : official journal of the Japanese Society of Neuropathology 27:494-506.

Wang A, Costello S, Cockburn M, Zhang X, Bronstein J, Ritz B. 2011. Parkinson's disease risk from ambient exposure to pesticides. European journal of epidemiology 26:547-555.

Wang W, Perovic I, Chittuluru J, Kaganovich A, Nguyen LT, Liao J, et al. 2011. A soluble alpha-synuclein construct forms a dynamic tetramer. Proceedings of the National Academy of Sciences of the United States of America 108:17797-17802.

Wang XF, Li S, Chou AP, Bronstein JM. 2006. Inhibitory effects of pesticides on proteasome activity: Implication in parkinson's disease. Neurobiology of disease 23:198-205.

Ward CD, Hess WA, Calne DB. 1983. Olfactory impairment in parkinson's disease. Neurology 33:943-946.

Wattendorf E, Welge-Lussen A, Fiedler K, Bilecen D, Wolfensberger M, Fuhr P, et al. 2009. Olfactory impairment predicts brain atrophy in parkinson's disease. The Journal of neuroscience : the official journal of the Society for Neuroscience 29:15410-15413.

Webb JL, Ravikumar B, Atkins J, Skepper JN, Rubinsztein DC. 2003. Alpha-synuclein is degraded by both autophagy and the proteasome. The Journal of biological chemistry 278:25009-25013.

Weinreb PH, Zhen W, Poon AW, Conway KA, Lansbury PT, Jr. 1996. Nacp, a protein implicated in alzheimer's disease and learning, is natively unfolded. Biochemistry 35:13709-13715.

Wen L, Wei W, Gu W, Huang P, Ren X, Zhang Z, et al. 2008. Visualization of monoaminergic neurons and neurotoxicity of mptp in live transgenic zebrafish. Developmental biology 314:84-92.

Williams A, Sarkar S, Cuddon P, Ttofi EK, Saiki S, Siddiqi FH, et al. 2008. Novel targets for huntington's disease in an mtor-independent autophagy pathway. Nature chemical biology 4:295-305.

Winner B, Jappelli R, Maji SK, Desplats PA, Boyer L, Aigner S, et al. 2011. In vivo demonstration that alpha-synuclein oligomers are toxic. Proceedings of the National Academy of Sciences of the United States of America 108:4194-4199.

Winslow AR, Rubinsztein DC. 2011. The parkinson disease protein alpha-synuclein inhibits autophagy. Autophagy 7:429-431.

Withers GS, George JM, Banker GA, Clayton DF. 1997. Delayed localization of synelfin (synuclein, nacp) to presynaptic terminals in cultured rat hippocampal neurons. Brain research Developmental brain research 99:87-94.

Wu F, Poon WS, Lu G, Wang A, Meng H, Feng L, et al. 2009. Alpha-synuclein knockdown attenuates mpp+ induced mitochondrial dysfunction of sh-sy5y cells. Brain research 1292:173-179.

Wu F, Xu HD, Guan JJ, Hou YS, Gu JH, Zhen XC, et al. 2015. Rotenone impairs autophagic flux and lysosomal functions in parkinson's disease. Neuroscience 284:900-911.

Xi Y, Noble S, Ekker M. 2011a. Modeling neurodegeneration in zebrafish. Current neurology and neuroscience reports 11:274-282.

Xi Y, Yu M, Godoy R, Hatch G, Poitras L, Ekker M. 2011b. Transgenic zebrafish expressing green fluorescent protein in dopaminergic neurons of the ventral diencephalon. Developmental dynamics : an official publication of the American Association of Anatomists 240:2539-2547.

Xie Z, Nair U, Klionsky DJ. 2008. Atg8 controls phagophore expansion during autophagosome formation. Molecular biology of the cell 19:3290-3298.

Yamano T, Morita S. 1995. Effects of pesticides on isolated rat hepatocytes, mitochondria, and microsomes ii. Archives of environmental contamination and toxicology 28:1-7.

Yang W, Tiffany-Castiglioni E. 2007. The bipyridyl herbicide paraquat induces proteasome dysfunction in human neuroblastoma sh-sy5y cells. Journal of toxicology and environmental health Part A 70:1849-1857.

Yavich L, Tanila H, Vepsalainen S, Jakala P. 2004. Role of alpha-synuclein in presynaptic dopamine recruitment. The Journal of neuroscience : the official journal of the Society for Neuroscience 24:11165-11170.

Yavich L, Jakala P, Tanila H. 2006. Abnormal compartmentalization of norepinephrine in mouse dentate gyrus in alpha-synuclein knockout and a30p transgenic mice. Journal of neurochemistry 99:724-732.

Yazdani U, German DC, Liang CL, Manzino L, Sonsalla PK, Zeevalk GD. 2006. Rat model of parkinson's disease: Chronic central delivery of 1-methyl-4-phenylpyridinium (mpp+). Experimental neurology 200:172-183.

Yonetani M, Nonaka T, Masuda M, Inukai Y, Oikawa T, Hisanaga S, et al. 2009. Conversion of wild-type alpha-synuclein into mutant-type fibrils and its propagation in the presence of a30p mutant. The Journal of biological chemistry 284:7940-7950.

Zang LY, Misra HP. 1993. Generation of reactive oxygen species during the monoamine oxidase-catalyzed oxidation of the neurotoxicant, 1-methyl-4-phenyl-1,2,3,6-tetrahydropyridine. The Journal of biological chemistry 268:16504-16512.

Zarranz JJ, Alegre J, Gomez-Esteban JC, Lezcano E, Ros R, Ampuero I, et al. 2004. The new mutation, e46k, of alpha-synuclein causes parkinson and lewy body dementia. Annals of neurology 55:164-173.

Zharikov AD, Cannon JR, Tapias V, Bai Q, Horowitz MP, Shah V, et al. 2015. Shrna targeting alpha-synuclein prevents neurodegeneration in a parkinson's disease model. The Journal of clinical investigation 125:2721-2735.

Zhou W, Milder JB, Freed CR. 2008. Transgenic mice overexpressing tyrosine-to-cysteine mutant human alpha-synuclein: A progressive neurodegenerative model of diffuse lewy body disease. The Journal of biological chemistry 283:9863-9870.

Zhou Y, Shie FS, Piccardo P, Montine TJ, Zhang J. 2004. Proteasomal inhibition induced by manganese ethylene-bis-dithiocarbamate: Relevance to parkinson's disease. Neuroscience 128:281-291.

Zimprich A, Biskup S, Leitner P, Lichtner P, Farrer M, Lincoln S, et al. 2004. Mutations in lrrk2 cause autosomal-dominant parkinsonism with pleomorphic pathology. Neuron 44:601-607.